

Effects of Green Infrastructure Implementation on Runoff Hydrology and Water Quality in the Clintonville Neighborhood of Columbus, Ohio

Kay Bernard¹, Kathryn Boening-Ulman, PhD., E.I.², R. Andrew Tirpak, PhD, P.E.³, Jay F. Martin, PhD, P.E.⁴, and Ryan J. Winston, PhD, P.E.⁵

Final Report Documenting Research from 2016-2023

Hydrology and Water Quality

Blueprint Columbus Monitoring

Written for the City of Columbus, Ohio

March 27, 2024

¹ PhD Candidate, Department of Food, Agricultural, and Biological Engineering, Ohio State University, 590 Woody Hayes Drive, 250 Agricultural Engineering Building, Columbus, OH 43210.

² Assistant Professor of Professional Practice, Department of Food, Agricultural, and Biological Engineering, Ohio State University, 590 Woody Hayes Drive, 262B Agricultural Engineering Building, Columbus, OH 43210. Boening-Ulman.1@osu.edu

³ Research Assistant Professor, Department of Food, Agricultural, and Biological Engineering, Ohio State University, 590 Woody Hayes Drive, 230A Agricultural Engineering Building, Columbus, OH 43210. tirpak.5@osu.edu

⁴ Professor, Department of Food, Agricultural, and Biological Engineering, Ohio State University, 590 Woody Hayes Drive, 228B Agricultural Engineering Building, Columbus, OH 43210. Martin.1130@osu.edu

⁵ Assistant Professor, Department of Food, Agricultural, and Biological Engineering & Civil, Environmental, and Geodetic Engineering, Ohio State University, 590 Woody Hayes Drive, 230 Agricultural Engineering Building, Columbus, OH 43210. winston.201@osu.edu

Table of Contents

TABLE OF CONTENTS	1
LIST OF FIGURES	2
LIST OF TABLES	7
EXECUTIVE SUMMARY	8
INTRODUCTION	11
PROJECT OVERVIEW	12
METHODS	14
<i>Description of Monitored Sewersheds</i>	14
<i>Project Timelines</i>	19
<i>Data Collection</i>	20
<i>Laboratory Methods</i>	21
<i>Data Analysis</i>	22
RESULTS	25
HYDROLOGY.....	25
<i>Observed Rainfall Events</i>	25
<i>Runoff Depth</i>	28
<i>Runoff Coefficient</i>	32
<i>Normalized Peak Flow Rate</i>	33
<i>Case Study: Simulated Storm Testing</i>	35
WATER QUALITY.....	38
<i>Nutrients</i>	38
<i>Metals</i>	41
<i>Sediment</i>	44
<i>Case Study: Park of Roses Wetland</i>	46
<i>Case Study: Unitarian Universalist Church Bioretention Cell</i>	48
CONCLUSIONS	51
REFERENCES	54
APPENDIX A: GIS ANALYSIS TO IDENTIFY DIFFERENT IMPERVIOUS SURFACE TYPES IN EACH SEWERSHED	59
APPENDIX B: MONITORING RESULTS FROM WHETSTONE AND STARRETT SEWERSHEDS	65
APPENDIX C: GRAPHICAL AND TABULAR ANALYSIS OF POLLUTANT CONCENTRATIONS AND LOADS	67
APPENDIX D: RAINFALL-WATER QUALITY CORRELATION ANALYSIS	87
APPENDIX E: WETLAND INLET AND OUTLET POLLUTANT CONCENTRATION SUMMARY TABLE AND FIGURES	97
APPENDIX F: LABORATORY METHODS	109

List of Figures

Figure 1: Four pillars of the Blueprint Columbus project.....	14
Figure 2: Boundaries of the six sewersheds monitored in this study. Distribution of bioretention cells (BRCs), monitoring locations, and land use within each sewershed are also shown. The remaining area within each sewershed not identified as commercial or institutional is residential.	16
Figure 3: The Blueprint Columbus project was implemented between 2017 and 2021 but construction did not occur uniformly across the three treatment sewersheds. These improvements included GI, sump pump installations, sanitary sewer lateral lining, and home downspout redirections. The resulting analysis periods and number of monitored storms within each period are included for each treatment sewershed.	20
Figure 4: Rain gage cluster (left), sample intake (clear plastic) and area velocity meter (black) in the Cooke-Glenmont outfall (center), and automated sampler at Beechwold (right).	21
Figure 5: Overview of ANOVA/ANCOVA statistical analysis and data preparation for water quality data.	25
Figure 6: Relationships between runoff depth (in) for the treatment and control (Beechwold) sewersheds during the various project periods. Note: runoff depths are log transformed.	31
Figure 7: Distribution of runoff coefficients during storm events in each of the treatment sewersheds by project phase. Statistically significant differences between phases for each sewershed are indicated by different letters derived from Tukey post-Hoc tests.	33
Figure 8: Area normalized peak flow rates (NPFR; cfs/mi ²) by project phase observed in the treatment compared to the control (Beechwold) sewersheds. Note that data were log transformed.	34
Figure 9: Pearson’s correlation matrix of simulated storm testing data. Only statistically significant ($p < 0.05$) correlations are included. The larger numbers and circles correspond to more highly correlated results.....	37
Figure 10: Boxplots of paired control-treatment concentrations and storm event loads for TN and TP by project phase.	39
Figure 11: Boxplots for paired control-treatment concentrations and storm event loads for Cu, Pb, and Zn by project phase.....	42
Figure 12: Boxplots of paired control-treatment concentrations and storm event loads for TSS by project phase.....	45
Figure 13: Boxplots showing concentrations of select pollutants present in paired water quality samples collected from the inlet and outlet of the Park of Roses wetland. Concentrations of TN, TP, and TSS are presented in mg/L; Zn and Pb are shown in $\mu\text{g/L}$	47
Figure 14. Photograph (at left) and planting plan and monitoring locations (at right) of Unitarian Universalist bioretention cell.....	48
Figure 15: Map showing impervious surface types in the Beechwold sewershed. Pervious areas in the sewershed are not highlighted with color.	59
Figure 16: Map showing impervious surface types in the Indian Springs sewershed. Pervious areas in the sewershed are not highlighted with color.	60
Figure 17: Map showing impervious surface types in the Cooke-Glenmont sewershed. Pervious areas in the sewershed are not highlighted with color.....	61

Figure 18: Map showing impervious surface types in the Blenheim sewershed. Pervious areas in the sewershed are not highlighted with color. 62

Figure 19: Map showing impervious surface types in the Starrett sewershed. Pervious areas in the sewershed are not highlighted with color. 63

Figure 20: Map showing impervious surface types in the Whetstone sewershed. Pervious areas in the sewershed are not highlighted with color. 64

Figure 21: Linear regressions comparing runoff and rainfall depths (in) across three monitoring years. . 65

Figure 22: Boxplot comparisons of runoff coefficients from the Starrett and Whetstone sewersheds across three monitoring years. 65

Figure 23: Summary statistics of TKN in water quality samples collected from Clintonville sewersheds and results of analyses comparing project phases. Significant differences ($p<0.05$), determined from Kruskal-Wallis/Dunn’s test with Bonferroni corrections, are represented by different letters in box plots. Asterisk denotes differences were significant at $p<0.1$ 68

Figure 24: Summary statistics of Nitrate in water quality samples collected from Clintonville sewersheds and results of analyses comparing project phases. Significant differences ($p<0.05$), determined from Kruskal-Wallis/Dunn’s test with Bonferroni corrections, are represented by different letters in box plots. Asterisk denotes differences were significant at $p<0.1$ 69

Figure 25: Summary statistics of Nitrite in water quality samples collected from Clintonville sewersheds and results of analyses comparing project phases. Significant differences ($p<0.05$), determined from Kruskal-Wallis/Dunn’s test with Bonferroni corrections, are represented by different letters in box plots. Asterisk denotes differences were significant at $p<0.1$ 70

Figure 26: Summary statistics of TN in water quality samples collected from Clintonville sewersheds and results of analyses comparing project phases. Significant differences ($p<0.05$), determined from Kruskal-Wallis/Dunn’s test with Bonferroni corrections, are represented by different letters in box plots. Asterisk denotes differences were significant at $p<0.1$ 71

Figure 27: Summary statistics of TAN in water quality samples collected from Clintonville sewersheds and results of analyses comparing project phases. Significant differences ($p<0.05$), determined from Kruskal-Wallis/Dunn’s test with Bonferroni corrections, are represented by different letters in box plots. Asterisk denotes differences were significant at $p<0.1$ 72

Figure 28: Summary statistics of OrgN in water quality samples collected from Clintonville sewersheds and results of analyses comparing project phases. Significant differences ($p<0.05$), determined from Kruskal-Wallis/Dunn’s test with Bonferroni corrections, are represented by different letters in box plots. Asterisk denotes differences were significant at $p<0.1$ 73

Figure 29: Summary statistics of OP in water quality samples collected from Clintonville sewersheds and results of analyses comparing project phases. Significant differences ($p<0.05$), determined from Kruskal-Wallis/Dunn’s test with Bonferroni corrections, are represented by different letters in box plots. Asterisk denotes differences were significant at $p<0.1$ 74

Figure 30: Summary statistics of TP in water quality samples collected from Clintonville sewersheds and results of analyses comparing project phases. Significant differences ($p<0.05$), determined from Kruskal-Wallis/Dunn’s test with Bonferroni corrections, are represented by different letters in box plots. Asterisk denotes differences were significant at $p<0.1$ 75

Figure 31: Summary statistics of PBP in water quality samples collected from Clintonville sewersheds and results of analyses comparing project phases. Significant differences ($p < 0.05$), determined from Kruskal-Wallis/Dunn's test with Bonferroni corrections, are represented by different letters in box plots. Asterisk denotes differences were significant at $p < 0.1$ 76

Figure 32: Summary statistics of TSS in water quality samples collected from Clintonville sewersheds and results of analyses comparing project phases. Significant differences ($p < 0.05$), determined from Kruskal-Wallis/Dunn's test with Bonferroni corrections, are represented by different letters in box plots. Asterisk denotes differences were significant at $p < 0.1$ 77

Figure 33: Summary statistics of Hardness in water quality samples collected from Clintonville sewersheds and results of analyses comparing project phases. Significant differences ($p < 0.05$), determined from Kruskal-Wallis/Dunn's test with Bonferroni corrections, are represented by different letters in box plots. Asterisk denotes differences were significant at $p < 0.1$ 78

Figure 34: Summary statistics of Alkalinity in water quality samples collected from Clintonville sewersheds and results of analyses comparing project phases. Significant differences ($p < 0.05$), determined from Kruskal-Wallis/Dunn's test with Bonferroni corrections, are represented by different letters in box plots. Asterisk denotes differences were significant at $p < 0.1$ 79

Figure 35: Summary statistics of *E. coli* in water quality samples collected from Clintonville sewersheds and results of analyses comparing project phases. Significant differences ($p < 0.05$), determined from Kruskal-Wallis/Dunn's test with Bonferroni corrections, are represented by different letters in box plots. Asterisk denotes differences were significant at $p < 0.1$ 80

Figure 36: Summary statistics of Cadmium in water quality samples collected from Clintonville sewersheds and results of analyses comparing project phases. Significant differences ($p < 0.05$), determined from Kruskal-Wallis/Dunn's test with Bonferroni corrections, are represented by different letters in box plots. Asterisk denotes differences were significant at $p < 0.1$ 81

Figure 37: Summary statistics of Chromium in water quality samples collected from Clintonville sewersheds and results of analyses comparing project phases. Significant differences ($p < 0.05$), determined from Kruskal-Wallis/Dunn's test with Bonferroni corrections, are represented by different letters in box plots. Asterisk denotes differences were significant at $p < 0.1$ 82

Figure 38: Summary statistics of Copper in water quality samples collected from Clintonville sewersheds and results of analyses comparing project phases. Significant differences ($p < 0.05$), determined from Kruskal-Wallis/Dunn's test with Bonferroni corrections, are represented by different letters in box plots. Asterisk denotes differences were significant at $p < 0.1$ 83

Figure 39: Summary statistics of Lead in water quality samples collected from Clintonville sewersheds and results of analyses comparing project phases. Significant differences ($p < 0.05$), determined from Kruskal-Wallis/Dunn's test with Bonferroni corrections, are represented by different letters in box plots. Asterisk denotes differences were significant at $p < 0.1$ 84

Figure 40: Summary statistics of Nickel in water quality samples collected from Clintonville sewersheds and results of analyses comparing project phases. Significant differences ($p < 0.05$), determined from Kruskal-Wallis/Dunn's test with Bonferroni corrections, are represented by different letters in box plots. Asterisk denotes differences were significant at $p < 0.1$ 85

Figure 41: Summary statistics of Zinc in water quality samples collected from Clintonville sewersheds and results of analyses comparing project phases. Significant differences ($p < 0.05$), determined from

Kruskal-Wallis/Dunn’s test with Bonferroni corrections, are represented by different letters in box plots. Asterisk denotes differences were significant at $p < 0.1$ 86

Figure 42: Spearman correlation matrices at Blenheim between rainfall characteristics and nutrient and metal concentrations across project phases. Statistically significant ($p < 0.05$) concentrations shown in correlograms 89

Figure 43: Spearman correlation matrices at Blenheim between rainfall characteristics and nutrient and metal loads across project phases. Statistically significant ($p < 0.05$) concentrations shown in correlograms 90

Figure 44: Spearman correlation matrices at Cooke-Glenmont between rainfall characteristics and nutrient and metal concentrations across project phases. Statistically significant ($p < 0.05$) concentrations shown in correlograms. 92

Figure 45: Spearman correlation matrices at Cooke-Glenmont between rainfall characteristics and nutrient and metal loads across project phases. Statistically significant ($p < 0.05$) concentrations shown in correlograms 93

Figure 46: Spearman correlation matrices at Indian Springs between rainfall characteristics and nutrient and metal concentrations across project phases. Statistically significant ($p < 0.05$) concentrations shown in correlograms. 95

Figure 47: Spearman correlation matrices at Indian Springs between rainfall characteristics and nutrient and metal loads across project phases. Statistically significant ($p < 0.05$) concentrations shown in correlograms 96

Figure 48: Summary statistics of alkalinity in water quality samples collected from the constructed wetland at the Clintonville Park of Roses receiving low flows from the Blenheim sewershed and results of analyses comparing season of collection. 98

Figure 49: Summary statistics of cadmium in water quality samples collected from the constructed wetland at the Clintonville Park of Roses receiving low flows from the Blenheim sewershed and results of analyses comparing season of collection. 98

Figure 50: Summary statistics of chromium in water quality samples collected from the constructed wetland at the Clintonville Park of Roses receiving low flows from the Blenheim sewershed and results of analyses comparing season of collection. 99

Figure 51: Summary statistics of copper in water quality samples collected from the constructed wetland at the Clintonville Park of Roses receiving low flows from the Blenheim sewershed and results of analyses comparing season of collection..... 99

Figure 52: Summary statistics of *E. coli* in water quality samples collected from the constructed wetland at the Clintonville Park of Roses receiving low flows from the Blenheim sewershed and results of analyses comparing season of collection..... 100

Figure 53: Summary statistics of hardness in water quality samples collected from the constructed wetland at the Clintonville Park of Roses receiving low flows from the Blenheim sewershed and results of analyses comparing season of collection. 100

Figure 54: Summary statistics of organic nitrogen in water quality samples collected from the constructed wetland at the Clintonville Park of Roses receiving low flows from the Blenheim sewershed and results of analyses comparing season of collection..... 101

Figure 55: Summary statistics of nickel in water quality samples collected from the constructed wetland at the Clintonville Park of Roses receiving low flows from the Blenheim sewershed and results of analyses comparing season of collection..... 101

Figure 56: Summary statistics of nitrate in water quality samples collected from the constructed wetland at the Clintonville Park of Roses receiving low flows from the Blenheim sewershed and results of analyses comparing season of collection..... 102

Figure 57: Summary statistics of nitrite in water quality samples collected from the constructed wetland at the Clintonville Park of Roses receiving low flows from the Blenheim sewershed and results of analyses comparing season of collection..... 102

Figure 58: Summary statistics of NO₂₃ in water quality samples collected from the constructed wetland at the Clintonville Park of Roses receiving low flows from the Blenheim sewershed and results of analyses comparing season of collection..... 103

Figure 59: Summary statistics of orthophosphate in water quality samples collected from the constructed wetland at the Clintonville Park of Roses receiving low flows from the Blenheim sewershed and results of analyses comparing season of collection..... 103

Figure 60: Summary statistics of inorganic nitrogen in water quality samples collected from the constructed wetland at the Clintonville Park of Roses receiving low flows from the Blenheim sewershed and results of analyses comparing season of collection..... 104

Figure 61: Summary statistics of lead in water quality samples collected from the constructed wetland at the Clintonville Park of Roses receiving low flows from the Blenheim sewershed and results of analyses comparing season of collection. 104

Figure 62: Summary statistics of particle-bound phosphorus in water quality samples collected from the constructed wetland at the Clintonville Park of Roses receiving low flows from the Blenheim sewershed and results of analyses comparing season of collection..... 105

Figure 63: Summary statistics of total ammoniacal nitrogen in water quality samples collected from the constructed wetland at the Clintonville Park of Roses receiving low flows from the Blenheim sewershed and results of analyses comparing season of collection..... 105

Figure 64: Summary statistics of total Kjeldahl nitrogen in water quality samples collected from the constructed wetland at the Clintonville Park of Roses receiving low flows from the Blenheim sewershed and results of analyses comparing season of collection..... 106

Figure 65: Summary statistics of total nitrogen in water quality samples collected from the constructed wetland at the Clintonville Park of Roses receiving low flows from the Blenheim sewershed and results of analyses comparing season of collection. 106

Figure 66: Summary statistics of total phosphorus in water quality samples collected from the constructed wetland at the Clintonville Park of Roses receiving low flows from the Blenheim sewershed and results of analyses comparing season of collection..... 107

Figure 67: Summary statistics of total suspended solids in water quality samples collected from the constructed wetland at the Clintonville Park of Roses receiving low flows from the Blenheim sewershed and results of analyses comparing season of collection..... 107

Figure 68: Summary statistics of zinc in water quality samples collected from the constructed wetland at the Clintonville Park of Roses receiving low flows from the Blenheim sewershed and results of analyses comparing season of collection. 108

List of Tables

Table 1: Land use and percent imperviousness (% Imp) in the six monitored sewersheds in Clintonville.	17
Table 2: Monitored Blueprint sewersheds and the number of implemented SCMs for each pillar of the Blueprint project as of December 2023. Note: monitored sewersheds are not equivalent to the complete project areas designated by the City, particularly for Cooke-Glenmont where infrastructure improvements were completed outside of the monitored area.	18
Table 3: Rainfall characteristics from all monitored events in the treatment sewersheds by project period. Significant differences in rainfall characteristics compared to the Pre-GI period are shown in italics.	27
Table 4: Summary statistics and ANCOVA results for comparisons of runoff depth (in) between treatment and control sewersheds. Statistically significant changes in LSM compared to pre-GI phase are denoted in bold ($p < 0.05$) and underlined ($p < 0.10$), indicating differences in runoff generation patterns in the treatment sewersheds compared to the control during the same period.	30
Table 5: Summary statistics for simulated storm testing in 2018-2022.	36
Table 6: Summary statistics of paired control-treatment concentrations and storm event loads for TN and TP by project phase. Significant differences based on ANCOVA analyses indicated by red (increase) and green (decrease) text.	40
Table 7: Summary statistics for paired control-treatment concentrations and storm event loads for Cu, Pb, and Zn by project phase. Significant differences based on ANCOVA analyses indicated by red (increase) and green (decrease) text.	43
Table 8: Summary statistics of paired control-treatment concentrations and storm event loads for TSS grouped by project phase.	46
Table 9: Summary statistics of concentrations of select pollutants present in paired water quality samples collected from the inlet and outlet of the Park of Roses wetland. Differences between inlet and outlet concentrations were all statistically significant ($p < 0.0001$).	47
Table 10: Summary statistics of concentrations of select pollutants present in paired water quality samples collected from the inlet and outlet of the Unitarian Universalist church bioretention cell. Nutrient and sediment concentrations are in mg/L, metals are in $\mu\text{g/L}$, and E. coli is in CFU/100mL. RE is the relative efficiency for that pollutant; multiplying the RE by 100 results in percent removal.	50
Table 11: Summary statistics of runoff depth (in) and runoff coefficients for Starrett and Whetstone.	66
Table 12: Summary statistics for wetland inlet and outlet data points for all monitored pollutants. Reported p-values based on Unpaired T-Test with Welch Corrections or Uncorrected Mann-Whitney test (based on normality). Significant p-values in bold; corresponding median percent reductions bolded and colored according to direction of change (green = decrease, red = increase).	97
Table 13: Sample collection, preservation, and laboratory testing methods as well as method detection limits (MDLs) for pollutants analyzed herein.	109

Executive Summary

To evaluate the holistic impacts of the Blueprint Columbus Project, stormwater runoff was monitored from July 2016 to October 2023 from three treatment sewersheds (Blenheim, Indian Springs, and Cooke-Glenmont) and a control sewershed (Beechwold) in the Clintonville neighborhood of Columbus. Differences in rainfall, hydrological, and water quality parameters were analyzed for 340-400 storm events spanning three separate phases of the Blueprint Columbus project (e.g., existing conditions [Pre-GI], following the installation of green infrastructure (GI) retrofits [i.e., bioretention cells, permeable pavements, and a constructed wetland; Post-GI], and after completion of additional infrastructure improvements [i.e., sump pumps, downspout disconnections, and sanitary sewer lateral lining; Post-AI²]). The overall goal of the Blueprint Columbus project was to decrease total suspended solids (TSS) loads by 20% and to “do no harm” in relation to other parameters (i.e., no increase in runoff volume from the sewersheds).

GI implementation did not significantly change runoff depths and peak flow rates in Cooke-Glenmont and Indian Springs. At the Blenheim sewershed, which was treated by the densest network of bioretention cells and a large constructed wetland (i.e., 90% of the sewershed area was treated), significant reductions in runoff depth and peak flow rate were observed post-GI. Post-AI², the additional infrastructure improvements added runoff to the storm sewer and reduced infiltration and inflow into the sanitary sewer. This resulted in a slight significant increase in runoff depth at Indian Springs, the sewershed that had the largest roof area draining to downspout redirections, indicating that the GI constructed in this area was not able to successfully mitigate the additional stormwater. For Blenheim and Cooke-Glenmont, no

significant difference in runoff response was observed post-AI² relative to the pre-GI period, suggesting that the overall effects of the four Blueprint pillars were negligible.

Significant changes in runoff quality were observed at the sewershed outlets between experimental phases. At Indian Springs, water quality post-GI was similar to pre-GI conditions; post-AI², loads for many metals increased and concentrations for many nutrients decreased relative to pre-GI. Notably, Indian Springs had a significant TSS load increase in the post-AI² phase relative to pre-GI. At Cooke-Glenmont, post-GI water quality improved for many pollutant loads and concentrations, most notably a TSS load decrease, suggesting that the GI was effectively sequestering pollutants. These significant improvements were mostly lost in the post-AI² phase due to the introduction of additional stormwater, reducing the effectiveness of the GI due to (presumed) increases in bypass or overflow. Concentrations of many pollutants, including TSS, increased post-GI at Blenheim, likely due to the addition of the Park of Roses constructed wetland which treated low flows. Post-GI water quality improvements relative to pre-GI were often absent in the post-AI² phase. For Blenheim, significant TSS load reductions were observed both in the post-GI and post-AI² phases, indicating that the City's TSS reduction goals were met in two of the three treatment sewersheds.

Summary of significant ($p < 0.05$) increases (↑) and decreases (↓) of hydrological and water quality parameters within each sewershed. ANCOVAs were used to compare pre-GI to post-GI values and pre-GI to post-AI² values. Dashes or parameters not mentioned coincide with no significant changes in the treatment compared to the same time period in the control sewershed.

Sewershed	Runoff Depth		Normalized Peak Flow Rate		Runoff Coefficient		TSS		Nutrients		Metals	
	Pre-GI to Post-GI	Pre-GI to Post-AI ²	Pre-GI to Post-GI	Pre-GI to Post-AI ²	Pre-GI to Post-GI	Pre-GI to Post-AI ²	Pre-GI to Post-GI	Pre-GI to Post-AI ²	Pre-GI to Post-GI	Pre-GI to Post-AI ²	Pre-GI to Post-GI	Pre-GI to Post-AI ²
Indian Springs	-	↑	-	-	↑	-	-	Load: ↑	Conc: OP ↓ TAN ↓ Load: OP ↓	Conc: OP ↓ TAN ↓ TP ↓ Load: NO ₂₋₃ ↓ OP ↓ PBP ↑ TAN ↓	-	Conc: Cu ↑ Load: Cd ↑ Cu ↑ Pb ↑
Cooke-Glenmont	-	-	-	-	-	-	Conc: ↓ Load: ↓	-	Conc: PBP ↓ TAN ↓ TN ↑ TP ↓ Load: TN ↓ TP ↓	Conc: OP ↑ Load: OP ↑ TK ↑	Conc: Cr ↓ Cu ↓ Ni ↑ Load: Cd ↓ Cr ↓ Cu ↓ Zn ↑	Load: Cd ↑
Blenheim Glencoe	↓	-	↓	-	↓	↓	Conc: ↑ Load: ↓	Load: ↓	Conc: OP ↓ PBP ↑ TAN ↑ TN ↑ TN ↑ Load: PBP ↓ TAN ↓ TKN ↓	Load: PBP ↓ TKN ↓ TP ↓	Conc: Cr ↑ Cu ↑ Load: Cr ↓ Cu ↓ Ni ↓ Pb ↓ Zn ↓	Conc: Cr ↓

Introduction

Urbanization results in the construction of impervious surfaces, mass grading, soil compaction, and removal of vegetative cover, reducing the combined effects of canopy interception, evapotranspiration, and infiltration in a watershed (Shuster et al. 2005). The consequence is increased stormwater runoff volumes traveling faster over hardened impervious surfaces, leading to instability in receiving streams, bed and bank erosion, loss of in-stream habitat, and imbalances in sediment transport (Walsh et al. 2005; Violin et al. 2011; Tillinghast et al. 2011; ten Veldhuis and Schleiss 2017). Furthermore, these increased volumes of stormwater runoff often carry higher pollutant loads from urbanized areas than other land uses (Line and White 2007; Line and White 2015; Chen et al. 2016). The severity of impacts to receiving streams varies and is dependent on the percentage of imperviousness in the watershed, topography, soils, vegetation, and other local factors (Bell et al. 2016).

To ameliorate some of these impacts, engineers design stormwater control measures (SCMs) such as bioretention and permeable pavement to detain, retain, infiltrate, and evapotranspire stormwater, reducing the rate and volume of flow discharged to receiving streams (Moore et al. 2017). These SCMs are central to Low Impact Development (LID) strategies, which aim to mimic pre-development hydrology more closely (Dietz 2007). Recent studies in Ohio have shown that bioretention and permeable pavement can substantially reduce runoff volumes even when constructed in clay soils (Winston et al. 2016b; Winston et al. 2018; Tirpak et al. 2021). Additionally, these SCMs often employ sedimentation, filtration, adsorption, and biological processes to sequester or remove pollutants from stormwater (Davis et al. 2009; Winston et al. 2016a). Many studies of single SCMs have shown that if designed, installed, and

maintained adequately, they function to reduce pollutant load to receiving streams, helping to meet total maximum daily load (TMDL) goals and reduce stream impairment.

A growing body of literature supports the use of LID with distributed SCMs in greenfield developments (Dietz and Clausen 2008; Line et al. 2012; Wilson et al. 2014). However, installing green infrastructure (GI) as part of new developments is substantially simpler, cheaper, and more effective than retrofitting GI into existing developments, where open space is limited and existing utilities abound. Modeling studies have shown that minor to vast differences in runoff reduction (10-70%) may be achieved when retrofitting SCMs depending on SCM type and scale of implementation (Wright et al. 2016). Field studies of retrofitted networks of SCMs in the municipal right-of-way support these findings (e.g., Page et al. 2015a, 2015b); however, more research is needed to quantify how targeted GI retrofits affect sewershed-scale hydrology and water quality. The goal of this research was to quantify the holistic impacts of GI implementation in the Clintonville neighborhood of Columbus, Ohio, as part of the Blueprint Columbus project. This report documents findings related to stormwater hydrology and water quality following the implementation of (1) SCMs and (2) other infrastructure improvements in the neighborhood by the City of Columbus.

Project Overview

Much of the City of Columbus has separated sewer systems. Sanitary sewer overflows (SSOs) remain a concern due to infiltration and inflow from leaky sewer pipes and porous utility trenches, causing capacity exceedance during rain events. In 2016, 127 SSO discharge events occurred across the remaining 34 SSO outfalls in Columbus (City of Columbus 2017a). These represent a significant public health risk (Liao et al. 2016) and the City of Columbus is under a United States EPA consent decree to eliminate SSOs and combined sewer overflows (CSOs)

within its boundaries. The City of Columbus responded by creating an infrastructure plan centered around SSO control while concurrently creating potential co-benefits (e.g., urban habitat, stormwater control, air quality, carbon sequestration, housing values, and beautification) provided by green infrastructure (GI) (Bolund and Hunhammar 1999; Arcadis 2015). The resulting multi-pronged Blueprint Columbus project includes the implementation of GI stormwater control measures (SCMs; bioretention, permeable pavement, and a constructed wetland), lining of sewer laterals, disconnection of roof downspouts to SCMs, and a voluntary sump pump program (Figure 1). It represents an unprecedented effort by the City of Columbus to retrofit a network of GI and improve grey infrastructure across the city to address numerous goals. This report details the findings based on a multi-year monitoring campaign to evaluate the benefits of Blueprint Columbus retrofits in Clintonville on runoff quantity and quality (City of Columbus 2017b). This will inform future decisions about SSO control strategies, providing the city with data to produce a more accurate and comprehensive cost benefit analysis. It will also guide the expansion of Blueprint Columbus to fulfill USEPA consent decree requirements to reduce SSOs in neighborhoods beyond Clintonville.



Figure 1: Four pillars of the Blueprint Columbus project.

Methods

Description of Monitored Sewersheds

Four sewersheds in the Clintonville neighborhood of Columbus, Ohio were monitored from 2016-2023 to characterize runoff hydrology and water quality. There were very few preexisting SCMs to treat and dissipate stormwater within this neighborhood prior to the onset of the Blueprint Columbus project. The City of Columbus has installed GI, disconnected downspouts, installed sump pumps, and lined sewer laterals in an effort to prevent SSOs in the Blenheim (also referred to as Blenheim-Glencoe; BG), Cooke-Glenmont (CG), and Indian Springs (IS) portions of the neighborhood (Figure 1, Figure 2). Because the majority of the Beechwold (BW) area of the neighborhood was not retrofitted with GI (i.e., only 2.2% of the watershed is treated by GI), it served as the control for the experiment. In 2019, monitoring commenced in two additional sewersheds in Clintonville, Whetstone (WH) and Starrett (ST), selected based on their proximity to the original four sewersheds and since they had no

preexisting stormwater controls. In addition, monitoring was conducted at a constructed wetland (Blenheim wetland), which was completed in late 2019; low flows from a portion of the Blenheim sewershed are shunted to this wetland for treatment using an in-sewer weir. Water quality and hydrology data for Blenheim accounted for flows from the wetland outlet data starting in 2020.



Figure 2: Boundaries of the six sewersheds monitored in this study. Distribution of bioretention cells (BRCs), monitoring locations, and land use within each sewershed are also shown. The remaining area within each sewershed not identified as commercial or institutional is residential.

Except for commercial and institutional land uses, Clintonville is a primarily residential neighborhood developed between 1910 and 1950. Six glacial ravines run east to west through Clintonville and eventually convey stormwater to the Olentangy River. Clintonville is drained with a system of separated storm sewers which generally outfall to the ravines. The CG, BG, and IS sewersheds drain to Overbrook ravine while the BW sewershed drains to the Beechwold ravine. ST and WH both discharge directly to the Olentangy River. The soils in the sewersheds are primarily mapped as silt loams in the Cardington and Bennington soil series. While the development patterns differ to some extent (Figure 15 to Figure 20), the neighborhood consists primarily of small lot, single family residential land use (Table 1).

Table 1: Land use and percent imperviousness (% Imp) in the six monitored sewersheds in Clintonville.

Sewershed	Area (ac)	% Imp	Land Use (ac)			Land Use (%)		
			Resid.	Comm.	Instit.	Resid.	Comm.	Instit.
BW	275.5	38.2	263.6	10.0	2.0	95.7	3.6	0.7
BG	151.4	44.5	134.2	7.4	9.9	88.6	4.9	6.5
CG	28.5	30.9	28.5	0	0	100	0	0
IS	118	40.3	89.3	9.0	20.5	75.0	7.6	17.4
ST	55	34.7	55	0	0	100	0	0
WH	56	35.3	46	0	10	82.1	0	17.9

Note: Residential, commercial, and institutional land use denoted as “Resid.”, “Comm.”, and “Instit.”, respectively.

Imperviousness within the six monitored sewersheds ranged from a minimum of 30.9% (Cooke-Glenmont; see Figure 17 in Appendix A) to a maximum of 44.6% (Blenheim; see Figure 18 in Appendix A) (Table 1). Roofs, roads, and driveways represented most of the impervious cover in all sewersheds. In each of the sewersheds, rooftops comprised approximately 40% of the total impervious area (TIA), while roads and driveways represented 20-30% and 15-25% of TIA, respectively.

The three treatment sewersheds had differing levels of GI implementation which facilitated comparisons of how GI density affects runoff quantity and quality at the sewershed

scale (Table 2). Because establishment of the Whetstone and Starrett monitoring locations occurred after GI implementation in the treatment sewersheds commenced, they were excluded from all pre- versus post-retrofit performance analyses (i.e., only the Beechwold sewershed was used as a control in this experiment). For reference, select hydrologic data collected from Whetstone and Starrett are summarized in Appendix B.

Table 2: Monitored Blueprint sewersheds and the number of implemented SCMs for each pillar of the Blueprint project as of December 2023. Note: monitored sewersheds are not equivalent to the complete project areas designated by the City of Columbus, particularly for Cooke-Glenmont where many infrastructure improvements were completed outside of the monitored sewershed.

	Blenheim	Cooke Glenmont	Indian Springs
% Sewershed Imperviousness	44.5	30.9	40.3
Sewershed Area (ac)	151.4	28.5	118.0
Number of homes	1251	139	549
Green Infrastructure Improvements			
# of BRCs	163	3	32
# of PP streets (acres)	0 (0)	0 (0)	6 (1.48)
# constructed wetlands (acres)	1 (0.52)	0	0
% of sewershed treated by GI	44, 90*	31	22
Additional Infrastructure Improvements			
Downspouts redirected (acres of redirected rooftops)	233 (2.57)	68 (2.44)	232 (5.17)
% of homes with disconnected downspouts	18.6	48.9	42.3
# Sump pumps installed	179	65	234
% of homes with sump pumps	14.3	46.8	42.6
# Lateral lining completed (# of homes)	688	78	284
% of homes with lateral lining	55.0	56.1	51.7

*GI in BG treated 44% of the sewershed; the addition of the constructed wetland increased the total sewershed area treated by GI to 90%

Project Timelines

Each sewershed was monitored during a pre-retrofit phase to establish baseline hydrologic response and runoff quality (referred to as the “Pre-GI” period; Figure 3). The infrastructure improvements of Blueprint Columbus were then implemented in a rolling fashion throughout the three monitored sewersheds. Generally, GI was constructed in the sewersheds, followed by sanitary sewer lateral lining and downspout redirections. The sump pump installation phase occurred over the longest period in each sewershed (approximately 3 years). To ensure the largest possible data sets for comparison, the period wherein GI was constructed and the other infrastructure improvements were being built is referred to as the “Post-GI” phase (Figure 3). In early 2020, the constructed wetland at Park of Roses was completed, receiving the low flows from the BG sewershed. Following GI retrofits, between 22% and 90% of the treatment sewersheds were treated by GI. By the end of 2019, the four pillars of Blueprint were completed in Indian Springs; the same threshold was reached in Cooke-Glenmont in 2020 and Blenheim in late 2021. The monitoring period following the completion of all infrastructure improvements associated with Blueprint Columbus was referred to as the “Post-AI²” phase.

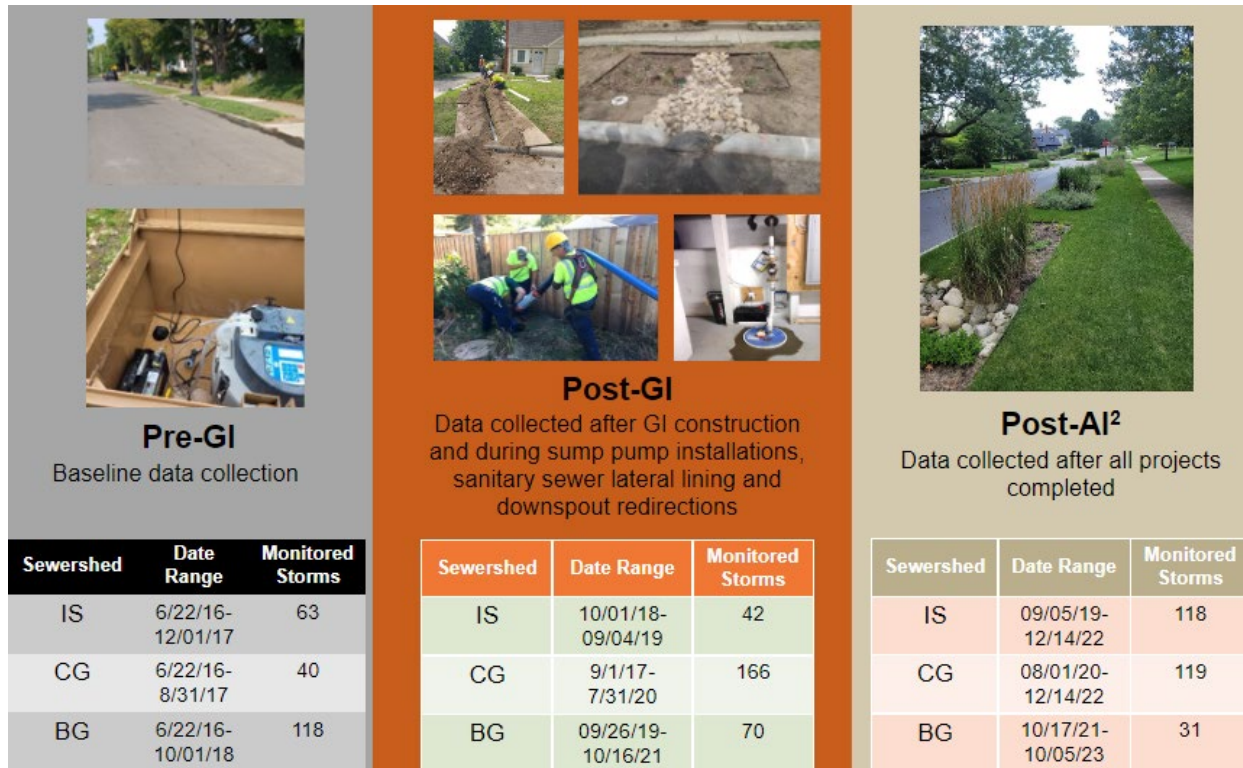


Figure 3: The Blueprint Columbus project was implemented between 2017 and 2021 but construction did not occur uniformly across the three treatment sewersheds. These improvements included GI, sump pump installations, sanitary sewer lateral lining, and home downspout redirections. The resulting analysis periods and number of monitored storms within each period are included for each treatment sewershed.

Data Collection

Rain gauge clusters, consisting of a 0.01-inch resolution tipping bucket and a manual gauge, were installed on a 6-ft post in an area free from overhead obstructions. A rain gauge cluster was installed in each monitored sewershed to collect rainfall data at 1-min intervals (Figure 4). Automated sampling equipment was used to monitor runoff hydrology and quality at the outfall of each sewershed. ISCO 750 area velocity meters (Teledyne ISCO, Lincoln, NE) were installed at the outfall of each sewershed and the inlet and outlet of the Blenheim wetland and measured velocity and depth of flow which, along with the known cross-section of the outfall, were used to determine flow rate on 1-minute intervals (Figure 4). ISCO 6712 and 3700 series samplers were used to collect runoff volume-proportional, composite stormflow samples

from each monitoring location. Sample aliquots collected during a storm event were composited into 18.9L containers, thus characterizing pollutant event mean concentrations (EMC). All composite samples were composed of a minimum of five and a maximum of 50, 350 mL aliquots describing greater than 80% of the pollutograph (U.S. EPA 2002). All samples were collected within 24 hours of the cessation of rainfall. Data were collected during the 87-month period between June 2016 to October 2023; data collection was discontinued between mid-December and mid-March in each year to prevent damage to monitoring equipment and/or collection of unreliable data due to winter weather conditions.



Figure 4: Rain gage cluster (left), sample intake (clear plastic) and area velocity meter (black) in the Cooke-Glenmont outfall (center), and automated sampler at Beechwold (right).

Laboratory Methods

Following the cessation of rainfall, each monitoring location was visited in succession to obtain samples and transport them to the City of Columbus laboratory for analysis, an approximately 4-hour effort. Composite samples collected in each ISCO were shaken vigorously to resuspend solids and were then subsampled into laboratory sample bottles for analysis of nutrients, metals, total suspended solids (TSS), and microbial contaminants (e.g., *E. coli*), among other pollutants. These constituents as well as corresponding preservation methods and method detection limits (MDLs) are presented in Table 13 in Appendix F. All water quality samples were immediately placed on ice and chilled to less than 4°C during transit to the City of Columbus laboratory, located approximately 10 miles from the sampling sites.

In addition to regular sampling, quarterly samples were collected and analyzed for chemical oxygen demand (COD), biochemical oxygen demand (BOD), and carbonaceous biochemical oxygen demand (cBOD) to meet National Pollutant Discharge Elimination System (NPDES) permit requirements for the City of Columbus. Quarterly grab samples of runoff were also collected for cyanide and oil and grease analysis. Quarterly spot measurements of runoff temperature and dissolved oxygen were also made using a YSI Pro 1020 instrument (YSI Incorporated, Yellow Springs, OH). Grab samples, runoff temperature, and dissolved oxygen measurements were obtained during the first two hours of a qualifying NPDES storm event once per quarter.

Data Analysis

Qualifying storm events were separated using the following criteria: a minimum antecedent dry period (ADP) of six hours and a minimum rainfall depth of 0.1 inches. Summary statistics for each rainfall event were calculated, including depth (in), duration (hrs), average intensity (in/hr), peak intensity (maximum over any 5-minute duration, in/hr), and ADP (days). Runoff volume was determined by integrating under the hydrograph, while peak flow rate was determined as the instantaneous 1-minute maximum flow rate that occurred during the flow duration. Runoff volume and peak flow rate were then normalized by sewershed area to allow for direct comparison between the sewersheds. Runoff and rainfall depth were separately summed across all qualifying hydrologic events (i.e., observed, pairable events between the treatment and control sewershed); the quotient of these metrics results in the runoff coefficient (C_R) for the sewershed. The timing of the beginning, peak, and end of runoff was utilized to determine the runoff duration and time to peak for each event. Following the completion of construction in

2019, flow from the Blenheim sewershed was comprised of flow measured at that outfall and the outlet of the wetland.

Beginning in 2020, reported concentration data for Blenheim was calculated by as the flow weighted average of runoff concentrations at Blenheim and the wetland outlet. In the event of missing hydrology data for either site, the median ratio of runoff for the two monitoring sites was used to estimate volume-weighted pollutant concentrations. For all sites, a value of one-half the detection limit was substituted for EMCs below the MDL (Antweiler and Taylor 2008).

Several data quality assurance procedures were implemented to remove erroneous data influenced by equipment malfunction or laboratory error. For example, data corresponding to storms with erroneous measurements from area velocity sensors (identified as instances where the recorded time of velocity measurements did not match the occurrence of rainfall, likely due to water main breaks or other non-rainfall sources of flow in the sewershed) were removed from the dataset prior to analysis. Similarly, pollutant concentrations associated with potential contamination or laboratory errors (identified in instances where concentrations were several orders of magnitude higher than values typically found in urban runoff) were removed from the dataset prior to analysis.

Pollutant loads at each monitoring location were determined as the product of pollutant EMC and runoff volume on a storm-by-storm basis. Area normalized pollutant loads (lb/ac) were calculated as quotient of pollutant load to sewershed area. Beginning in 2020, reported load data for Blenheim were presented as the total load from the wetland outlet and the Blenheim outfall. Summary statistics (i.e., range, mean, median, and standard deviation) for pollutant concentrations and loads were developed for each monitored outfall for each phase of the experiment.

Hydrology and water quality data were log transformed to satisfy requirements of statistical tests. Analysis of covariance (ANCOVA) was used to identify differences in runoff hydrology or water quality between pre-GI and post-GI phases and pre-GI and post-AI² phases. A visual overview of this process is shown below in Figure 5. This method controls for seasonal, temporal, and other variability by using a control sewershed and allows for confidence in the conclusion that observed changes in a given parameter were specifically due to Blueprint Columbus-related modifications to the sewershed. Percent changes in pollutant concentration and load were calculated and reported using results of least squares means (LSM) analysis and the following equation:

$$Change (\%) = \left(\frac{10^{u_T}}{10^{u_C}} - 1 \right) \times 100$$

where u_T is the control-treatment LSM during the post-AI² phase and u_C is the control-treatment LSM during the pre-GI phase. Following results of statistical testing (which revealed no significant differences between phases pre-GI and GI construction phases in Cooke-Glenmont and Blenheim), rainfall, hydrology, and water quality data collected during these phases in Cooke-Glenmont and Blenheim were combined to increase the sample size and bolster the strength of statistical testing. Water quality data collected from each treatment sewershed were paired with samples collected from the control sewershed, and summaries of minimum, median, interquartile range, and maximum values were generated separately for treatment and control data.

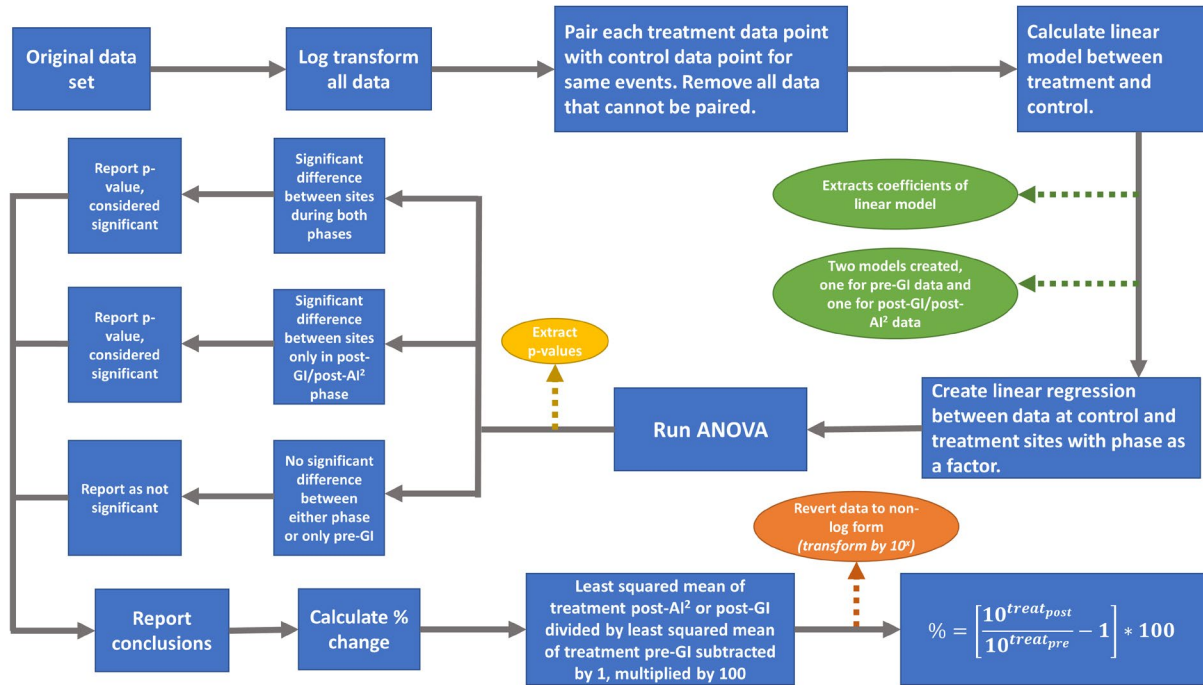


Figure 5: Overview of ANOVA/ANCOVA statistical analysis and data preparation for water quality data.

All data analysis was completed using R statistical software version 4.2.2 (R Core Team 2023). Except where noted, a criterion of 95% confidence ($\alpha=0.05$) was used to determine statistically significant results.

Results

Hydrology

Observed Rainfall Events

Between 346 and 401 rainfall events were monitored in the four sewersheds during the 87-month period from June 2016 – October 2023. The average rainfall depth for all events in the sewersheds ranged from 0.32-0.44 inches, while median rainfall depth for qualifying hydrologic events ranged from 0.45-0.47 inches. Rainfall depth, average rainfall intensity, and ADP did not significantly differ across project periods for any of the monitored sewersheds. Significant differences in peak rainfall intensities across project phases were observed; higher peak

intensities were observed during the post- AI^2 phase in each sewershed (Table 3). The seasonal distribution of storm events and the timeline for each project period (Figure 3) may be responsible for the observed increase in peak intensities. In previous analysis of rainfall characteristics within Columbus, Ohio, peak rainfall intensities were generally greater in the summer than in fall and spring, and average rainfall intensities were generally greater in summer than in fall (Smith et al. 2020). This is likely due to convective thunderstorms that frequently occur in the Columbus area during the summer season (Fritsch et al. 1986).

Table 3: Rainfall characteristics from all monitored events in the treatment sewersheds by project period. Significant differences in rainfall characteristics compared to the Pre-GI period are shown in italics.

	Blenheim-Glencoe			Cooke-Glenmont			Indian Springs		
	Pre-GI	Post-GI	Post-AI ²	Pre-GI	Post-GI	Post-AI ²	Pre-GI	Post-GI	Post-AI ²
Number of Monitored Events	140	156	109	70	185	144	86	50	210
Total Precipitation (in)	90.6	77.9	65.5	39.0	110.6	82.2	49.6	29.1	117.0
Median Rainfall Depth (in)	0.44	0.35	0.32	0.37	0.38	0.39	0.38	0.45	0.34
Median Peak Intensity (in/hr)	0.80	0.84	<i>0.96</i>	0.84	0.72	<i>0.93</i>	0.54	0.54	<i>0.78</i>
Median ADP (d)	3.1	2.6	3.4	3.3	3.0	2.8	3.2	3.2	2.9
Median Average Intensity (in/hr)	0.09	0.08	0.08	0.10	0.07	0.08	0.08	0.07	0.08
Number of Storm Events >0.75 in	35	30	30	18	45	35	22	12	26
90 th Percentile Storm Depth (in)	1.54	1.26	1.50	1.41	1.28	1.26	<i>1.49</i>	1.10	1.26

Runoff Depth

Runoff depths were not significantly different between the pre-GI and post-GI phases at CG and IS compared to runoff depths at the control (Table 4, Figure 6). Past research has attributed runoff volume reductions to BRC design parameters such as media infiltration rates, surface storage volumes, and inclusion of internal water storage zones (Brown and Hunt 2011; Hunt et al. 2012; Winston et al. 2016). The total storage volume added to each sewershed following the construction of GI varied, ranging from approximately 3160 ft³ in IS to approximately 6640 ft³ in CG. Total storage in IS was equivalent to a runoff depth of just 0.007 inches, while storage provided by the BRCs in CG was equal to approximately 0.06 inches of runoff (Table 1). The BRCs implemented in Clintonville had perforated underdrains that did not have upturned elbows or other devices to promote internal water storage, thus limiting the retention time. Limited surface and subsurface storage along with the high infiltration rates observed via simulated storm events (see *Case Study: Simulated Storm Testing*) indicate the BRCs were primarily functioning as filters with limited retention time. Due to the “no net change” goal of the Blueprint Columbus project and the strategies used to design the BRCs, these results are not necessarily surprising nor are they in conflict with desired project outcomes. Should future iterations of the Blueprint Columbus project desire to have larger runoff reduction benefits, changes to the GI design (e.g., creation of internal water storage zone, increased bowl volumes, decreased saturated conductivity of media blends) which increase storage and prolonged retention times should be considered.

Runoff depths in IS significantly increased ($p < 0.004$) between the pre-GI and post-AI² phases compared to the control sewershed (Table 4, Figure 6). The significant differences in regression slopes observed between the project phases at Indian Springs suggest changes in

runoff generation patterns occurred within the sewershed during the post-AI² phase that did not occur in the control. However, the mean runoff depth in the treatment sewershed was just 20% higher post-AI² compared to pre-GI period and, moreover, no discernable change in the median runoff depth in IS was observed between the project phases (Table 4). This was likely related to the additional volumes redirected to the outfall resulting from downspout disconnection, lateral lining, and sump pumps installed in the sewershed (Table 4). These additional infrastructure improvements represent increases to the directly connected impervious area (DCIA) in the sewershed. Unlike the control sewershed, where runoff from smaller events may be fully abstracted by pervious areas receiving flow from rooftops or leaking sanitary sewer laterals accepting stormwater, runoff from these areas (now DCIA in the treatment sewersheds) was directly routed into the storm sewer network due to the additional infrastructure improvements. LSM comparisons also increased in CG, however; these changes were not found to be statistically significant (Table 4). A higher percentage of the watershed was treated in CG (31% treated) compared to IS (22% treated), but when comparing the rooftop redirections in IS to CG, over twice the rooftop area was redirected in IS (Table 2). Despite the additional runoff routed to the outfall, runoff volume remained unchanged in CG between the pre-GI and post-AI² phases, likely attributable to the larger surface area and GI storage volumes in this sewershed. Thus, the larger, regional bioretention cells in CG appear to have provided better mitigation of increased stormwater volumes compared to the smaller BRCs implemented in IS.

Table 4: Summary statistics and ANCOVA results for comparisons of runoff depth (in) between treatment and control sewersheds. Statistically significant changes in LSM compared to pre-GI phase are denoted in bold ($p < 0.05$) and underlined ($p < 0.10$), indicating differences in runoff generation patterns in the treatment sewersheds compared to the control during the same period.

	Indian Springs			Cooke-Glenmont			Blenheim		
	<i>Pre-GI</i> (<i>n=56</i>)	<i>Post-GI</i> (<i>n=39</i>)	<i>Post-AP²</i> (<i>n=131</i>)	<i>Pre-GI</i> (<i>n=40</i>)	<i>Post-GI</i> (<i>n=147</i>)	<i>Post-AP²</i> (<i>n=111</i>)	<i>Pre-GI</i> (<i>n=106</i>)	<i>Post-GI</i> (<i>n=64</i>)	<i>Post-AP²</i> (<i>n=45</i>)
Mean Runoff Depth (in)	0.20	0.21	0.24	0.16	0.16	<u>0.23</u>	0.19	0.07	0.10
Median Runoff Depth (in)	0.12	0.13	0.12	0.08	0.07	0.08	0.10	0.04	0.07
Mean (Median) Percent Difference	-	5% (8%)	20% (0%)	-	0% (-13%)	44% (0%)	-	-63% (-60%)	-47% (-30%)
Mean Normalized Peak Flow Rate (cfs/mi²)	104.2	<u>67.1</u>	<u>61.2</u>	114.6	49.8	117.0	69.6	15.8	58.1
Median Normalized Peak Flow Rate (cfs/mi²)	52.9	34.0	33.8	77.4	25.6	77.7	35.0	7.5	19.1
Mean (Median) Percent Difference	-	-36% (-36%)	-41% (-36%)	-	-57% (-67%)	2% (0.4%)	-	-54% (-79%)	-17% (-45%)
Mean Runoff Coefficient	0.38	0.50	0.42	0.34	0.36	0.36	0.36	0.09	0.16
Median Runoff Coefficient	0.26	0.29	0.25	0.16	0.16	0.21	0.19	0.09	0.13
Mean (Median) Percent Difference	-	32% (12%)	11% (-4%)	-	6% (0%)	6% (31%)	-	-75% (-53%)	-56% (-32%)

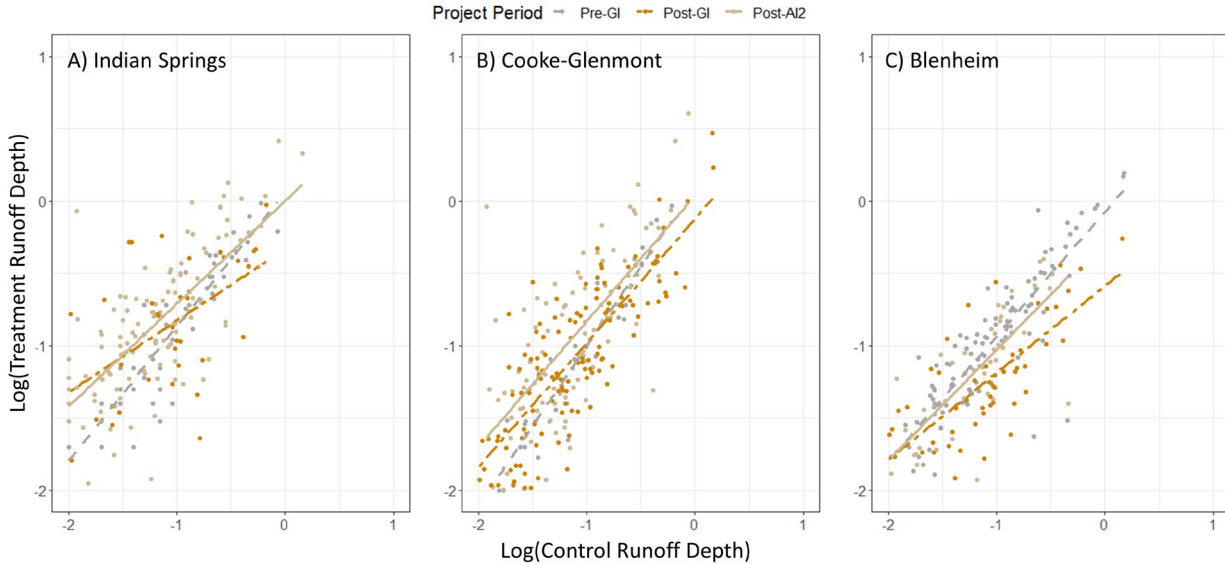


Figure 6: Relationships between runoff depth (in) for the treatment and control (Beechwood) sewersheds during the various project periods. Note: runoff depths are log transformed.

Unlike the other treatment sewersheds, regression slopes at BG decreased significantly ($p < 0.03$) between the pre-GI and post-GI phases (Figure 6). The most notable difference between BG and the other treatment sewersheds was the Park of Roses constructed wetland installed to treat low flows from much of the sewershed (Table 2). The wetland provided additional detention in the watershed but also greatly reduced runoff volumes during dry periods (e.g., late summer and autumn of 2022 and 2023). The reduction in runoff depths observed in BG during the post-GI period is likely attributable to the storage capacity of the constructed wetland. After completion of the additional infrastructure improvements, decreases in runoff depth were observed compared to pre-GI levels, however; these decreases were not significantly different when compared to the control sewershed. Thus, it can be concluded that the additional inflows from other infrastructure improvements were successfully mitigated by the constructed wetland and GI within the BG sewershed.

Runoff Coefficient

Median runoff coefficients for the BG sewershed significantly decreased by 0.06-0.10 between the pre-GI to post-GI and pre-GI to post-AI² phases (Figure 7; Table 4). This is likely due to the runoff volumes diverted to the Park of Roses constructed wetland in the post-GI and post-AI² phases, which substantially increased the storage in the sewershed. Runoff coefficients in the post-GI phase increased at IS ($p < 0.05$) and CG (not significant; Figure 7). Differences in placement of GI compared to outfall locations and GI design (e.g., lack of internal water storage) may explain this result, especially in the case of Indian Springs, where rainfall characteristics did not vary significantly across project periods (Ran et al. 2012; Table 3). Runoff coefficients in IS and CG did not significantly change following the installation of all Blueprint Columbus pillars (Table 4).

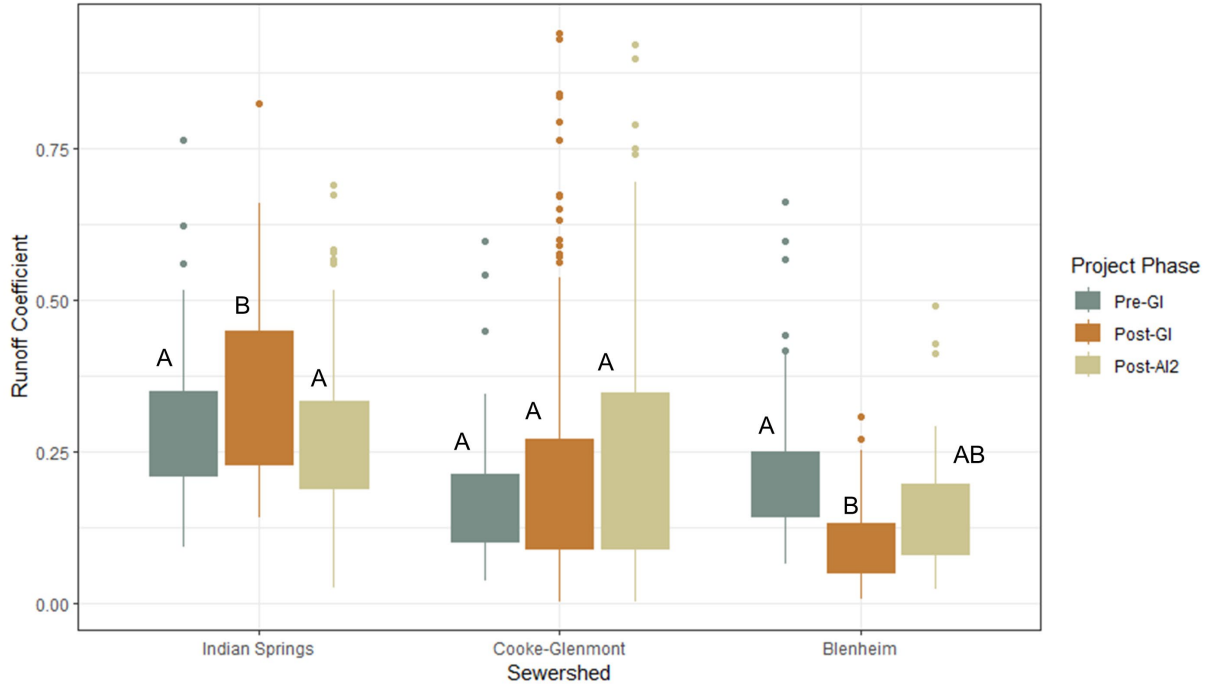


Figure 7: Distribution of runoff coefficients during storm events in each of the treatment sewersheds by project phase. Statistically significant differences between phases for each sewershed are indicated by different letters derived from Tukey post-Hoc tests.

Normalized Peak Flow Rate

Median normalized peak flow rates significantly decreased at Blenheim ($p < 0.002$) and Indian Springs ($p < 0.08$) during the post-GI phase (Table 4, Figure 8). While peak flow rates decreased in Cooke-Glenmont during the same period, the decreases were not significant when compared to the control sewershed. Hunt et al. (2012) reported that peak flow mitigation from individual bioretention cells was directly related to the amount of storage volume and infiltration rates of the practices. These critical aspects of bioretention cells are determined during the design phase based on objectives such as capturing runoff from a target storm event depth (in this case 0.75 inches). Because CG has the smallest sewershed area, the effects of travel time and soil storage on the hydrograph are less pronounced. Holding other factors constant, less mitigation of peak flow rates will occur as the area of the sewershed becomes smaller (Goodrich et al. 1997; Moody and Martin 2001).

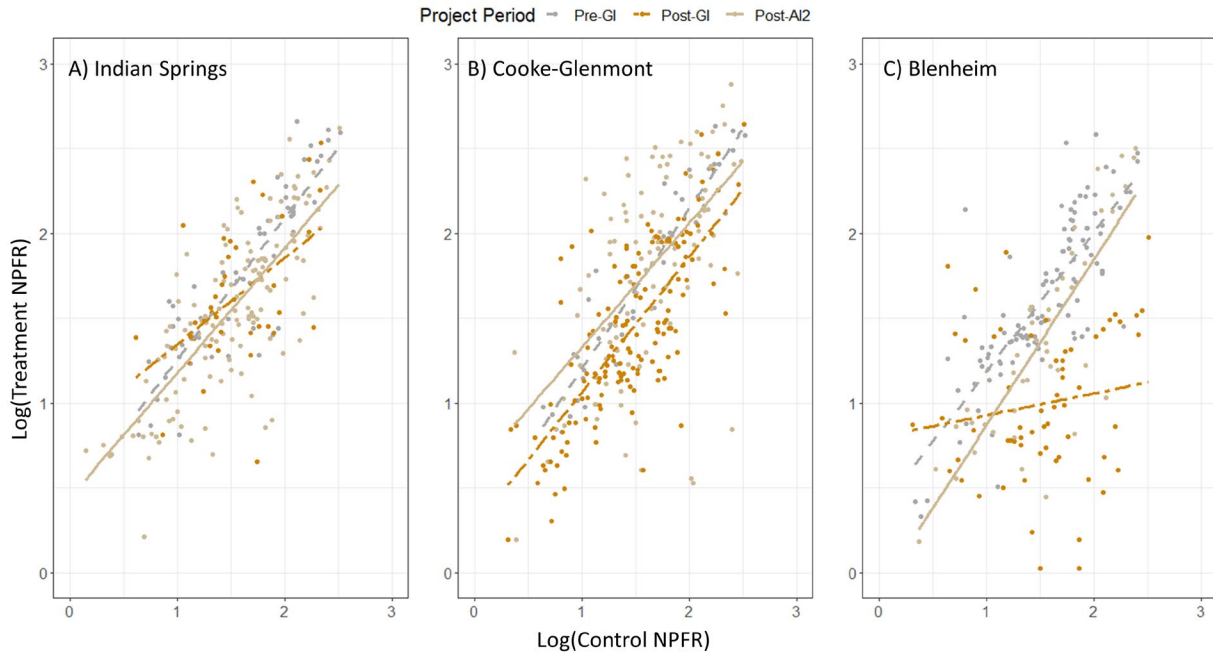


Figure 8: Area normalized peak flow rates (NPFR; cfs/mi²) by project phase observed in the treatment compared to the control (Beechwald) sewersheds. Note that data were log transformed.

The variability of the normalized peak flow rates increased following the completion of the four Blueprint Columbus pillars in the treatment sewersheds, likely due to the increase in DCIA in the sewersheds (Figure 8). Similarly, weaker linear relationships and larger standard deviations between the treatment and control sewersheds were observed in the post-AI² phases for each of the three treatment sewersheds. During the post-AI² phase, peak flows trended toward pre-GI levels in the Indian Springs and Blenheim sewersheds (Table 4, Figure 8). The higher intensity rain events observed during the post-AI² phase (Table 3) may have led to increased bypass of the bioretention cells, resulting in a portion of runoff conveyed directly into the storm sewer without treatment (similar to the condition of the sewersheds in the pre-GI phase). However, the very small magnitude change in peak runoff flow rates in the sewersheds indicates the post AI² effects of Blueprint Columbus were minimal.

Case Study: Simulated Storm Testing

Simulated storm tests were conducted to quantify bioretention cell performance under semi-controlled conditions. In total, 56 tests were conducted between 2018 and 2022 on 11 bioretention cells in three sewersheds in Clintonville (i.e., Cooke-Glenmont, Indian Springs, and Schreyer-Springs). Simulated storm testing procedures varied depending on the surface area of the bioretention cell. Bioretention cells with surface areas greater than 300 ft² required a fire hydrant, while those less than 300 ft² were tested using a 400-gallon tank. Flow from the tanks was measured using graduated buckets, while a mechanical flow meter was implemented on hydrant tests. A 2L pan was used to quantify outflow from the cells. Beginning in 2021, efforts focused on replicating testing for the previously tested bioretention cells and water quality performance by adding chemicals to influent water sources to simulate the quality of actual runoff.

Summary statistics from simulated storm testing completed in 2018-2021 are presented in Table 5. Data from simulated storm testing was analyzed based on year, project area, and BRC design (i.e., whether the cell was installed in the right-of-way (ROW) or as a curb bump-out which extended into the roadside parking area). The mean volume reduction for all tests was 69%; bump-out BRCs in Cooke-Glenmont yielded the highest mean volume and peak flow reductions (88% and 95%, respectively), while the lowest volume reductions (mean 56%) were observed at ROW-style BRCs in Schreyer-Springs.

Table 5: Summary statistics for simulated storm testing in 2018-2022.

Dataset (number of tests)	Volume Reduction (%)		Peak Flow Reduction (%)		Lag Time (min)	
	Mean	St. Dev.	Mean	St. Dev.	Mean	St. Dev.
All Tests (53)	69	26	76	19	8	4
Indian Springs BRCs (22)	66	26	67	15	7	2
Cooke-Glenmont BRCs (15)	88	7	95	3	9	3
Schreyer-Springs BRCs (17)	56	30	70	10	10	3
ROW BRCs (30)	54	24	64	16	9	3
Bump Out BRCs (24)	88	9	90	10	4	3

The project sewershed and BRC style (i.e., ROW versus Bump-Out), were the most positively significantly correlated to hydrologic performance ($r=0.56$ and $r=0.7$; Figure 9). Bump-out style BRCs provided larger volume (34%) and peak flow (26%) reductions than ROW-style BRCs. Similarly, larger BRCs provided greater hydrologic mitigation than smaller BRCs during testing. A possible explanation for the higher volume reductions observed from the bump-out BRCs is the proximity to subsurface infrastructure (e.g., utility lines, sanitary and storm sewers) which may provide preferential hydrologic pathways for water percolating through the BRCs that bypass the underdrain.

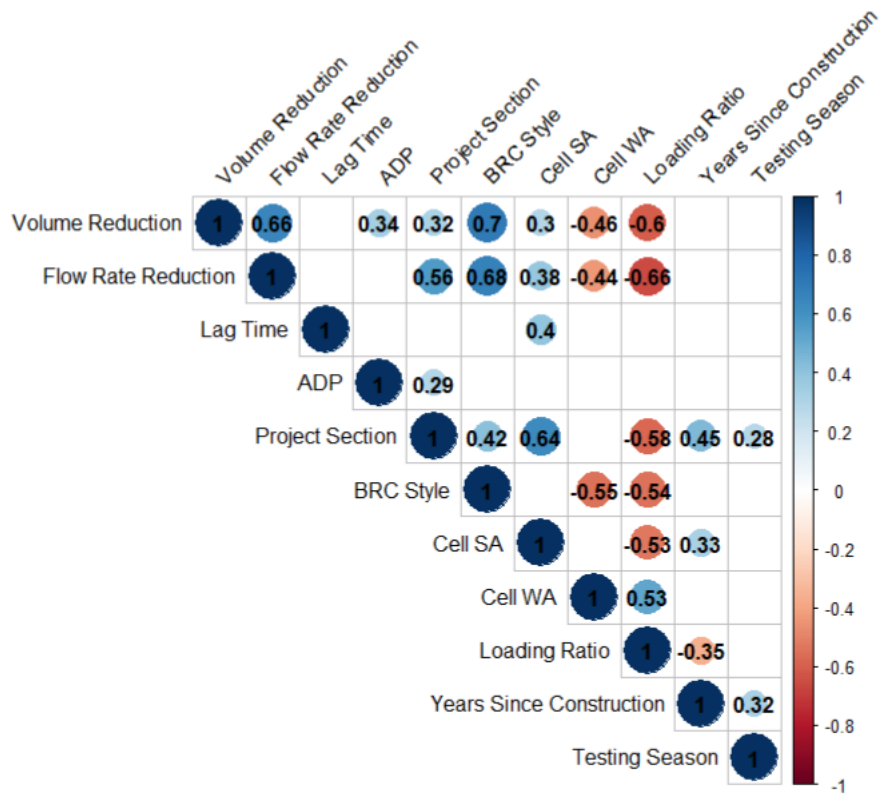


Figure 9: Pearson's correlation matrix of simulated storm testing data. Only statistically significant ($p < 0.05$) correlations are included. The larger numbers and circles correspond to more highly correlated results.

The contributing drainage area for a BRC was negatively correlated to its hydrologic response ($r = -0.46$; Figure 9). The drainage areas for the BRCs tested herein ranged from 0.3-3.28ac with a mean drainage area of 1.09 ac. Simulated testing revealed significantly lower hydrologic responses for cells with larger loading ratios (i.e., the ratio of drainage area to BRC surface area; $r = -0.66$; Figure 9). The largest loading ratio was observed for a ROW cell in IS (973:1) which produced mean volume reductions of 41% and mean peak flow reductions of 52%. In contrast, the smallest loading ratio was observed for a bump-out BRC in CG (29:1), which provided two-fold greater volume and peak flow reductions (89% and 95% respectively). Previous studies have observed decreases in GI performance when large loading ratios were used due to larger inflow volumes and an increased chance of media clogging (Shrestha et al. 2018;

Mahmoud et al. 2019). Because of these results, greater hydrologic benefits may be achieved if loading ratios are reduced in future iterations of the Blueprint Columbus project.

Water Quality

The following section contains a brief discussion of the main findings related to the water quality analysis based on data collected since 2016; the full suite of water quality data collected during the study are presented in Appendix C.

Nutrients

Significant reductions in nitrogen species concentrations between pre-GI and post-GI phases were observed only at CG for TAN (26.9% reduction) and at IS for TAN (12.1% reduction); significant increases in nitrogen concentrations between these same phases were observed at BG for TAN and TN (102.1% and 6.2%, respectively) and CG for TN (5.9%). Between these same phases, the only significant load changes occurred at BG for TAN and TKN (reductions of 73.5% and 54.3%, respectively) and CG for TN (55.6% reduction). Between pre-GI and post-AI², significant changes at IS were limited to concentrations of TAN and TN, which were reduced by 33.6% and 9.2%, respectively. Significant load changes at BG (38.5% TKN reduction) and IS (decreases in NO₂₋₃ and TKN loads of 6.1% and 12.6%, respectively) were also observed between these phases.

Significant changes in phosphorus species concentrations between pre-GI and post-GI phases were observed at BG (22.7% OP reduction; increases of 35.2% and 12.4% for PBP and TP, respectively), CG (reductions of 44.8% and 27.0% for PBP and TP, respectively), and IS (20.7% OP decrease). Between these same phases, load reductions were observed at BG for PBP (73.6%) and at CG for TP (17.6%). One significant load increase was observed at IS for OP in the post-GI phase (3.6%). Between pre-GI and post-AI², significant changes in concentrations of

phosphorus species were observed at IS for OP (36.4% decrease) and TP (18.0% decrease) and CG for OP (1.2% increase). Significant load changes were observed at BG (59.6% PBP and 61.4% TP reductions), CG (201.4% OP increase), and IS (18.7% OP reduction; 47.6% PBP increase) between these same phases. Boxplots for TN and TP are shown in Figure 10, while concentrations and loads of these pollutants at the treatment sites by project phase are shown in Table 6.

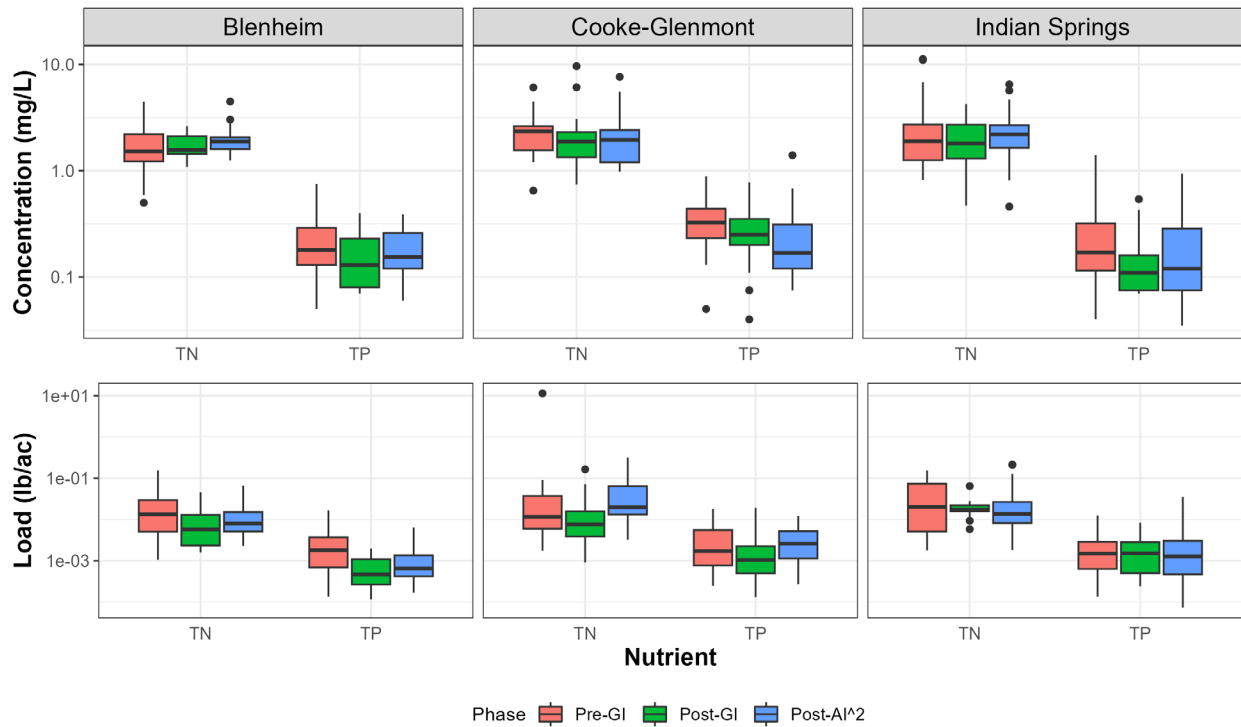


Figure 10: Boxplots of paired control-treatment concentrations and storm event loads for TN and TP by project phase.

Table 6: Summary statistics of paired control-treatment concentrations and storm event loads for TN and TP by project phase. Significant differences based on ANCOVA analyses indicated by red (increase) and green (decrease) text.

	Data Type	Pol.	Pre-GI		Post-GI				Post-AI ²			
			n	Med.	n	Med.	p-value	LSM % Diff.	n	Med.	p-value	LSM % Diff.
BG	Conc. (mg/L)	TN	35	1.52	17	1.57	6.81E-04	6.17	21	1.89	AOV not sig.	4.67
		TP	37	0.18	17	0.13	1.85E-10	12.38	20	0.16	AOV not sig.	-29.56
	Load (lb/ac)	TN	32	0.01	14	0.01	0.08	-46.73	20	0.01	0.10	-32.43
		TP	33	1.80E-03	14	4.86E-04	AOV not sig.	-66.82	20	6.52E-04	0.03	-61.36
CG	Conc. (mg/L)	TN	17	2.35	45	1.89	3.49E-03	5.85	25	1.95	0.06	-15.81
		TP	20	0.33	48	0.25	1.17E-03	-26.97	24	0.17	0.21	-33.12
	Load (lb/ac)	TN	15	0.01	44	0.01	2.39E-05	-55.55	19	0.02	0.53	117.69
		TP	16	1.73E-03	45	1.04E-03	0.01	-17.64	19	2.60E-03	0.92	122.67
IS	Conc. (mg/L)	TN	23	1.90	18	1.81	AOV not sig.	34.63	52	2.20	2.65E-03	-9.16
		TP	23	0.17	18	0.11	AOV not sig.	12.69	51	0.12	1.31E-03	-18.00
	Load (lb/ac)	TN	21	0.02	16	0.02	AOV not sig.	-8.22	45	0.01	0.71	22.42
		TP	20	1.49E-03	16	1.51E-03	AOV not sig.	-4.28	44	1.27E-03	0.10	28.05

Data from the International Stormwater BMP Database (ISBMPD) support the occurrence of nitrification in individual bioretention cells, and this was also observed at the sewershed scale herein (Clary & Jones 2016; Bedan & Clausen 2009; Page et al. 2015a). TAN concentrations and storm event loads generally decreased while NO₃ concentrations and storm event loads generally increased in the treatment sewersheds post-GI. However, TAN concentrations and loads did not universally decrease across the sites in the post-GI phase, indicating that establishment of microbial communities responsible for nitrogen cycling may still have been taking place. It was expected that concentrations and loads of TAN and NO₂₋₃ would decline with establishment of plant roots and microbial communities in bioretention cells in the post-AI² phase (Hopkinson & Giblin, 2008). The decrease of TAN and NO₂₋₃ concentrations and

loads in the post-AI² phase indicated the maturation of soil systems in the GI which support nitrogen cycling processes.

Particulate TKN removal has been shown to occur in bioretention and permeable pavement primarily through sedimentation and filtration processes (Li & Davis, 2014; Winston et al. 2016a). Decreased TKN loads and concentrations have been attributed to decreased mineralization processes in soils and immobilization of organic nitrogen from mulch and other woody materials (Lynn et al. 2015; Mullane et al. 2015).

TP reductions observed across phases at CG, BG, and IS were likely due to sedimentation of particulate phosphorus in bioretention in the sewersheds (Hsieh & Davis, 2005; Roy-Poirier et al. 2010). Studies generally report a net export of OP within bioretention, with median influent and effluent concentrations of 0.02 to 0.27 mg/L, respectively, reported in the ISBMPD (Clary & Jones, 2016). Increases in OP concentrations have also been attributed to decomposition and leaching of organic matter in bioretention (Passeport et al. 2009). Increased OP loads were observed at CG and IS across phases. Leaching of organic matter from bioretention media is expected to decrease over time, which may explain why OP concentrations and loads at IS were not elevated in the post-AI² phase.

Metals

Runoff pollutant concentrations and loads for three metals of interest (i.e., Cu, Pb, Zn) are presented in Figure 11 and Table 7. Significant changes in heavy metal concentrations between pre-GI and post-GI phases were mixed at BG (Cr 51.0% increase and Cu 19.2% increase) and CG (Cr 14.7% and Cu 11.3% decreases; Ni 30.7% increase). Post GI loads decreased at BG for Cr (623%), Cu (54.7%), Ni (45.2%), Pb (63.2%), and Zn (63.6%), and at CG for Cd (40.4%), Cr (26.0%), and Cu (29.7%). Zn loads increased in the post-GI phase at CG

by 6.0%. In the post-AI² phase, significant changes to metal concentrations were limited to BG (Cr 1.9% decrease) and IS (Cu 8.4% increase). Load increases in metals in the post-AI² phase were detected at CG (Cd 109.3%) and IS (Cd 66.5%, Cu 51.1%, Pb 35.6%).

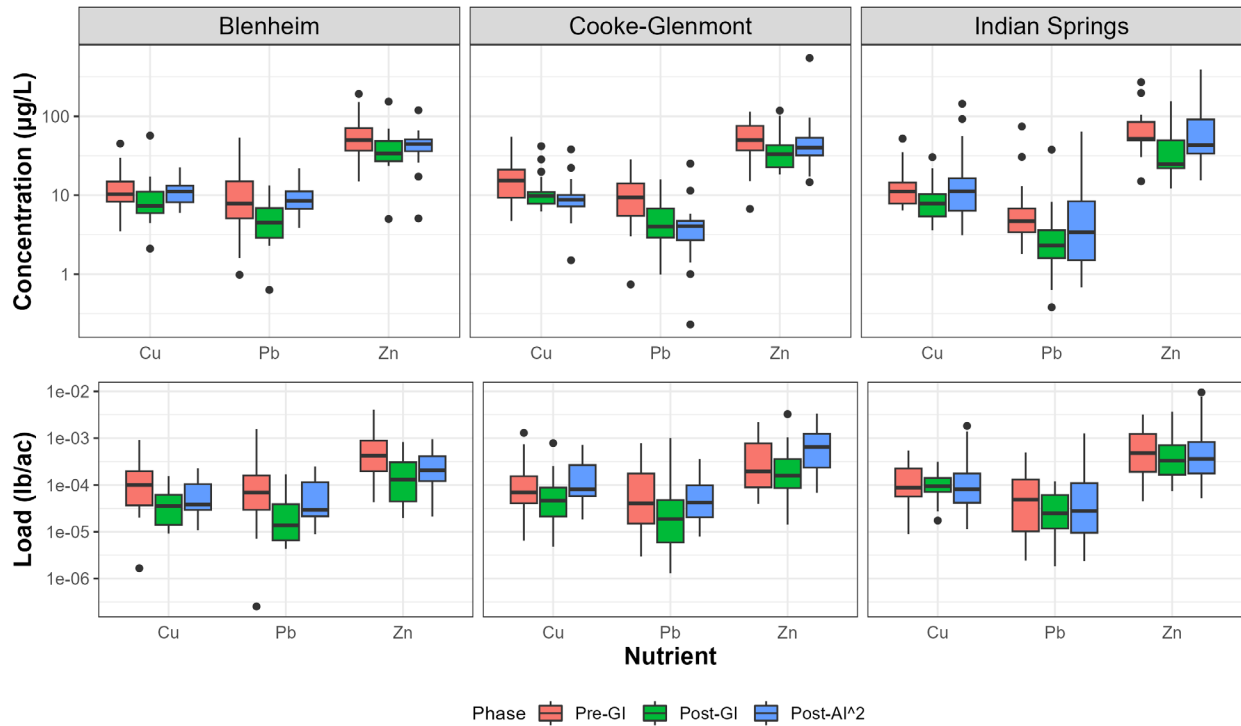


Figure 11: Boxplots for paired control-treatment concentrations and storm event loads for Cu, Pb, and Zn by project phase.

Table 7: Summary statistics for paired control-treatment concentrations and storm event loads for Cu, Pb, and Zn by project phase. Significant differences based on ANCOVA analyses indicated by red (increase) and green (decrease) text.

	Data Type	Pol.	Pre-GI		Post-GI				Post-AI ²			
			n	Med.	n	Med.	p-value	LSM % Diff.	n	Med.	p-value	LSM % Diff.
BG	Conc. (µg/L)	Cu	37	10.30	17	7.33	6.29E-04	19.21	20	11.13	AOV not sig.	-5.84
		Pb	37	7.80	17	4.50	AOV not sig.	71.26	20	8.50	AOV not sig.	-6.15
		Zn	37	50.00	17	33.65	AOV not sig.	6.58	19	44.55	AOV not sig.	-31.59
	Load (lb/ac)	Cu	33	9.98E-05	14	3.56E-05	0.02	-53.77	20	3.84E-05	0.48	-39.30
		Pb	33	6.90E-05	14	1.48E-05	0.03	-63.24	20	2.96E-05	0.42	-38.92
		Zn	33	4.23E-04	14	1.36E-04	0.03	-63.63	19	2.04E-04	0.15	-57.66
CG	Conc. (µg/L)	Cu	19	15.35	47	9.80	7.34E-06	-11.34	24	8.75	AOV not sig.	-39.87
		Pb	19	9.40	47	4.00	0.22	-16.20	24	4.05	AOV not sig.	-46.59
		Zn	19	50.00	47	33.10	0.44	-2.64	24	40.05	0.47	24.36
	Load (lb/ac)	Cu	16	6.95E-05	44	4.63E-05	0.02	-29.69	19	8.11E-05	AOV not sig.	124.35
		Pb	16	4.04E-05	44	1.88E-05	0.35	-39.07	19	4.21E-05	0.26	112.84
		Zn	16	1.95E-04	44	1.58E-04	0.01	5.96	19	6.47E-04	0.54	306.57
IS	Conc. (µg/L)	Cu	22	11.15	17	7.80	0.48	28.83	51	11.20	0.02	8.44
		Pb	21	4.70	17	2.30	AOV not sig.	54.62	51	3.40	AOV not sig.	-24.06
		Zn	21	51.80	17	24.80	AOV not sig.	19.65	51	43.00	AOV not sig.	-2.49
	Load (lb/ac)	Cu	19	8.77E-05	15	9.41E-05	AOV not sig.	2.57	44	8.13E-05	3.53E-09	51.09
		Pb	18	4.92E-05	15	2.47E-05	AOV not sig.	-28.73	44	2.78E-05	0.03	35.58
		Zn	18	4.81E-04	15	3.31E-04	AOV not sig.	8.63	44	3.60E-04	0.27	57.29

While IS loads and concentrations increased for a number of metals in the post-AI² phase, the actual values remained below levels of concern. For example, reported toxicity thresholds in freshwater aquatic environments for Cu, Pb, and Zn range from 10 to 20 µg/L, 47 to 3,323 µg/L, and 21 to 3,704 µg/L, respectively (National Academy of Science 1986; Mebane et al. 2012).

Sediment

The distribution of TSS concentrations and loads and results of statistical tests to identify changes therein are presented in Figure 12 and Table 8. In the post-GI phase, significant changes in TSS were observed for both concentration and load at BG (17.6% increase and 61.8% decrease, respectively) and CG (29.1% and 68.1% decreases, respectively). Results for TSS in the post-AI² phase were mixed; for example, a TSS load reduction of 46.2% was observed at BG, while a TSS load increase of 24.1% was observed at IS. Filtration and sedimentation occurring in GI in the treatment sewersheds are likely responsible for these TSS reductions at BG and CG.

Bioretention cells effectively decrease TSS concentrations through sedimentation and filtration, at times by several orders of magnitude (Trowsdale & Simcock, 2011). However, in the case of IS, the additional drainage area from redirected downspouts added substantial runoff volumes in the post-AI² phase that likely increased TSS loads. The acreage of rooftops that received downspout redirections in the Indian Springs catchment (5.17 ac) was more than twice that of the other treatment catchments (2.57 ac in Blenheim; 2.44 ac in Cooke-Glenmont). This factor likely explains why increases in TSS loads were only observed in IS. Meanwhile, the significant TSS loads reductions observed at BG in the post-AI² phase were likely due to the constructed wetland which significantly reduced almost all studied pollutants, including TSS (see *Case Study: Park of Roses Wetland*) and resulted in 90% of BG being treated by GI.

Other residential and commercial GI studies reported significant differences in TSS concentration; Page et al. (2015) reported an 82% decrease in TSS, from 54 to 7 mg/L, and Line et al. (2012) reported a 97% decrease, from 244 to 8 mg/L. Coupled with previous research, the data presented herein support the conclusion that the percent TSS concentration reduction in

residential sewersheds can be substantial after GI implementation. However, additional inflow volumes added in the redirection of rooftops and other impervious areas (as observed in the post-AI² phase) to GI must be addressed in the design phase to ensure treatment remains effective.

This information is valuable to engineers and regulators as they try to meet local TSS concentration regulations.

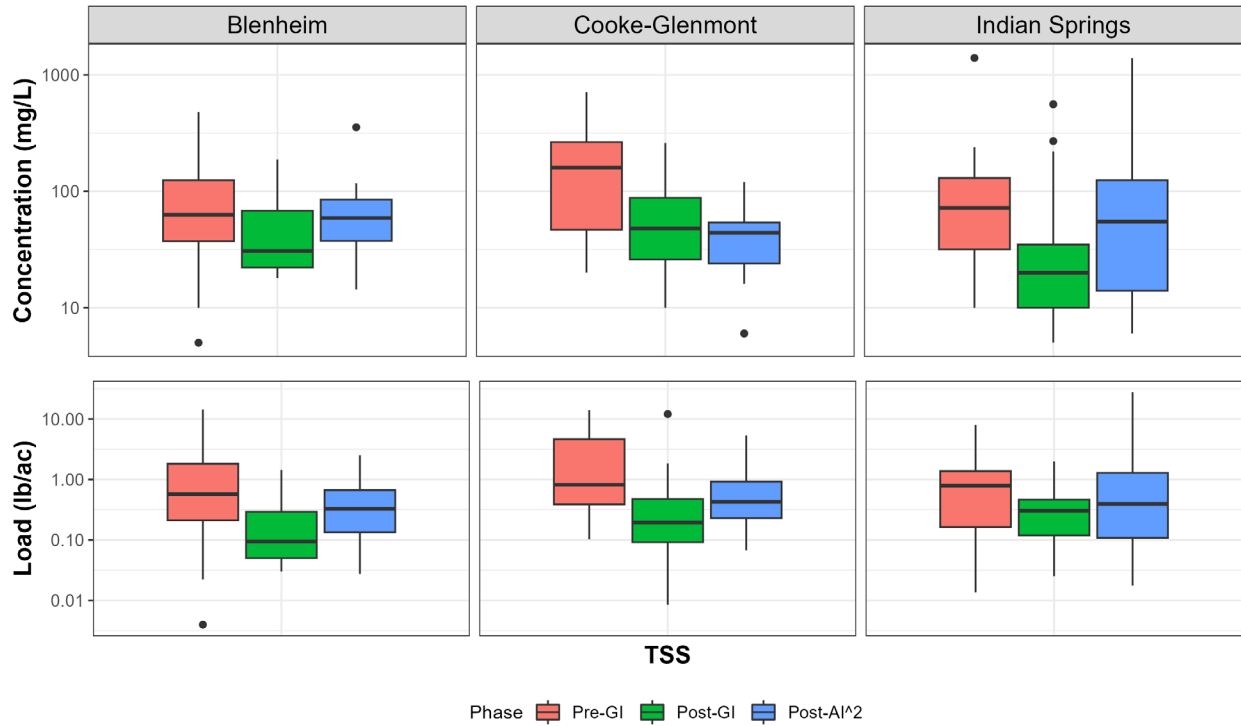


Figure 12: Boxplots of paired control-treatment concentrations and storm event loads for TSS by project phase.

Table 8: Summary statistics of paired control-treatment concentrations and storm event loads for TSS grouped by project phase.

	Data Type	Pre-GI		Post-GI				Post-AI ²			
		n	Med.	n	Med.	p-value	LSM % Diff.	n	Med.	p-value	LSM % Diff.
BG	Conc. (mg/L)	34	63.00	17	30.75	5.87E-05	17.62	20	59.11	AOV not sig.	-19.43
	Load (lb/ac)	31	0.57	14	0.09	3.60E-03	-61.75	19	0.33	0.02	-46.15
CG	Conc. (mg/L)	19	160.00	47	48.00	9.95E-05	-29.13	25	44.00	AOV not sig.	-67.13
	Load (lb/ac)	14	0.83	44	0.19	1.78E-03	-68.08	19	0.43	0.45	-9.67
IS	Conc. (mg/L)	20	72.00	18	20.00	AOV not sig.	56.40	52	55.00	0.49	-24.99
	Load (lb/ac)	17	0.79	16	0.31	AOV not sig.	-52.68	45	0.39	1.11E-04	24.07

Case Study: Park of Roses Wetland

Following the completion of construction activities, the Park of Roses constructed wetland began treating low flows from the BR sewershed in 2020. Automated sampling equipment was installed at the inlet and outlet of the wetland shortly thereafter. Full summary data for all monitored water quality parameters are presented in Appendix E. Concentrations of select pollutants (i.e., TN, TP, TSS, Zn, Pb) from paired inlet-outlet samples are presented in Figure 13 and Table 9.

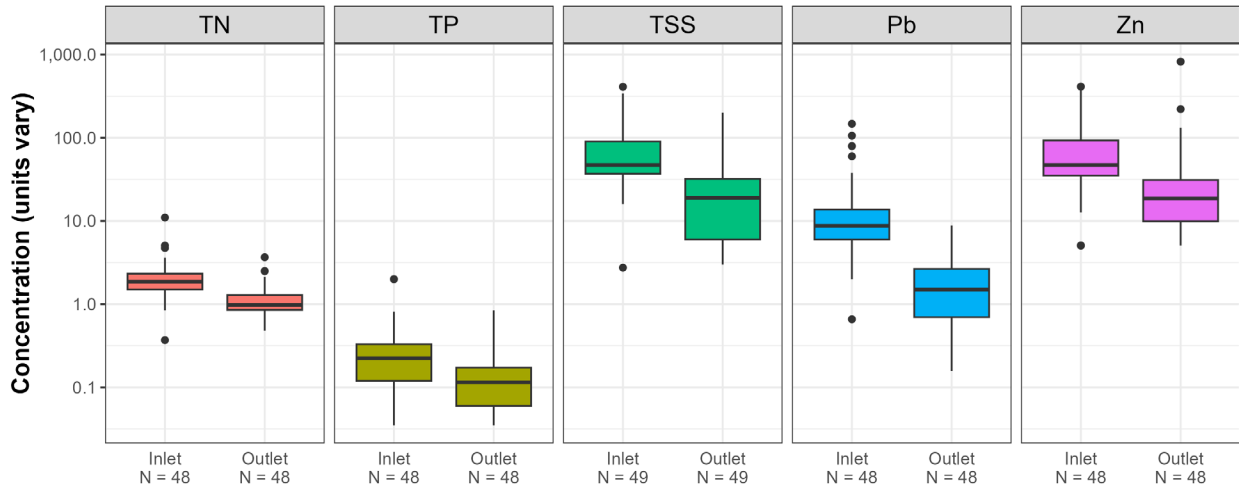


Figure 13: Boxplots showing concentrations of select pollutants present in paired water quality samples collected from the inlet and outlet of the Park of Roses wetland. Concentrations of TN, TP, and TSS are presented in mg/L; Zn and Pb are shown in µg/L.

Table 9: Summary statistics of concentrations of select pollutants present in paired water quality samples collected from the inlet and outlet of the Park of Roses wetland. Differences between inlet and outlet concentrations were all statistically significant ($p < 0.0001$).

Pollutant	Number of Samples		Median Concentration		Median % Reduction
	Inlet	Outlet	Inlet	Outlet	
TN (mg/L)	48	48	1.86	0.98	45.7
TP (mg/L)	48	48	0.23	0.12	42.0
TSS (mg/L)	49	49	47	19	69.6
Pb (µg/L)	48	48	8.75	1.50	82.0
Zn (µg/L)	48	48	47.1	18.7	64.4

Significant pollutant concentration changes between the inlet and the outlet were observed for all pollutants except Ni. Aside from alkalinity and hardness (which increased by 95.7% and 47.1%, respectively), all pollutants significantly decreased between the inlet and outlet of the wetland (see Appendix E). Pollutant removal in the wetland varied seasonally; the removal rates of most pollutants were highest in spring, moderate in summer, and lowest or moderate in fall. Data from the ISBMPD show that the performance of the Park of Roses

constructed wetland was similar to other wetlands for some pollutants (e.g., TSS and Zn) and outperformed other wetlands for others (e.g., Pb, TN, TP, and OP).

Case Study: Unitarian Universalist Church Bioretention Cell

Intensive monitoring was conducted on the bioretention cell located at the Unitarian Universalist (UU) church on Weisheimer Rd from October 2021 to December 2022. This bioretention cell was constructed in 2014 prior to the Blueprint program with older bioretention mix design specifications; thus, based on 10 samples the media was measured as a silt loam texture, which is quite dissimilar to the loamy sand or sandy loam texture recommended today. As the bioretention cell was nearly 10 years old during the sampling window, the plants were mature with 8-10 ft tall shrubs (Figure 14) and frequent observations of ground-dwelling mammals and birds were made in the bioretention cell. Flow monitoring and water quality samplers were installed at the inlet and outlet of the bioretention cell; runoff volume and peak flow reductions as well as changes in pollutant concentrations and loads were calculated in the same manner as the sewershed scale data described in this report.

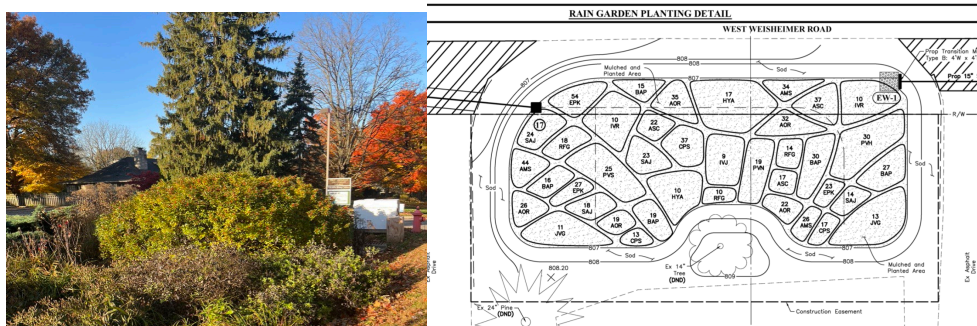


Figure 14. Photograph (at left) and planting plan and monitoring locations (at right) of Unitarian Universalist bioretention cell.

A total of 74 storm events were observed during the monitoring period. Nearly all storms <0.5 inches in depth had runoff volume reductions >70%. Overall average runoff volume reduction was 75% while that for peak flow mitigation was 87.9%. It should be noted that the

data set was dominated by smaller rainfall events (mean 0.64 inches). Sampled storms tended to be larger in depth (mean 0.84 inches).

Pollutant concentrations at the inlet and outlet of the UU church bioretention cell are presented in Table 10. Given that the bioretention cell did not employ internal water storage, it was not surprising to observe nitrification and therefore significant increase in NO_{2-3} through the bioretention cell. However, excellent sequestration of TSS (95% reduction) and particulate phosphorus and nitrogen resulted in substantial TN (22%) and TP (66%) reduction in the UU church bioretention cell. Orthophosphate concentrations increased significantly, similar to other studies of bioretention cells in Ohio with substantial compost content in the soil media. All six heavy metals studied were significantly reduced by the bioretention cell (Table 10). *E. coli* concentrations increased through the bioretention cell by 140%, perhaps related to the frequent observations of wildlife inhabiting this bioretention cell and the dense vegetation which may prevent the penetration of UV to the surface of the filter.

Table 10: Summary statistics of concentrations of select pollutants present in paired water quality samples collected from the inlet and outlet of the Unitarian Universalist church bioretention cell. Nutrient and sediment concentrations are in mg/L, metals are in µg/L, and E. coli is in CFU/100mL. RE is the relative efficiency for that pollutant; multiplying the RE by 100 results in percent removal.

Pollutant	Monitoring Location	Concentration				
		Range	Median	Mean	SD	RE
NO ₂₃	Inlet	0.08 - 2.61	0.354	0.43	0.523	-
	Outlet	0.325 - 2.244	1.005	1.1	0.58	-1.839
TN	Inlet	0.93 - 6.244	2.154	2.51	1.29	-
	Outlet	0.34 - 2.8183	1.681	1.64	0.701	0.220
OP	Inlet	0.0195 - 0.13	0.073	0.0627	0.0338	-
	Outlet	0.1 - 0.25	0.14	0.149	0.0401	-0.918
TP	Inlet	0.075 - 0.81	0.35	0.355	0.184	-
	Outlet	0.075 - 0.39	0.12	0.182	0.0981	0.657
TSS	Inlet	17 - 300	120	128	73.9	-
	Outlet	11841.00	6	8.67	6.35	0.950
Cu	Inlet	5.6 - 83.4	12.8	16.5	15.5	-
	Outlet	2.6 - 6.7	4.6	4.76	1.09	0.641
Pb	Inlet	3.9 - 61.2	13.7	16.4	11.7	-
	Outlet	0.37 - 4.9	1.1	1.42	0.991	0.920
Zn	Inlet	45.6 - 251	69.4	82.5	45.6	-
	Outlet	8.1 - 72.3	16.5	21.1	8.1	0.762
<i>E.coli</i>	Inlet	25 - 52200	1300	5310	11800	-
	Outlet	125 - 26000	3170	4800	6370	-1.438

Conclusions

This report details holistic hydrologic and water quality monitoring activities undertaken by Ohio State University to quantify and compare the effects of installing green infrastructure in the Clintonville neighborhood of Columbus, Ohio, over the eight-year period between 2016 and 2023. The following conclusions were drawn from data collected:

- (1) Runoff generation from the Blenheim sewershed was impacted by the construction of the Park of Roses wetland which brought total sewershed treatment by GI to 90%. Both the median runoff depth and runoff coefficient for the sewershed significantly decreased (by 60% and 50%, respectively) in the post-GI phase. While runoff depth in Indian Springs significantly increased in the post-GI phase, the mean increase was less than 20% and can be attributed to IS having the lowest percentage of the sewershed treated (22% treatment) and lower storage volume compared to other treatment sewersheds. Further, IS had the greatest number of additional infrastructure improvements, which resulted in significant increases in runoff depth post-AI². Conversely, despite the completion of additional infrastructure improvements in CG, neither runoff depth nor peak flow rates increased significantly during the post-AI² phase, suggesting that the larger, regional BRCs constructed in the sewershed provided better mitigation of the increased runoff volumes which resulted from downspout disconnection, sump pump installation, and sewer lateral lining efforts. Future iterations of Blueprint would benefit from GI designed with larger surface and subsurface storage volumes to provide extended hydrological benefits.
- (2) Simulated storm testing revealed that bump-out style BRCs provide greater hydrologic mitigation than ROW-style BRCs. Greater hydrologic benefits were observed for BRCs

with lower loading ratios (i.e., ratio of drainage area to BRC surface area). Limiting loading ratios whenever possible in future Blueprint Columbus projects is recommended.

- (3) Instances of significant pollutant removal improvements in the treatment sewersheds between the pre-GI and post-GI phases were mixed. At Blenheim, loads for many pollutants significantly improved following GI retrofits while some concentrations significantly increased. Water quality in Cooke-Glenmont mostly improved in this period, with significant reductions in concentrations and loads of TP and TSS. Loads of TSS, TN, and TP also significantly decreased at Cooke-Glenmont in the post-GI phase. During the post-GI phase, pollutant concentrations and loads at IS were mostly unchanged. In the post-AI² phase, Blenheim pollutant concentrations were similar to pre-GI concentrations; however, significant load reductions were observed for multiple nutrients and TSS. The only significant concentrations change observed at Cooke-Glenmont during the post-AI² phase was a 1.2% increase in OP while OP and Cd loads increased by 201.4% and 109.3%, respectively. Mixed results were observed in Indian Springs in the post-AI² phase. Increased export of many metal loads was observed; trends in loads for many nitrogen and phosphorus species were mixed. Notably, TSS loads were significantly increased during this period, likely associated with the relatively high impervious area (i.e., rooftops) routed to the GI in this sewershed in the post-AI² phase compared to the other treatment sewersheds.
- (4) The Park of Roses wetland provided substantial mitigation of many pollutants, including TN, TP, TSS, Zn, and Pb, discharged from the Blenheim sewershed. Seasonal trends in performance were observed, with pollutant removal generally highest in the spring and declining into summer and fall. The Park of Roses constructed wetland continues to

perform similarly to or better than other documented constructed wetlands. Many of the improved water quality outcomes observed at Blenheim are attributed to the constructed wetland.

- (5) The Unitarian Universalist church bioretention cell exhibited excellent performance over a 14-month monitoring period from October 2021 to December 2022. Runoff reduction was greater than 70% and the concentrations of many pollutants, including TSS, TN, TP, and all heavy metals analyzed, were reduced substantially as water passed through the filter. Nitrate-nitrite nitrogen and *E. coli* concentrations increased during biofiltration at the UU church. Overall, this bioretention cell indicates that mid-life bioretention cells still perform well, perhaps better than newly installed systems.

References

American Public Health Association (APHA), American Water Works Association (AWWA), and Water Environment Federation (WEF). (2012). *Standard methods for the examination of water and wastewater*, Ed. Laura Bridgewater. 22nd ed., Washington, DC.

Antweiler, R.C., and Taylor, H.E. (2008). "Evaluation of statistical treatments of left-censored environmental data using coincident uncensored data sets: 1. Summary statistics." *Environmental Science and Technology*. 42(10), 3732–3738.

Arcadis. (2015). *The City of Columbus integrated plan and 2015 WWMP update report*. Prepared for City of Columbus Department of Public Utilities Division of Sewerage and Drainage.

Bedan, E.S., and Clausen, J.C. (2009). "Stormwater runoff quality and quantity from traditional and low impact development watersheds." *Journal of the American Water Resources Association*, 45(4), 998-1008.

Bell, C.D., McMillan, S.K., Clinton, S.M., and Jefferson, A.J. (2016). "Hydrologic response to stormwater control measures in urban watersheds." *Journal of Hydrology*, 541, 1488-1500.

Benallal, H., Mouchid, Y., Abouelaziz, I., Alfalou, A., Tairi, H., Riffi, J., & El Hassouni, M. (2022, May). A new approach for removing point cloud outliers using box plot. In *Pattern recognition and tracking XXXIII* (Vol. 12101, pp. 63-69). SPIE.

Bolund, P., and Hunhammar, S. (1999). "Ecosystem services in urban areas." *Ecological Economics*, 29(2), 293-301.

Brown, R. A., & Hunt III, W. F. (2011). Impacts of media depth on effluent water quality and hydrologic performance of undersized bioretention cells. *Journal of Irrigation and Drainage Engineering*, 137(3), 132-143.

Chen, X., Zhou, W., Pickett, S.T., Li, W., and Han, L. (2016). "Spatial-temporal variations of water quality and its relationship to land use and land cover in Beijing, China." *International Journal of Environmental Research and Public Health*, 13(5), 449.

City of Columbus (2017a). "Sewer overflow discharge information."
<<https://eapp.columbus.gov/ssocso/mnmap.aspx>> (Jan 11, 2018).

City of Columbus. (2017b). "Blueprint Columbus."
<<https://www.columbus.gov/utilities/projects/blueprint/>> (Jan 11, 2018).

Clary, J., and Jones, J. (2016). International Stormwater BMP Database (ISBMPD - 2016 Summary Statistics. In *Wetf*. <https://doi.org/C-ITS Platform>

Davis, A.P., Hunt, W.F., Traver, R.G., and Clar, M. (2009). "Bioretention technology: Overview of current practice and future needs." *Journal of Environmental Engineering*, 135(3), 109-117.

- Dietz, M. E. (2007). "Low impact development practices: A review of current research and recommendations for future directions." *Water, Air, and Soil Pollution*, 186(1-4), 351-363.
- Dietz, M. E., and Clausen, J.C. (2008). "Stormwater runoff and export changes with development in a traditional and low impact subdivision." *Journal of Environmental Management*, 87(4), 560-566.
- Fritsch, J.M., Kane, R.J., and Chelius, C. R. (1986). "The contribution of mesoscale convective weather systems to the warm-season precipitation in the United States." *Journal of Climate and Applied Meteorology*, 25(10), 1333-1345.
- Goodrich, D.C., Lane, L.J., Shillito, R.M., Miller, S.N., Syed, K.H., and Woolhiser, D.A. (1997). "Linearity of basin response as a function of scale in a semiarid watershed." *Water Resources Research*, 33(12), 2951-2965.
- Hopkinson, C. S., & Giblin, A. E. (2008). "Nitrogen Dynamics of Coastal Salt Marshes". In *Nitrogen in the Marine Environment*.
- Hsieh, C., Davis, A. P., & Needelman, B. A. (2007). "Nitrogen Removal from Urban Stormwater Runoff Through Layered Bioretention Columns". *Water Environment Research*, 79(12), 2404–2411.
- Hunt, W. F., Allen P. Davis, and Robert G. Traver (2012). "Meeting Hydrologic and Water Quality Goals through Targeted Bioretention Design." *Journal of Environmental Engineering* 138(6): 698–707.
- Liao, H., Krometis, L.A.H., and Kline, K. (2016). "Coupling a continuous watershed-scale microbial fate and transport model with a stochastic dose-response model to estimate risk of illness in an urban watershed." *Science of the Total Environment*, 551, 668-675.
- Li, L., and Davis, A. P. (2014). "Urban stormwater runoff nitrogen composition and fate in bioretention systems". *Environmental Science and Technology*, 48(6), 3403–3410.
- Line, D.E., Brown, R.A., Hunt, W.F., and Lord, W.G. (2012). "Effectiveness of LID for commercial development in North Carolina." *Journal of Environmental Engineering*, 138(6), 680-688.
- Line, D. E., and White, N.M. (2007). "Effects of development on runoff and pollutant export." *Water Environment Research*, 79(2), 185-190.
- Line, D. E., and White, N.M. (2015). "Runoff and pollutant export from a LID subdivision in North Carolina." *Journal of Environmental Engineering*, 142(1), 04015052.

- Lynn, T. J., Yeh, D. H., & Ergas, S. J. (2015). Performance of denitrifying stormwater biofilters under intermittent conditions. *Environmental Engineering Science*, 32(9), 796–805.
- Mahmoud, A., Alam, T., Rahman, M. Y. A., Sanchez, A., Guerrero, J., and Jones, K. D. (2019). “Evaluation of field-scale stormwater bioretention structure flow and pollutant load reductions in a semi-arid coastal climate”. *Ecological Engineering*, 142, 100007.
- Mebane, C. A., Dillon, F. S., & Hennessy, D. P. (2012). Acute toxicity of cadmium, lead, zinc, and their mixtures to stream-resident fish and invertebrates. *Environmental Toxicology and Chemistry*, 31(6), 1334–1348.
- Moody, J.A., and Martin, D.A. (2001). “Post-fire, rainfall intensity–peak discharge relations for three mountainous watersheds in the western USA.” *Hydrological Processes*, 15(15), 2981–2993.
- Moore, T.L., Rodak, C.M., and Vogel, J.R. (2017). “Urban stormwater characterization, control, and treatment.” *Water Environment Research*, 89(10), 1876–1927.
- Mullane, J. M., Flury, M., Iqbal, H., Freeze, P. M., Hinman, C., Cogger, C. G., & Shi, Z. (2015). Intermittent rainstorms cause pulses of nitrogen, phosphorus, and copper in leachate from compost in bioretention systems. *Science of The Total Environment*, 537, 294–303.
- National Academy of Science. (1986). Health effects of excess copper. Chapter 5. In Copper in drinking water. National Academy Press. Washington DC.
- Page, J. L., Winston, R.J., Mayes, D.B., Perrin, C.A., and Hunt, W.F. (2015a). “Retrofitting residential streets with stormwater control measures over sandy soils for water quality improvement at the catchment scale.” *Journal of Environmental Engineering*, 141(4), 04014076.
- Page, J. L., Winston, R.J., Mayes, D.B., Perrin, C., and Hunt, W.F. (2015b). “Retrofitting with innovative stormwater control measures: Hydrologic mitigation of impervious cover in the municipal right-of-way.” *Journal of Hydrology*, 527, 923–932.
- Passeport, E., Hunt, W. F., Line, D. E., Smith, R. A., & Brown, R. A. (2009). Field study of the ability of two grassed bioretention cells to reduce storm-water runoff pollution. *Journal of Irrigation and Drainage Engineering*, 135(4), 505–510. [https://doi.org/10.1061/\(ASCE\)IR.1943-4774.00000006](https://doi.org/10.1061/(ASCE)IR.1943-4774.00000006)
- Ran, Q., Su, D., Li, P., & He, Z. (2012). Experimental study of the impact of rainfall characteristics on runoff generation and soil erosion. *Journal of Hydrology*, 424, 99–111.
- R Core Team (2023). *A language and environment for statistical computing*. R Foundation for Statistical Computing. Vienna, Austria.
- Roy-Poirier, A., Champagne, P., & Filion, Y. (2010). “Bioretention processes for phosphorus pollution control”. *Environmental Reviews*, 18(1), 159–173.

- Shrestha, P., Hurley, S. E., and Wemple, B. C. (2018). "Effects of different soil media, vegetation, and hydrologic treatments on nutrient and sediment removal in roadside bioretention systems". *Ecological Engineering*, 112, 116-131
- Shuster, W.D., Bonta, J., Thurston, H., Warnemuende, E., and Smith, D.R. (2005) "Impacts of impervious surface on watershed hydrology: a review." *Urban Water Journal*. 2: 263–275.
- Smith, J. S., Winston, R. J., Tirpak, R. A., Wituszynski, D. M., Boening, K. M., & Martin, J. F. (2020). The seasonality of nutrients and sediment in residential stormwater runoff: Implications for nutrient-sensitive waters. *Journal of Environmental Management*, 276, 111248.
- ten Veldhuis, M.C., and Schleiss, M. (2017). "Statistical analysis of hydrological response in urbanising catchments based on adaptive sampling using inter-amount times." *Hydrology and Earth System Sciences*, 21(4), 1991.
- Tillinghast, E. D., Hunt, W.F., and Jennings, G.D. (2011). "Stormwater control measure (SCM) design standards to limit stream erosion for Piedmont North Carolina." *Journal of Hydrology*, 411(3), 185-196.
- Tirpak, R. A., Winston, R. J., Simpson, I. M., Dorsey, J. D., Grimm, A. G., Pieschek, R. L.... & Carpenter, D. D. (2021). Hydrologic impacts of retrofitted low impact development in a commercial parking lot. *Journal of Hydrology*, 592, 125773.
- U.S. Environmental Protection Agency (USEPA). (1983). *Methods of chemical analysis of water and waste*. EPA-600/4-79-020, Cincinnati, Ohio.
- U.S. Environmental Protection Agency (2002). *2002 Integrated Water Quality Monitoring and Assessment Report Guidance*. U.S. EPA, Office of Wetlands, Oceans, and Watersheds, Washington, D.C.
- U.S. Environmental Protection Agency. (2006). Method 1603 *Escherichia coli* (*E. coli*) in water by membrane filtration using modified membrane-thermotolerant *Escherichia coli* Agar (Modified mTEC).
- Violin, C.R., Cada, P., Sudduth, E.B., Hassett, B.A., Penrose, D.L. and Bernhardt, E.S. (2011). "Effects of urbanization and urban stream restoration on the physical and biological structure of stream ecosystems." *Ecological Applications*, 21(6), 1932-1949.
- Walsh, C.J., Roy, A.H., Feminella, J.W., Cottingham, P.D., Groffman, P.M., and Morgan, R.P. (2005). "The urban stream syndrome: current knowledge and the search for a cure." *Journal of the North American Benthological Society*, 24(3), 706-723.
- Wilson, C.E., Hunt, W.F., Winston, R.J., and Smith, P. (2014). "Comparison of runoff quality and quantity from a commercial low-impact and conventional development in Raleigh, North Carolina." *Journal of Environmental Engineering*, 141(2), 05014005.

Winston, R.J., Davidson-Bennett, K.M., Buccier, K.M., and Hunt, W.F. (2016a). “Seasonal variability in stormwater quality treatment of permeable pavements situated over heavy clay and in a cold climate. *Water, Air, and Soil Pollution*, 227(5), 140.

Winston, R.J., Dorsey, J.D., and Hunt, W.F. (2016b). “Quantifying volume reduction and peak flow mitigation for three bioretention cells in clay soils in northeast Ohio.” *Science of the Total Environment*, 553, 83-95.

Winston, R.J., Dorsey, J.D., Smolek, A.P., and Hunt, W.F. (2018). “Hydrologic performance of four permeable pavement systems constructed over low-permeability soils in northeast Ohio.” *Journal of Hydrologic Engineering*. 23(4), 04018007.

Wright, T.J., Liu, Y., Carroll, N.J., Ahiablame, L.M., and Engel, B.A. (2016). “Retrofitting LID practices into existing neighborhoods: is it worth it?” *Environmental Management*, 57(4), 856-867.

Appendix A: GIS Analysis to Identify Different Impervious Surface Types in Each Sewershed

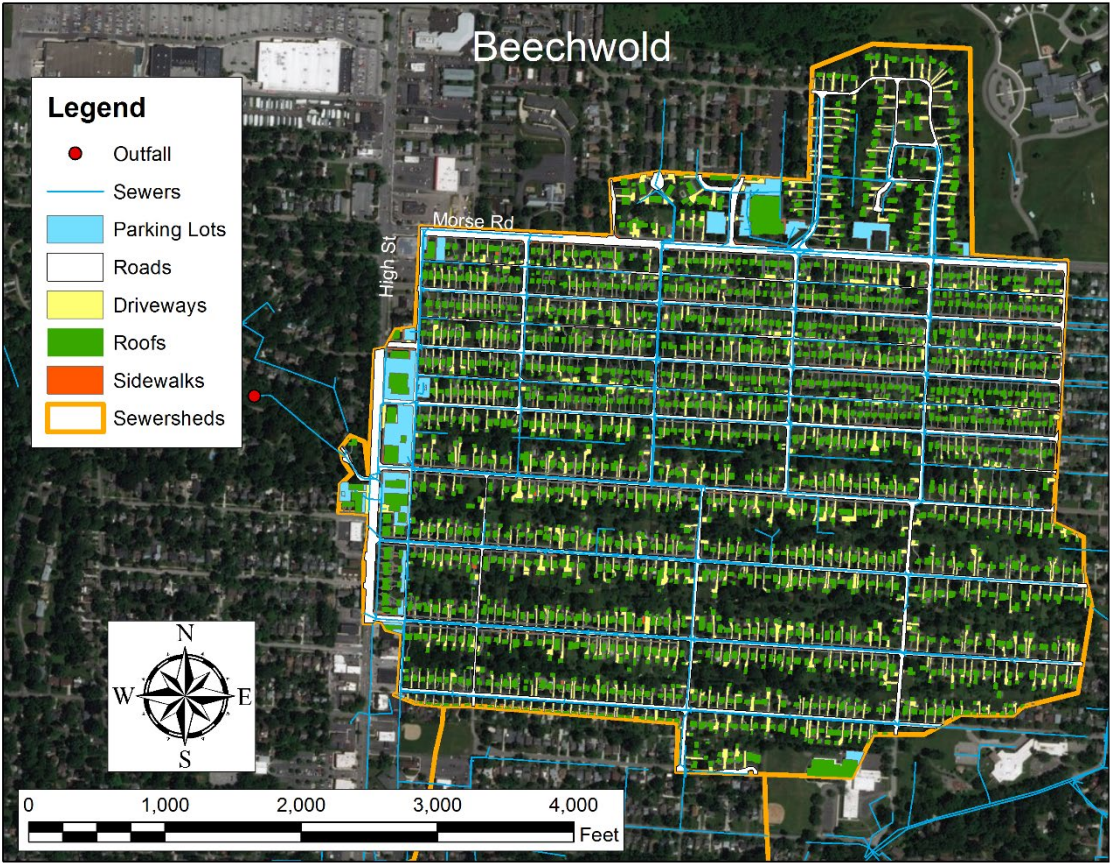


Figure 15: Map showing impervious surface types in the Beechwold sewershed. Pervious areas in the sewershed are not highlighted with color.

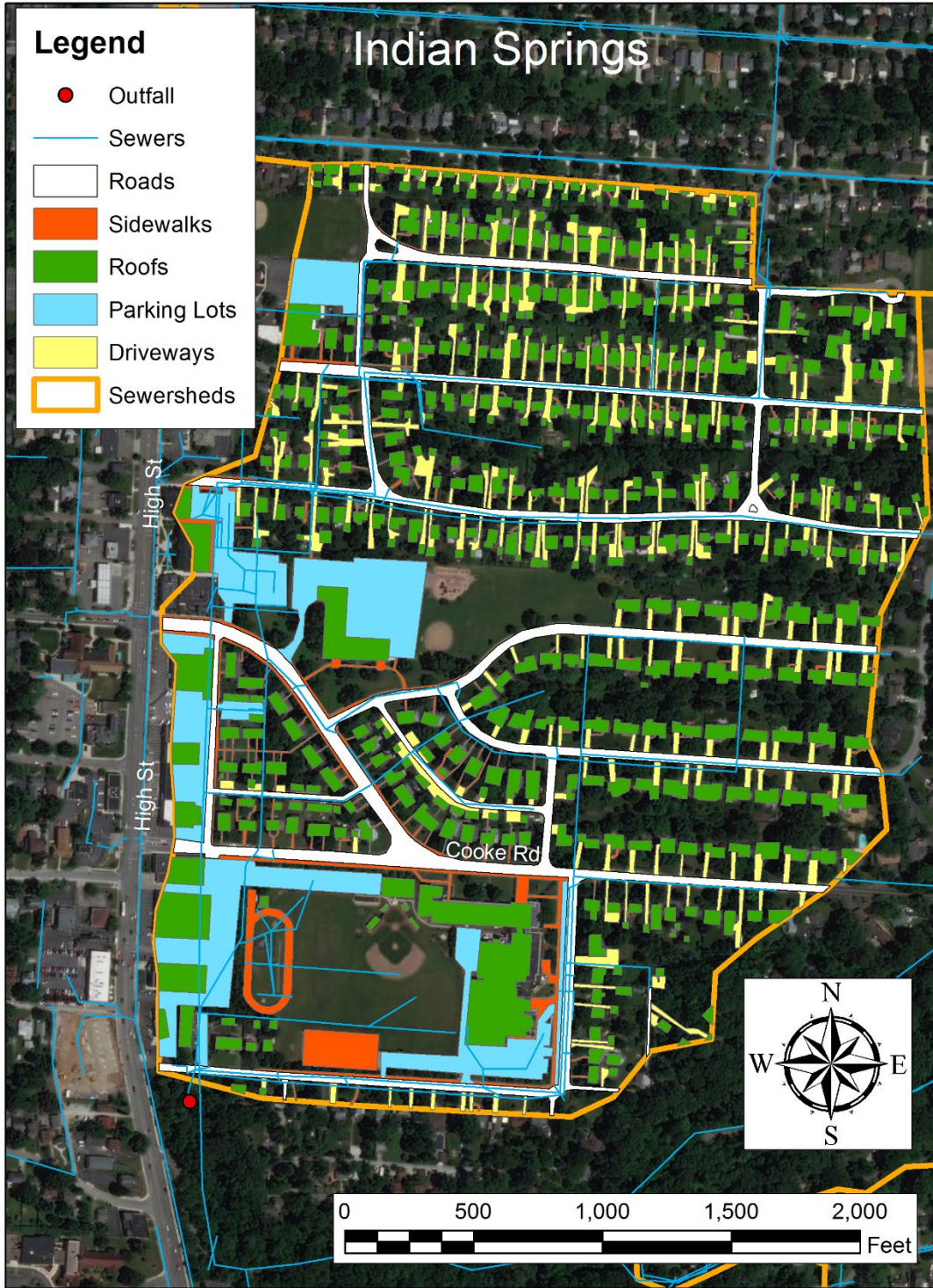


Figure 16: Map showing impervious surface types in the Indian Springs sewershed. Pervious areas in the sewershed are not highlighted with color.

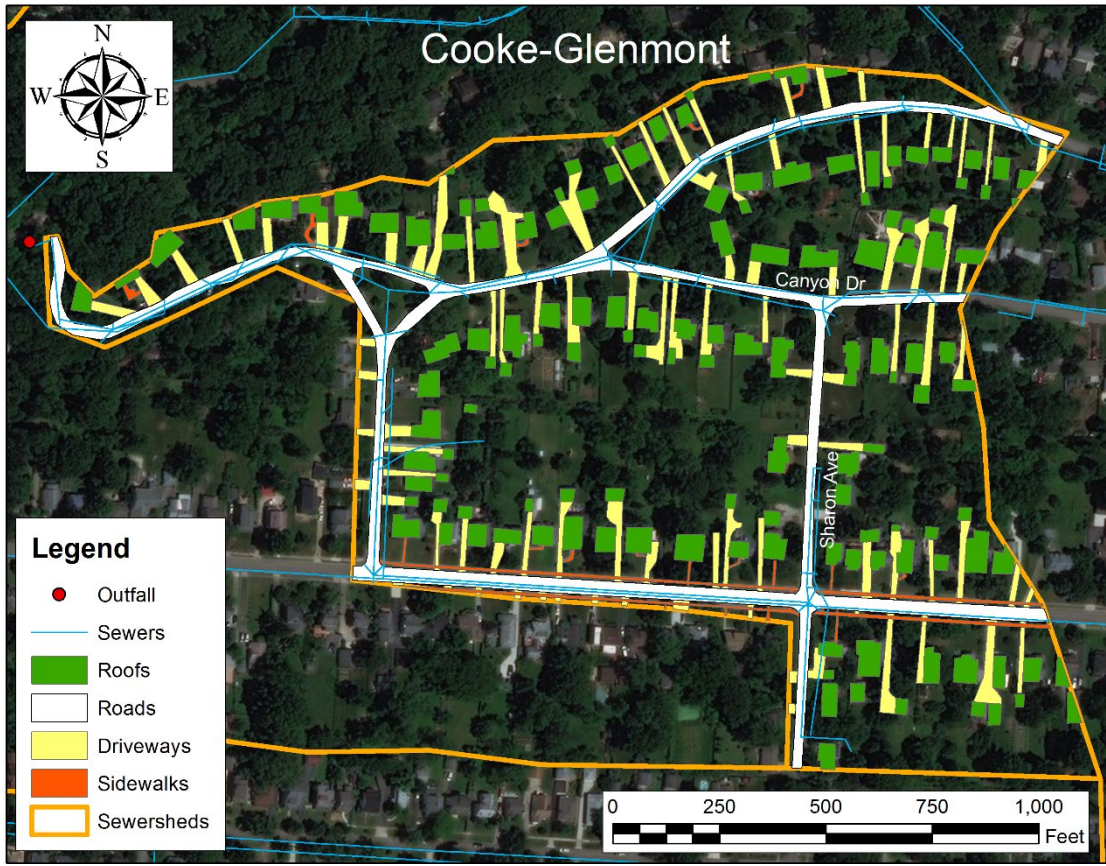


Figure 17: Map showing impervious surface types in the Cooke-Glenmont sewershed. Pervious areas in the sewershed are not highlighted with color.

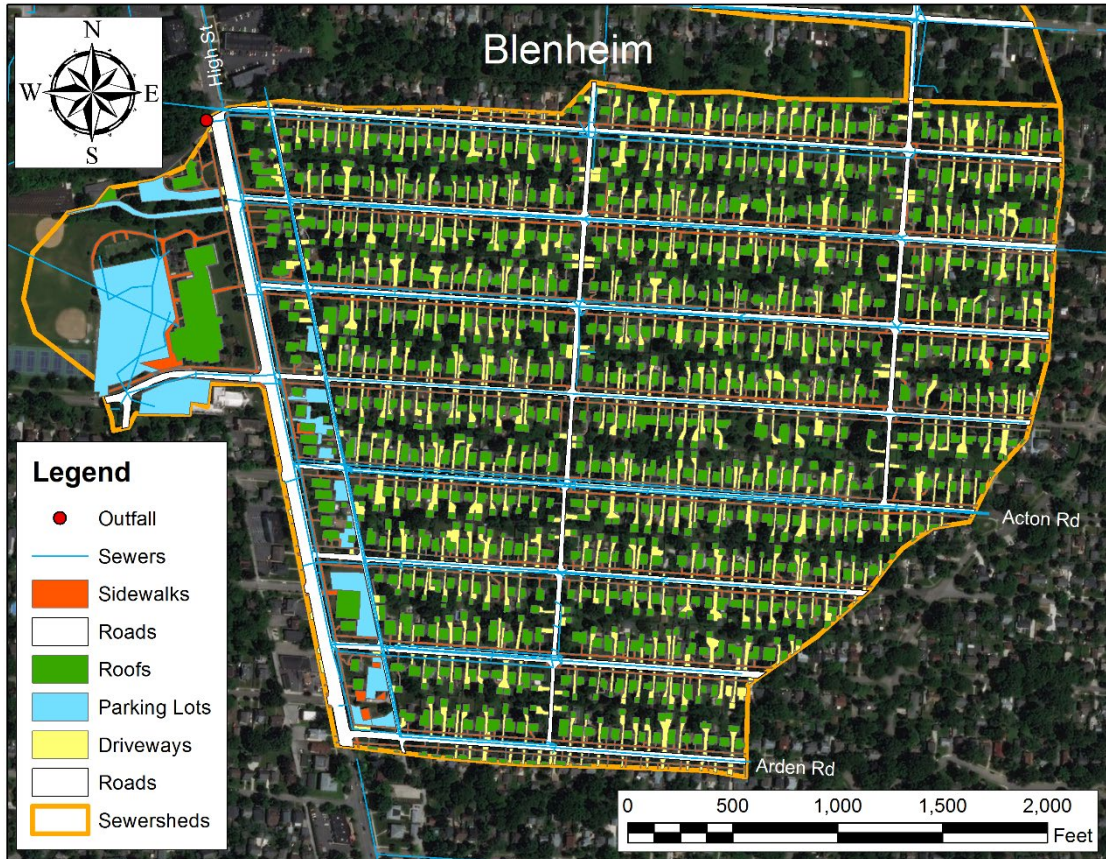


Figure 18: Map showing impervious surface types in the Blenheim sewershed. Pervious areas in the sewershed are not highlighted with color.



Figure 19: Map showing impervious surface types in the Starrett sewershed. Pervious areas in the sewershed are not highlighted with color.

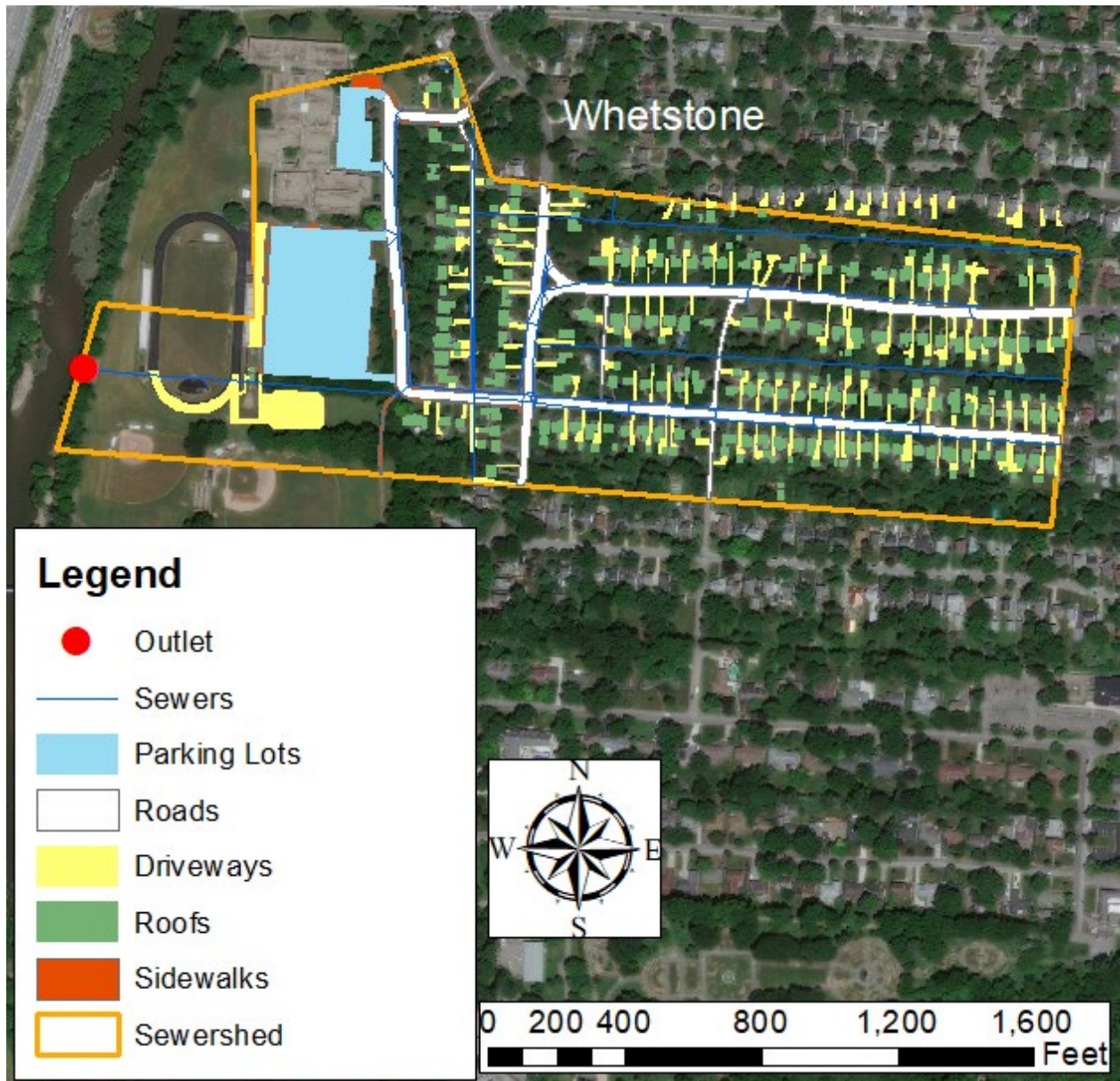


Figure 20: Map showing impervious surface types in the Whetstone sewershed. Pervious areas in the sewershed are not highlighted with color.

Appendix B: Monitoring Results from Whetstone and Starrett Sewersheds

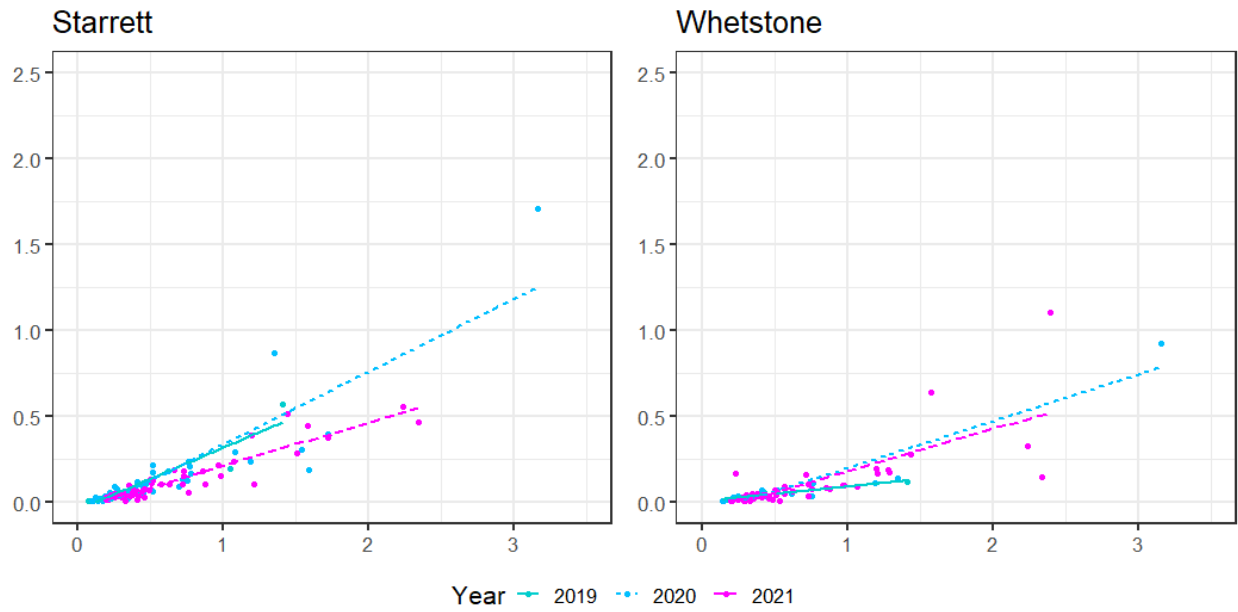


Figure 21: Linear regressions comparing runoff and rainfall depths (in) across three monitoring years.

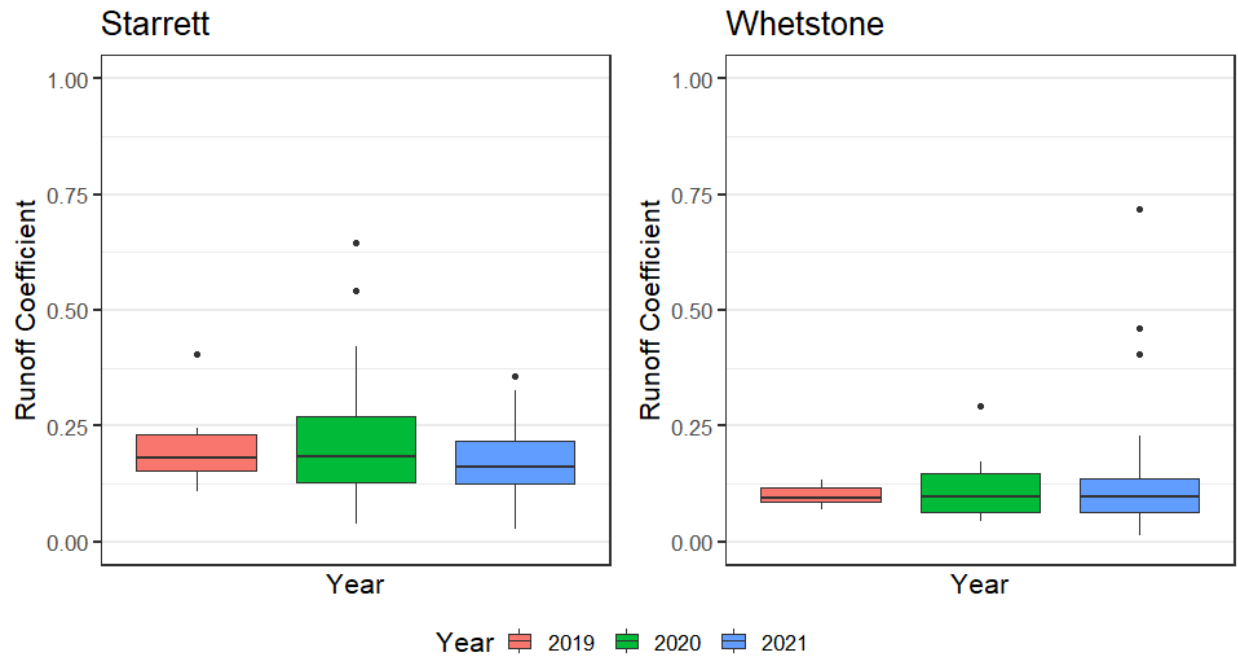


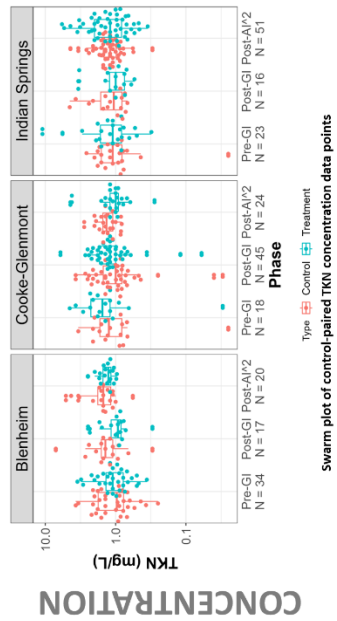
Figure 22: Boxplot comparisons of runoff coefficients from the Starrett and Whetstone sewersheds across three monitoring years.

Table 11: Summary statistics of runoff depth (in) and runoff coefficients for Starrett and Whetstone.

Sewershed	Parameter	2019	2020	2021
Starrett	Median Runoff Depth (in)	0.04	0.07	0.07
	Median Runoff Coefficient	0.18	0.19	0.16
Whetstone	Median Runoff Depth (in)	0.03	0.04	0.04
	Median Runoff Coefficient	0.09	0.10	0.10

Appendix C: Graphical and Tabular Analysis of Pollutant Concentrations and Loads

Treatment Sewershed	Pre-GI			Post-GI			Post-GI Summary Statistics			Post-AI ²			Post-AI ² Summary Statistics				
	n	Control Median (mg/L)	Treatment Median (mg/L)	n	Control Median (mg/L)	Treatment Median (mg/L)	p-value	LSM % Phase Difference	n	Control Median (mg/L)	Treatment Median (mg/L)	p-value	LSM % Phase Difference	n	Control Median (mg/L)	Treatment Median (mg/L)	p-value
Blenheim	34	0.97	1.10	17	1.40	0.93	0.70	20.97	20	1.50	1.27	AOV not significant	2.73				
Cooke-Glenmont	18	1.25	1.55	45	1.00	1.20	0.18	-14.84	24	1.35	1.00	0.06	-22.82				
Indian Springs	23	1.10	1.10	16	1.07	1.00	0.19	21.24	51	1.20	1.20	0.77	-6.25				



Treatment Sewershed	Pre-GI			Post-GI			Post-GI Summary Statistics			Post-AI ²			Post-AI ² Summary Statistics				
	n	Control Median (lb/ac)	Treatment Median (lb/ac)	n	Control Median (lb/ac)	Treatment Median (lb/ac)	p-value	LSM % Phase Difference	n	Control Median (lb/ac)	Treatment Median (lb/ac)	p-value	LSM % Phase Difference	n	Control Median (lb/ac)	Treatment Median (lb/ac)	p-value
Blenheim	31	0.01	0.01	14	0.01	3.29E-03	1.94E-05	-54.31	20	0.01	0.01	2.13E-04	-38.46				
Cooke-Glenmont	15	0.01	0.01	42	0.01	0.01	0.96	-21.46	19	0.01	0.01	5.38E-05	126.08				
Indian Springs	21	0.01	0.01	14	0.01	0.01	AOV not significant	-8.07	44	4.28E-03	0.01	0.44	21.27				

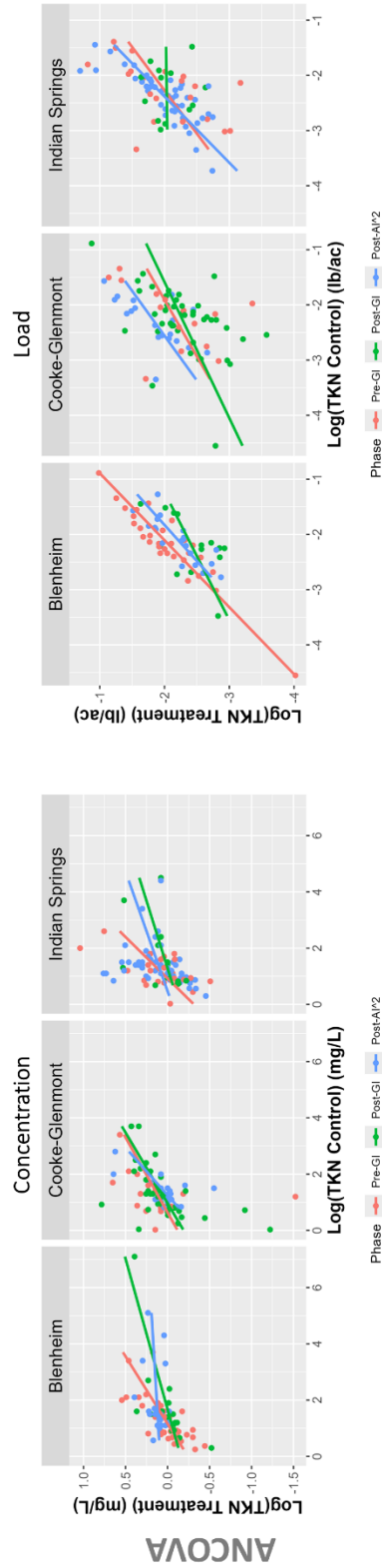
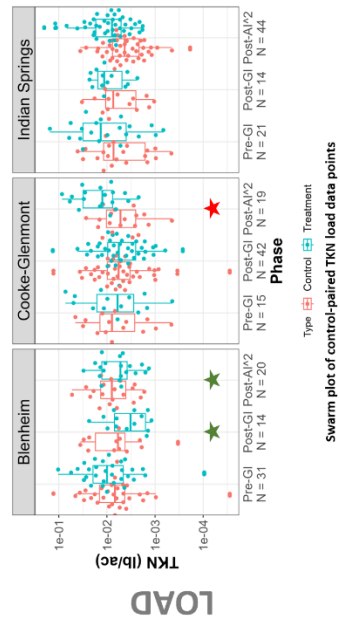
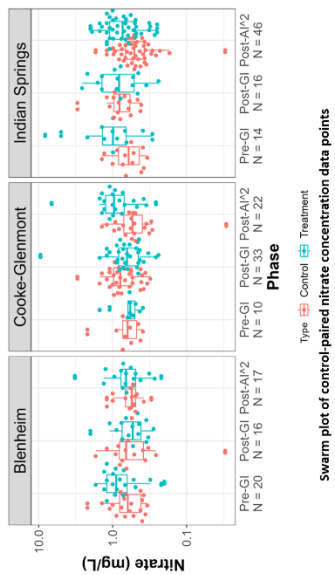


Figure 23: Summary statistics of TKN in water quality samples collected from Clintonville sewersheds and results of analyses comparing project phases. Significant differences ($p < 0.05$), determined from Kruskal-Wallis/Dunn's test with Bonferroni corrections, are represented by different letters in box plots. Asterisk denotes differences were significant at $p < 0.1$.

Treatment Sewershed	Pre-GI			Post-GI			Post-GI Summary Statistics			Post-AI2 Summary Statistics			
	n	Control Median (mg/L)	Treatment Median (mg/L)	n	Control Median (mg/L)	Treatment Median (mg/L)	p-value	LSM % Phase Difference	n	Control Median (mg/L)	Treatment Median (mg/L)	p-value	LSM % Phase Difference
Blenheim	20	0.63	0.90	16	0.66	0.54	AOV not significant	9.46	17	0.55	0.66	0.58	-10.38
Cooke-Glenmont	10	0.63	0.58	33	0.79	0.64	AOV not significant	40.87	22	0.54	0.96	AOV not significant	43.98
Indian Springs	14	0.61	0.99	16	0.81	0.82	AOV not significant	10.41	46	0.51	0.74	0.61	-20.09



Treatment Sewershed	Pre-GI			Post-GI			Post-GI Summary Statistics			Post-AI2 Summary Statistics			
	n	Control Median (lb/ac)	Treatment Median (lb/ac)	n	Control Median (lb/ac)	Treatment Median (lb/ac)	p-value	LSM % Phase Difference	n	Control Median (lb/ac)	Treatment Median (lb/ac)	p-value	LSM % Phase Difference
Blenheim	18	3.90E-03	0.01	14	2.12E-03	1.94E-03	AOV not significant	-49.02	16	2.22E-03	2.29E-03	0.79	-38.87
Cooke-Glenmont	10	0.01	0.01	32	3.05E-03	2.65E-03	0.09	-60.08	17	1.24E-03	0.01	AOV not significant	249.34
Indian Springs	14	4.07E-03	0.01	14	2.82E-03	0.01	AOV not significant	12.81	40	1.56E-03	4.86E-03	0.01	-5.67

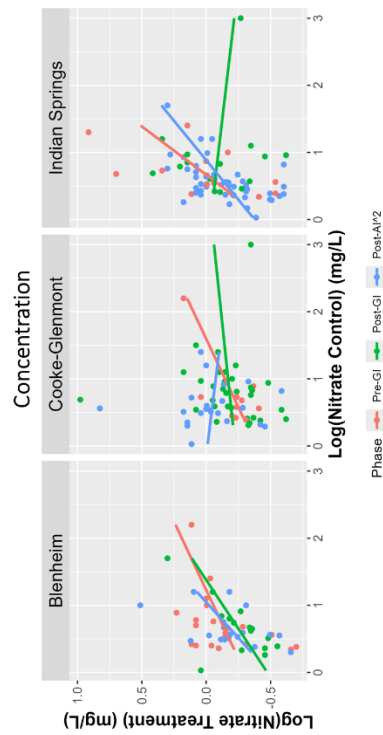
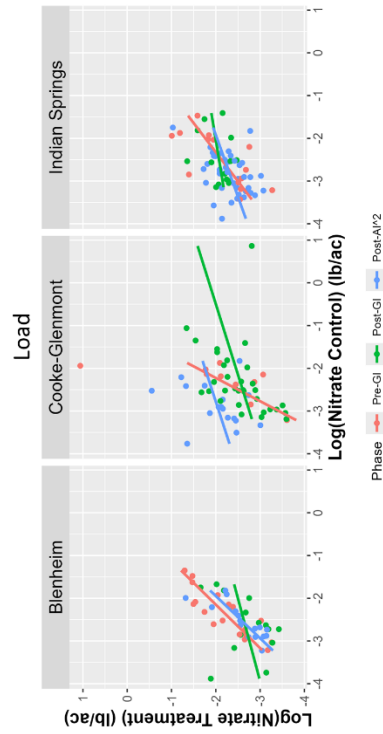
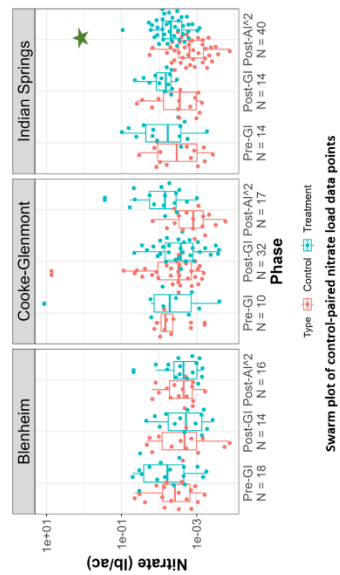
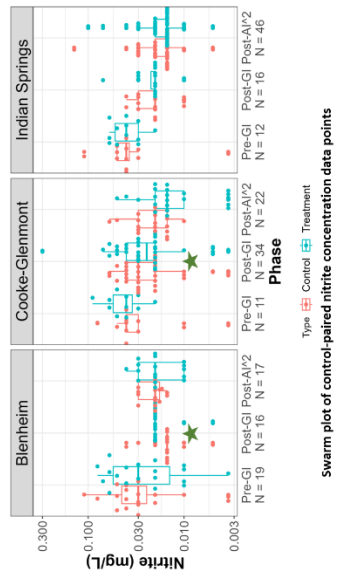


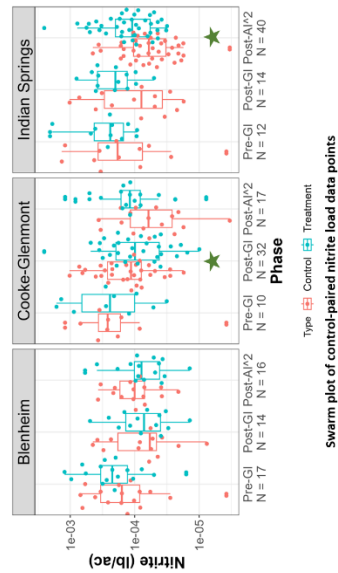
Figure 24: Summary statistics of Nitrate in water quality samples collected from Clintonville sewersheds and results of analyses comparing project phases. Significant differences ($p < 0.05$), determined from Kruskal-Wallis/Dunn's test with Bonferroni corrections, are represented by different letters in box plots. Asterisk denotes differences were significant at $p < 0.1$.

Treatment Sewershed	Pre-GI			Post-GI			Post-GI Summary Statistics			Post-AI ²			Post-AI ² Summary Statistics		
	n	Control Median (mg/L)	Treatment Median (mg/L)	n	Control Median (mg/L)	Treatment Median (mg/L)	p-value	LSM % Phase Difference	n	Control Median (mg/L)	Treatment Median (mg/L)	p-value	LSM % Phase Difference		
Blenheim	16	0.04	0.03	16	0.02	0.02	0.05	-16.60	17	0.02	0.02	AOV not significant	-8.03		
Cooke-Glenmont	10	0.04	0.04	31	0.03	0.03	0.01	-39.82	22	0.02	0.02	AOV not significant	-59.70		
Indian Springs	11	0.04	0.04	16	0.02	0.02	0.93	-11.73	46	0.02	0.02	0.62	-34.83		



Swarm plot of control-paired nitrite concentration data points

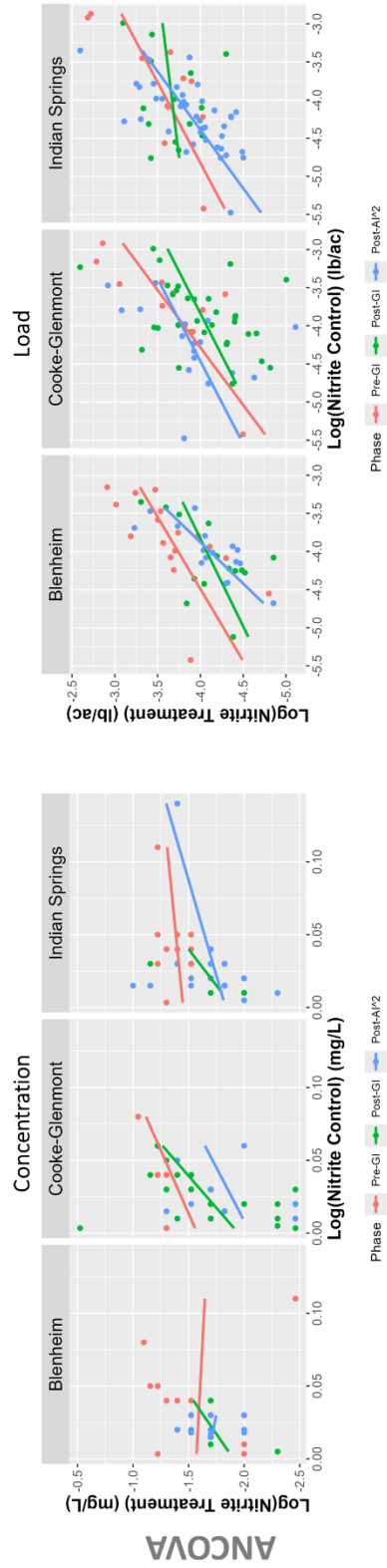
Treatment Sewershed	Pre-GI			Post-GI			Post-GI Summary Statistics			Post-AI ²			Post-AI ² Summary Statistics		
	n	Control Median (lb/ac)	Treatment Median (lb/ac)	n	Control Median (lb/ac)	Treatment Median (lb/ac)	p-value	LSM % Phase Difference	n	Control Median (lb/ac)	Treatment Median (lb/ac)	p-value	LSM % Phase Difference		
Blenheim	15	1.61E-04	2.72E-04	14	5.82E-05	7.21E-05	AOV not significant	-38.51	16	1.00E-04	7.88E-05	0.81	-35.85		
Cooke-Glenmont	9	2.67E-04	2.79E-04	30	1.14E-04	1.13E-04	0.04	-43.23	17	6.11E-05	1.19E-04	AOV not significant	12.50		
Indian Springs	11	1.92E-04	2.43E-04	14	7.87E-05	2.00E-04	AOV not significant	-18.09	40	6.02E-05	1.09E-04	0.01	-12.81		



Swarm plot of control-paired nitrite load data points

CONCENTRATION

LOAD



CONCENTRATION

LOAD

Figure 25: Summary statistics of Nitrite in water quality samples collected from Clintonville sewersheds and results of analyses comparing project phases. Significant differences ($p < 0.05$), determined from Kruskal-Wallis/Dunn's test with Bonferroni corrections, are represented by different letters in box plots. Asterisk denotes differences were significant at $p < 0.1$.

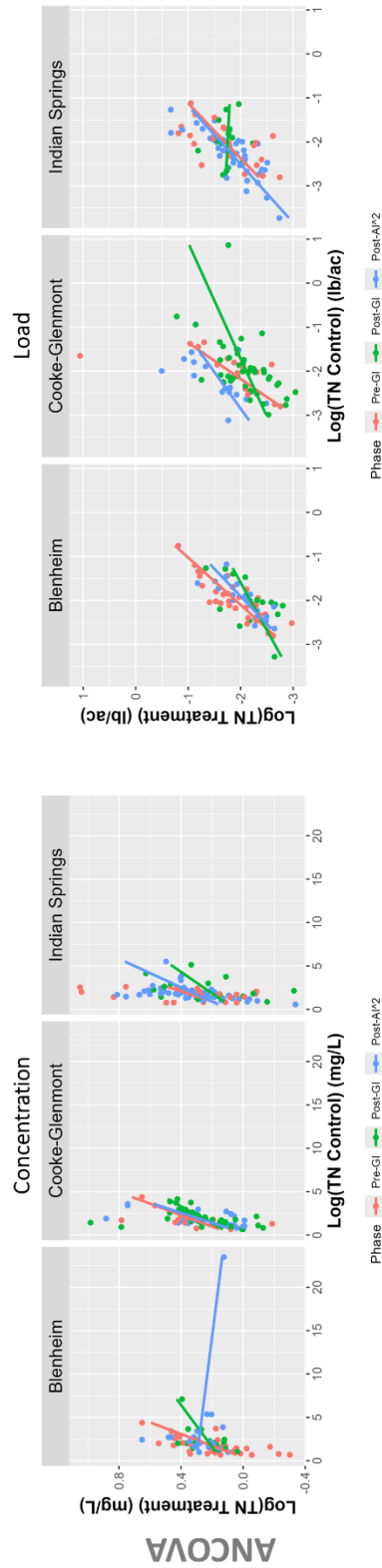
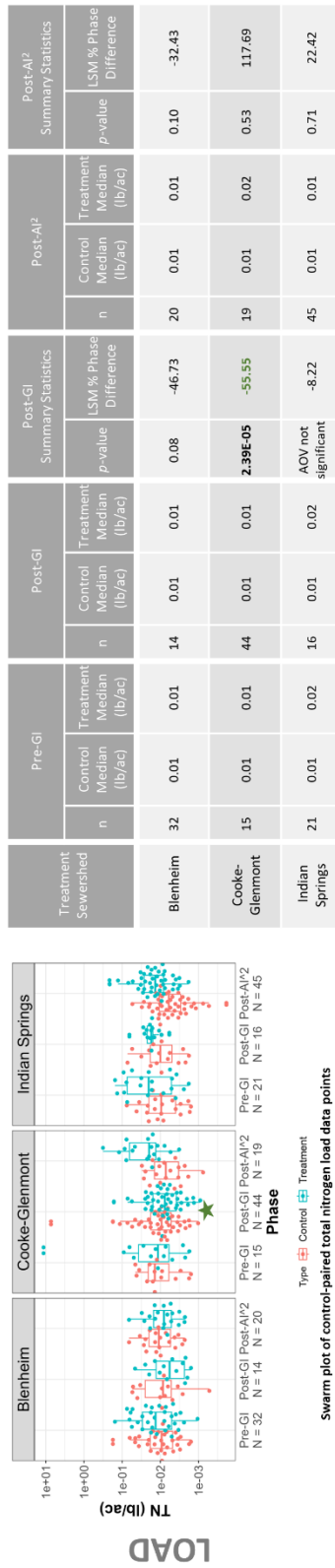
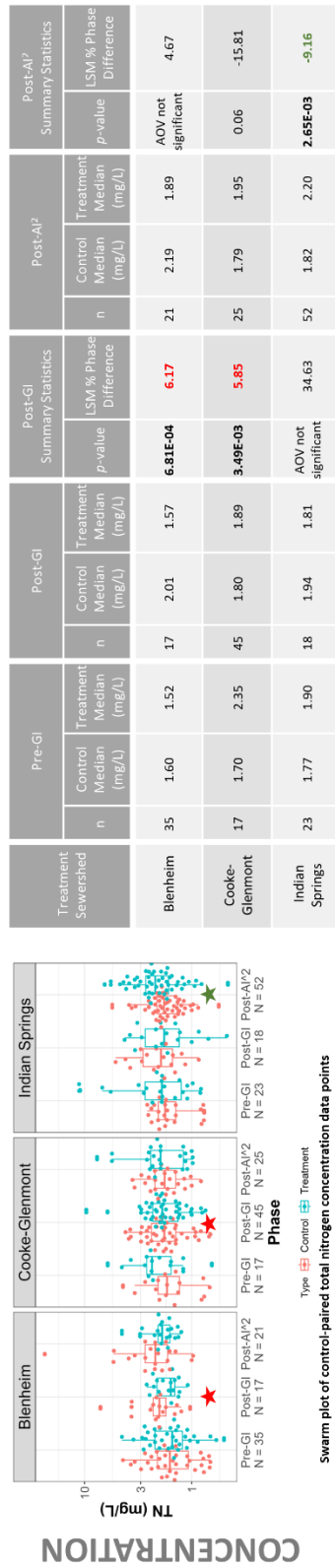
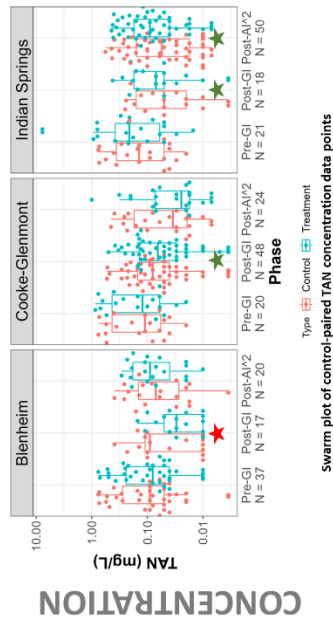


Figure 26: Summary statistics of TN in water quality samples collected from Clintonville sewersheds and results of analyses comparing project phases. Significant differences ($p < 0.05$), determined from Kruskal-Wallis/Dunn's test with Bonferroni corrections, are represented by different letters in box plots. Asterisk denotes differences were significant at $p < 0.1$.

Treatment Sewershed	Pre-GI			Post-GI			Post-GI Summary Statistics			Post-AI ²			Post-AI ² Summary Statistics		
	n	Control Median (mg/L)	Treatment Median (mg/L)	n	Control Median (mg/L)	Treatment Median (mg/L)	p-value	LSM % Phase Difference	n	Control Median (mg/L)	Treatment Median (mg/L)	p-value	LSM % Phase Difference		
Blenheim	36	0.09	0.08	17	0.09	0.03	3.62E-03	102.06	20	0.07	0.09	0.08	15.69		
Cooke-Glenmont	20	0.11	0.13	42	0.09	0.08	6.91E-05	-26.85	24	0.04	0.03	AOV not significant	-53.22		
Indian Springs	21	0.14	0.21	15	0.08	0.12	4.47E-04	-12.08	50	0.06	0.09	2.11E-03	-33.57		



Treatment Sewershed	Pre-GI			Post-GI			Post-GI Summary Statistics			Post-AI ²			Post-AI ² Summary Statistics		
	n	Control Median (lb/ac)	Treatment Median (lb/ac)	n	Control Median (lb/ac)	Treatment Median (lb/ac)	p-value	LSM % Phase Difference	n	Control Median (lb/ac)	Treatment Median (lb/ac)	p-value	LSM % Phase Difference		
Blenheim	31	8.30E-04	1.19E-03	14	2.77E-04	9.97E-05	2.08E-03	-73.54	20	3.73E-04	3.45E-04	0.25	-16.05		
Cooke-Glenmont	16	8.82E-04	5.20E-04	39	5.15E-04	3.13E-04	0.08	-39.37	19	3.14E-04	4.16E-04	AOV not significant	-6.51		
Indian Springs	18	7.47E-04	1.28E-03	14	6.06E-04	1.00E-03	AOV not significant	14.98	44	2.09E-04	6.16E-04	2.41E-04	-12.63		

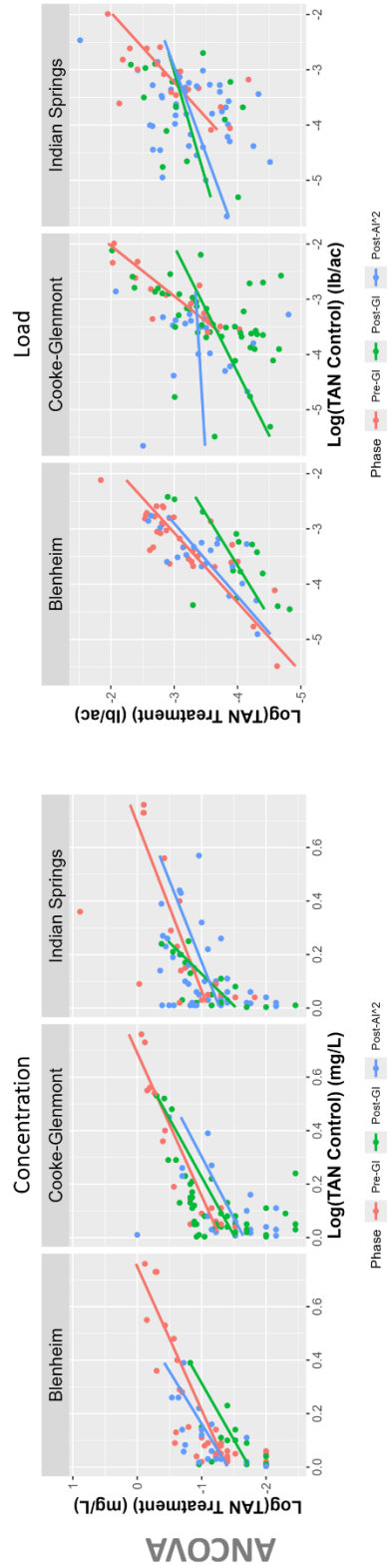
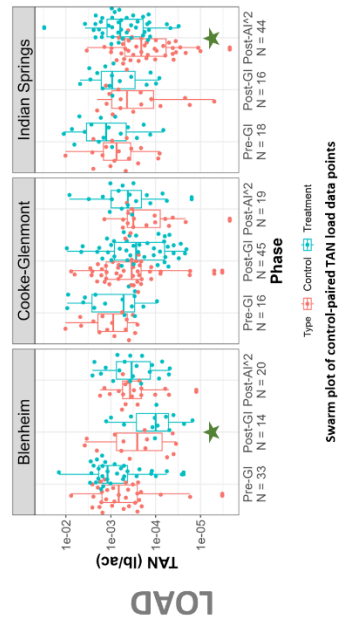
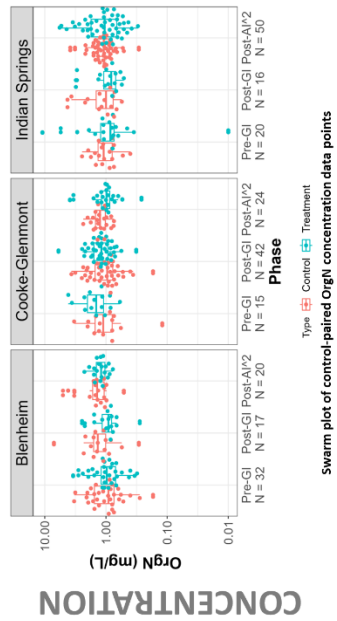


Figure 27: Summary statistics of TAN in water quality samples collected from Clintonville sewersheds and results of analyses comparing project phases. Significant differences ($p < 0.05$), determined from Kruskal-Wallis/Dunn's test with Bonferroni corrections, are represented by different letters in box plots. Asterisk denotes differences were significant at $p < 0.1$.

Treatment Sewershed	Pre-GI			Post-GI			Post-GI Summary Statistics			Post-AI ²			Post-AI ² Summary Statistics		
	n	Control Median (mg/L)	Treatment Median (mg/L)	n	Control Median (mg/L)	Treatment Median (mg/L)	p-value	LSM % Phase Difference	n	Control Median (mg/L)	Treatment Median (mg/L)	p-value	LSM % Phase Difference		
Blenheim	32	0.91	0.98	17	1.36	0.91	0.93	17.01	20	1.39	1.20	AOV not significant	4.10		
Cooke-Glenmont	15	1.11	1.44	42	0.96	1.19	0.08	-20.37	24	1.25	0.98	0.07	-36.33		
Indian Springs	20	1.09	0.85	16	1.00	0.82	0.95	20.11	50	1.09	1.05	0.82	11.93		



Treatment Sewershed	Pre-GI			Post-GI			Post-GI Summary Statistics			Post-AI ²			Post-AI ² Summary Statistics		
	n	Control Median (lb/ac)	Treatment Median (lb/ac)	n	Control Median (lb/ac)	Treatment Median (lb/ac)	p-value	LSM % Phase Difference	n	Control Median (lb/ac)	Treatment Median (lb/ac)	p-value	LSM % Phase Difference		
Blenheim	29	0.01	0.01	14	0.01	3.23E-03	1.94E-04	-51.01	20	0.01	0.01	1.48E-03	-36.55		
Cooke-Glenmont	12	0.01	0.01	40	0.01	0.01	1.63E-05	-22.80	19	0.01	0.01	0.50	127.64		
Indian Springs	18	0.01	0.01	14	0.01	0.01	AOV not significant	37.17	44	4.25E-03	0.01	0.13	107.57		

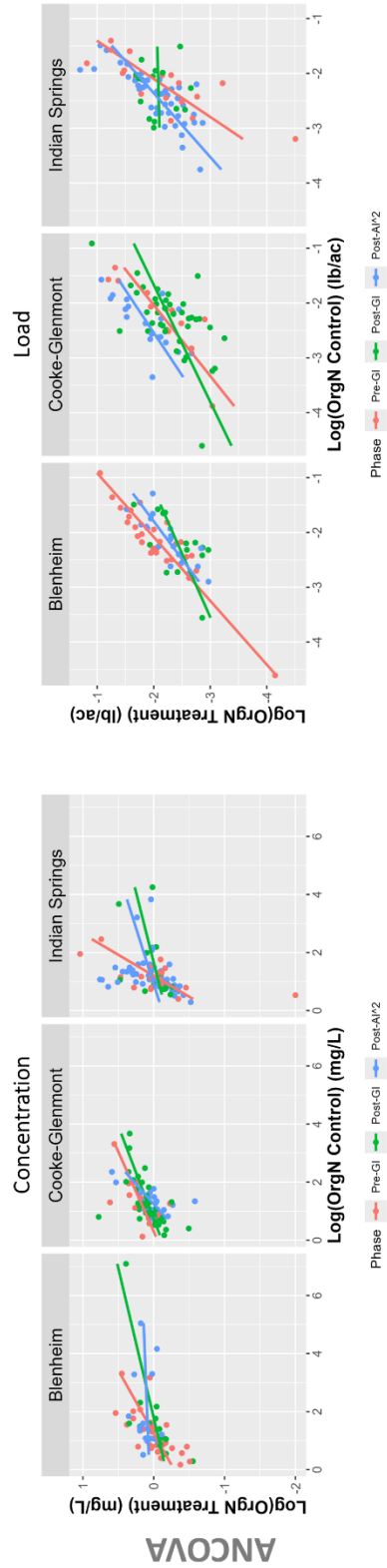
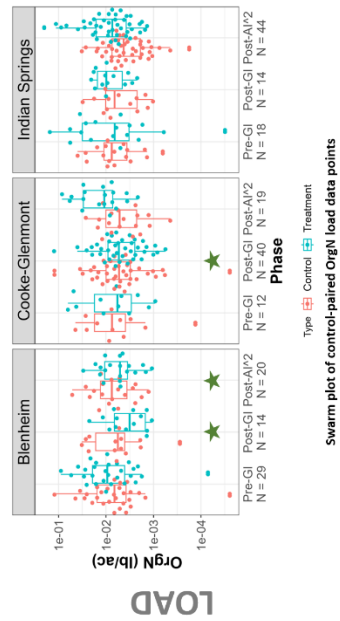
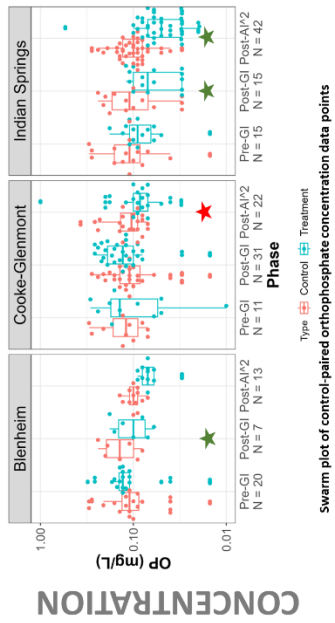


Figure 28: Summary statistics of OrgN in water quality samples collected from Clintonville sewersheds and results of analyses comparing project phases. Significant differences ($p < 0.05$), determined from Kruskal-Wallis/Dunn's test with Bonferroni corrections, are represented by different letters in box plots. Asterisk denotes differences were significant at $p < 0.1$.

Treatment Sewershed	Pre-GI			Post-GI			Post-GI Summary Statistics			Post-AI ²			Post-AI ² Summary Statistics		
	n	Treatment Median (mg/L)	Control Median (mg/L)	n	Treatment Median (mg/L)	Control Median (mg/L)	p-value	LSM % Phase Difference	n	Treatment Median (mg/L)	Control Median (mg/L)	p-value	LSM % Phase Difference		
Blenheim	20	0.11	0.13	7	0.14	0.10	3.51E-03	-22.71	13	0.10	0.07	AOV not significant	-38.49		
Cooke-Glenmont	11	0.12	0.14	31	0.11	0.13	0.06	-34.15	22	0.11	0.09	0.01	1.20		
Indian Springs	15	0.11	0.09	15	0.11	0.07	1.31E-09	-20.70	42	0.10	0.05	8.80E-07	-36.42		



Treatment Sewershed	Pre-GI			Post-GI			Post-GI Summary Statistics			Post-AI ²			Post-AI ² Summary Statistics		
	n	Treatment Median (lb/ac)	Control Median (lb/ac)	n	Treatment Median (lb/ac)	Control Median (lb/ac)	p-value	LSM % Phase Difference	n	Treatment Median (lb/ac)	Control Median (lb/ac)	p-value	LSM % Phase Difference		
Blenheim	18	4.26E-04	8.81E-04	6	5.16E-04	7.59E-04	AOV not significant	-7.23	13	4.33E-04	2.86E-04	0.29	-60.54		
Cooke-Glenmont	10	8.20E-04	5.37E-04	29	3.76E-04	3.17E-04	0.94	29.07	18	3.73E-04	7.84E-04	1.79E-03	201.43		
Indian Springs	15	4.30E-04	6.48E-04	13	3.18E-04	4.32E-04	1.06E-03	3.62	37	3.97E-04	3.78E-04	4.40E-03	-18.65		

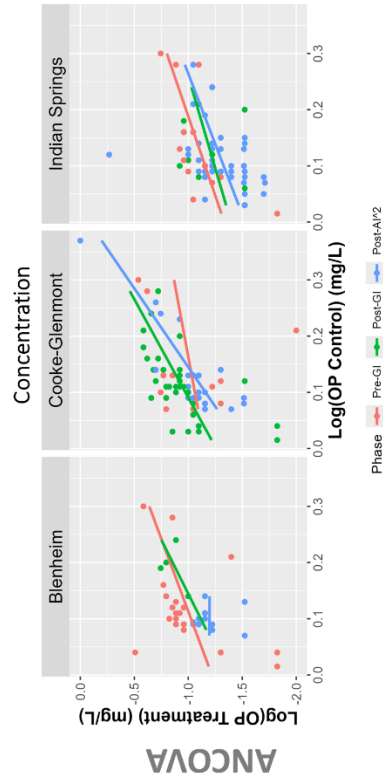
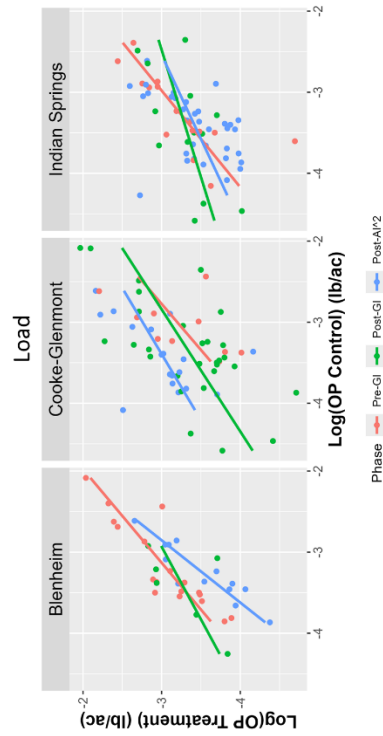
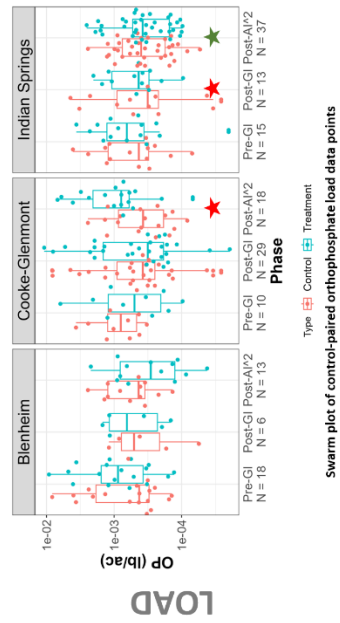
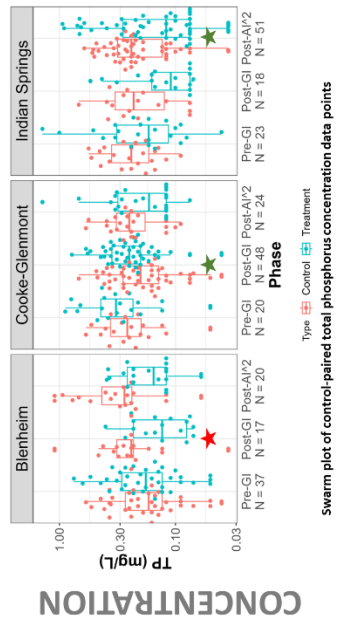


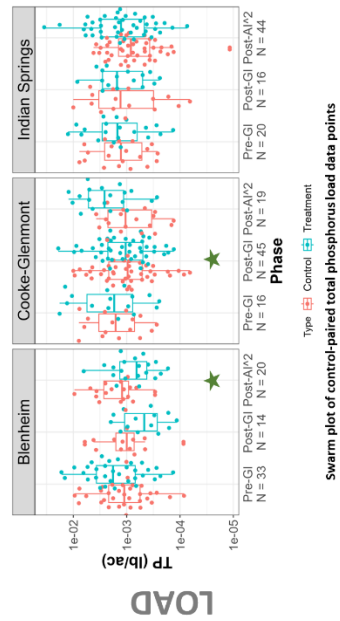
Figure 29: Summary statistics of OP in water quality samples collected from Clintonville sewersheds and results of analyses comparing project phases. Significant differences ($p < 0.05$), determined from Kruskal-Wallis/Dunn's test with Bonferroni corrections, are represented by different letters in box plots. Asterisk denotes differences were significant at $p < 0.1$.

Treatment Sewershed	Pre-GI			Post-GI			Post-AI ²			Post-AI ²			
	n	Control Median (mg/L)	Treatment Median (mg/L)	n	Control Median (mg/L)	Treatment Median (mg/L)	n	Control Median (mg/L)	Treatment Median (mg/L)	p-value	LSM % Phase Difference	p-value	LSM % Phase Difference
Blenheim	37	0.17	0.18	17	0.24	0.13	20	0.28	0.16	1.85E-10	12.38	AOV not significant	-29.56
Cooke-Glenmont	20	0.26	0.33	48	0.20	0.25	24	0.25	0.17	1.17E-03	-26.97	0.21	-33.12
Indian Springs	23	0.24	0.17	18	0.23	0.11	51	0.24	0.12	AOV not significant	12.69	1.31E-03	-18.00



Swarm plot of control-paired total phosphorus concentration data points

Treatment Sewershed	Pre-GI			Post-GI			Post-AI ²			Post-AI ²			
	n	Control Median (lb/ac)	Treatment Median (lb/ac)	n	Control Median (lb/ac)	Treatment Median (lb/ac)	n	Control Median (lb/ac)	Treatment Median (lb/ac)	p-value	LSM % Phase Difference	p-value	LSM % Phase Difference
Blenheim	33	1.11E-03	1.80E-03	14	9.96E-04	4.86E-04	20	1.22E-03	6.52E-04	AOV not significant	-66.82	0.03	-61.36
Cooke-Glenmont	16	1.62E-03	1.73E-03	45	9.58E-04	1.04E-03	19	1.05E-03	2.60E-03	0.01	-17.64	0.92	122.67
Indian Springs	20	1.28E-03	1.49E-03	16	1.33E-03	1.51E-03	44	8.36E-04	1.27E-03	AOV not significant	-4.28	0.10	28.05



Swarm plot of control-paired total phosphorus load data points

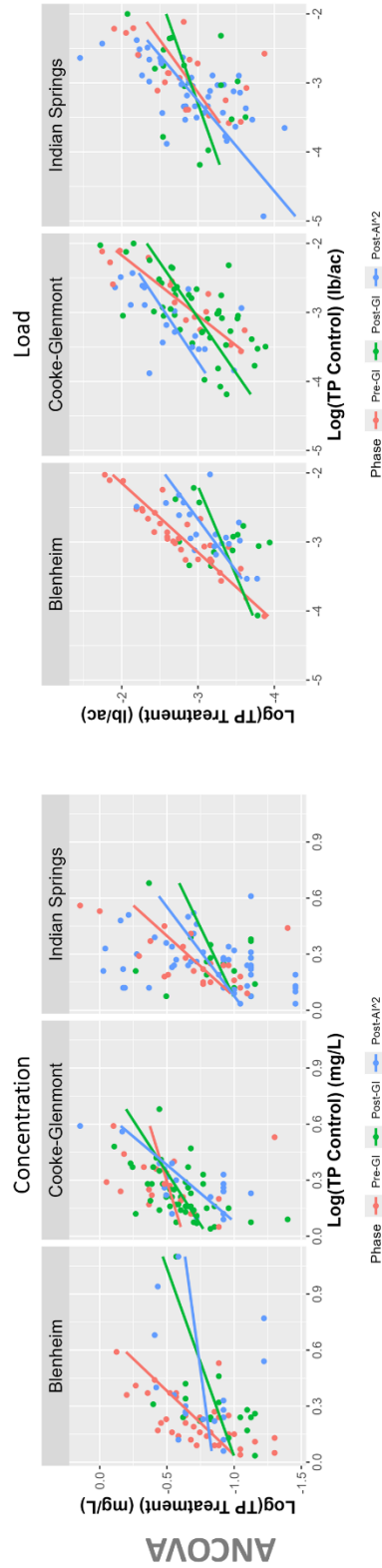


Figure 30: Summary statistics of TP in water quality samples collected from Clintonville sewersheds and results of analyses comparing project phases. Significant differences ($p < 0.05$), determined from Kruskal-Wallis/Dunn's test with Bonferroni corrections, are represented by different letters in box plots. Asterisk denotes differences were significant at $p < 0.1$.

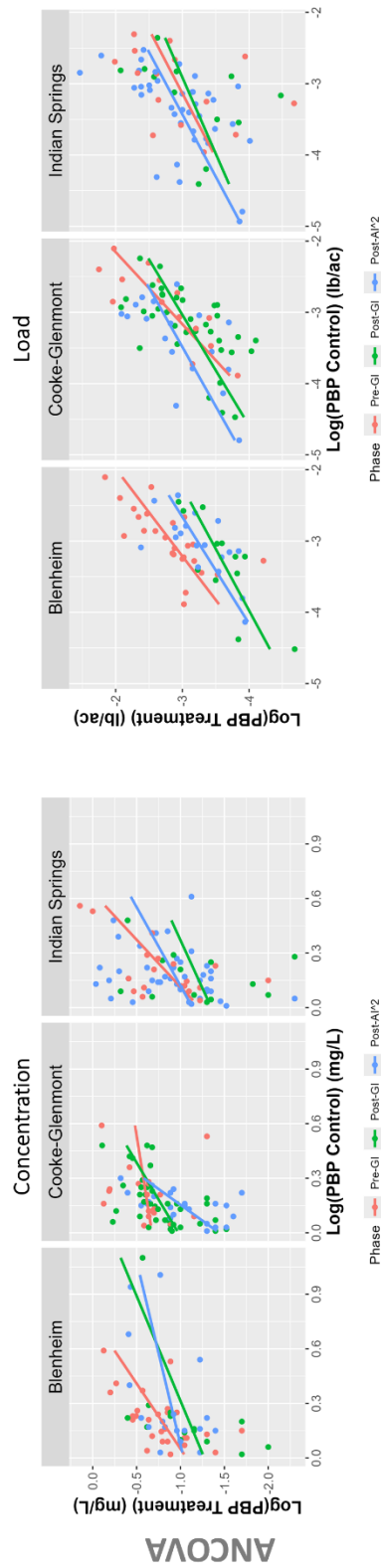
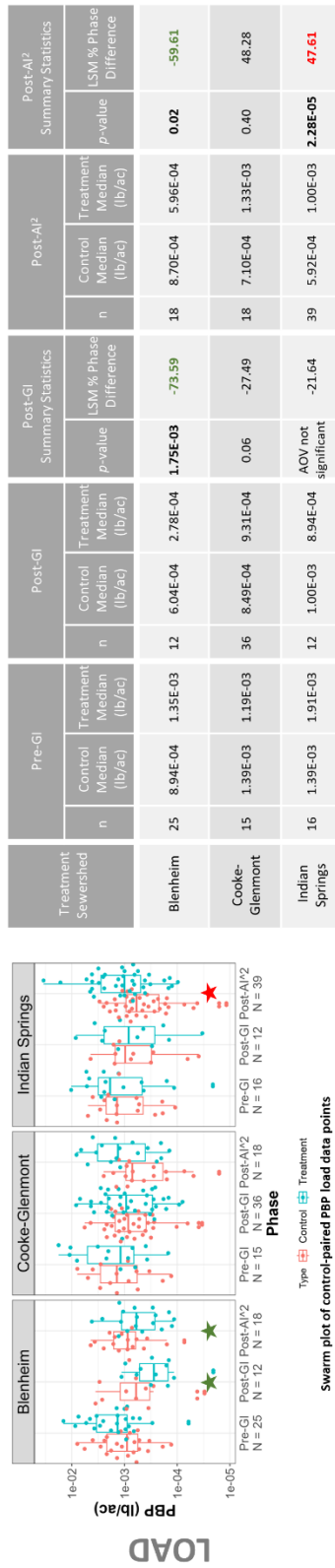
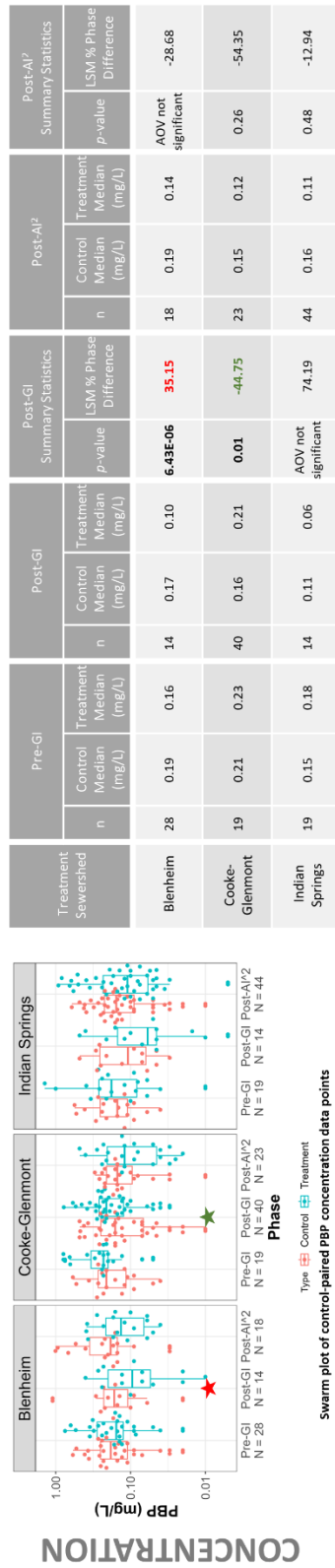


Figure 31: Summary statistics of PBP in water quality samples collected from Clintonville sewersheds and results of analyses comparing project phases. Significant differences ($p < 0.05$), determined from Kruskal-Wallis/Dunn's test with Bonferroni corrections, are represented by different letters in box plots. Asterisk denotes differences were significant at $p < 0.1$.

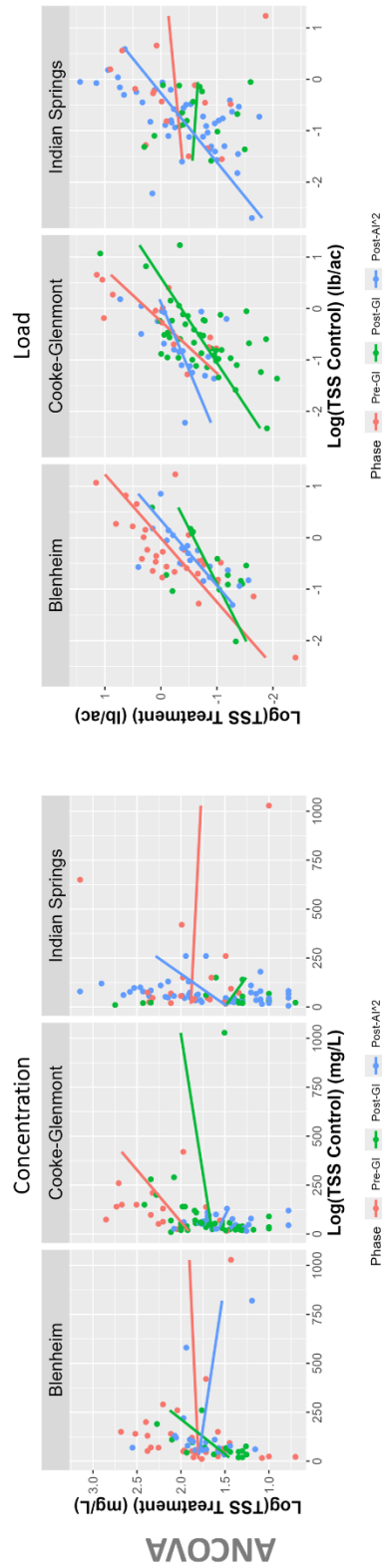
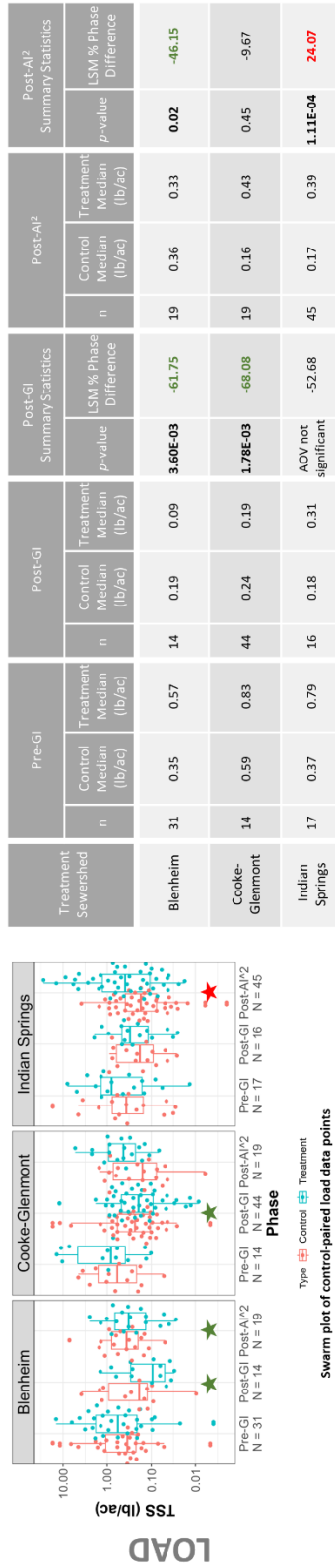
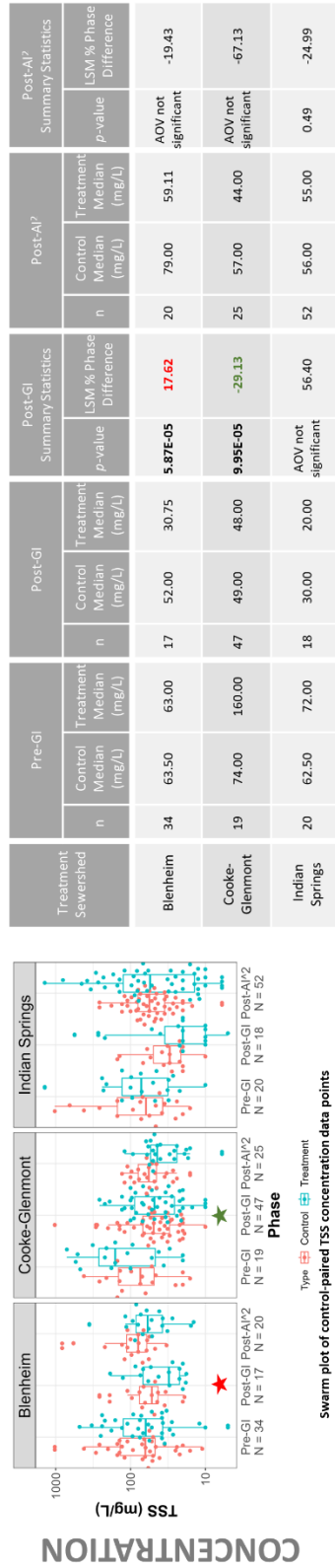
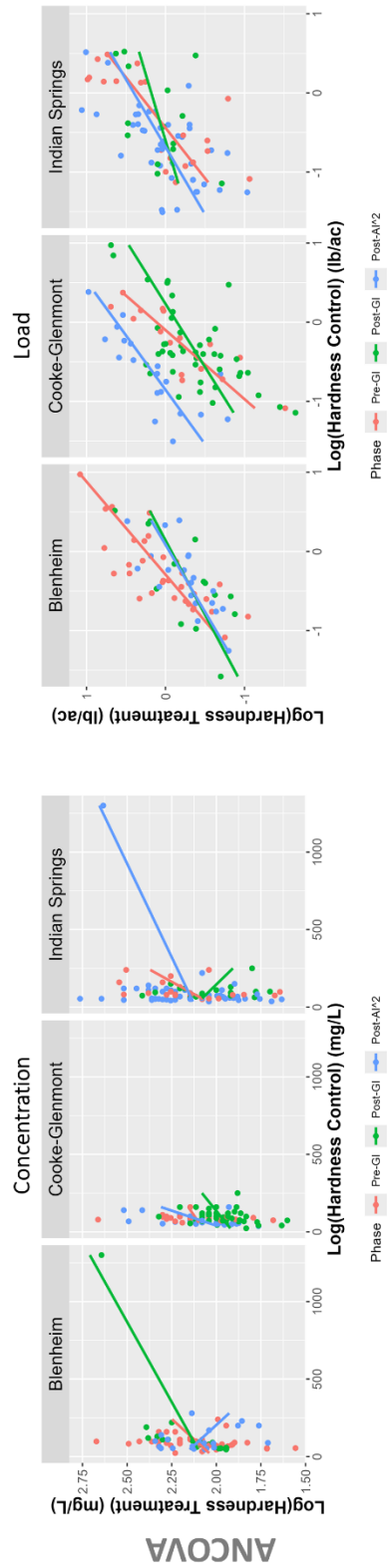
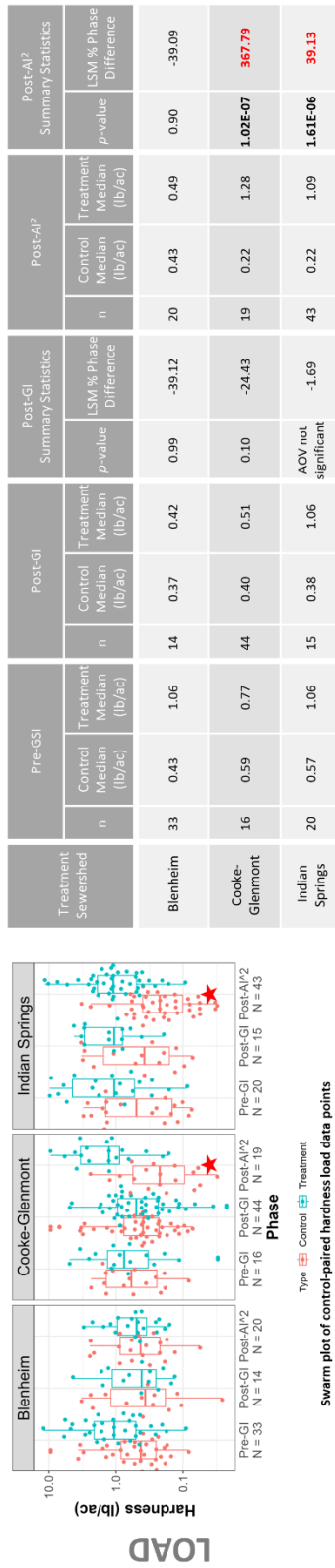
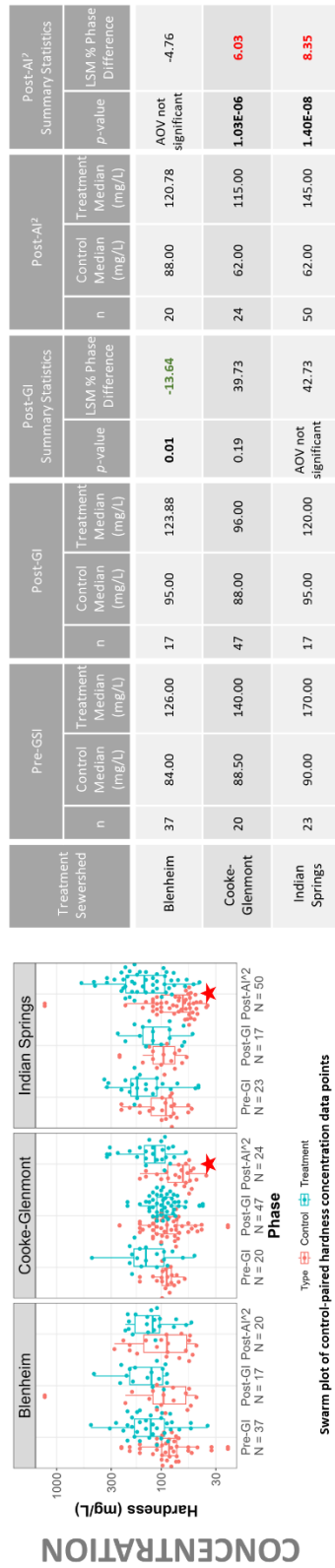


Figure 32: Summary statistics of TSS in water quality samples collected from Clintonville sewersheds and results of analyses comparing project phases. Significant differences ($p < 0.05$), determined from Kruskal-Wallis/Dunn's test with Bonferroni corrections, are represented by different letters in box plots. Asterisk denotes differences were significant at $p < 0.1$.

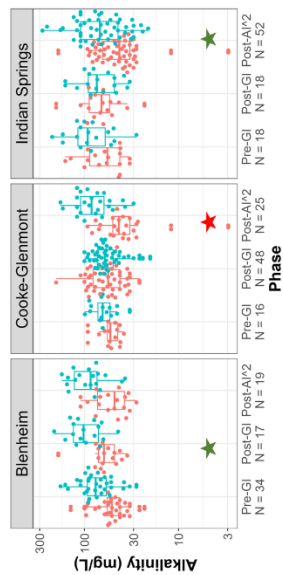


Treatment Sewsershed	Pre-GSI			Post-GI			Post-GI Summary Statistics			Post-AI ²			
	n	Control Median (mg/L)	Treatment Median (mg/L)	n	Control Median (mg/L)	Treatment Median (mg/L)	p-value	LSM % Phase Difference	n	Control Median (mg/L)	Treatment Median (mg/L)	p-value	LSM % Phase Difference
Blenheim	37	84.00	126.00	17	95.00	123.88	0.01	-13.64	20	88.00	120.78	AOV not significant	-4.76
Cooke-Glenmont	20	88.50	140.00	47	88.00	95.00	0.19	39.73	24	62.00	115.00	1.08E-06	6.03
Indian Springs	23	90.00	170.00	17	95.00	120.00	AOV not significant	42.73	50	62.00	145.00	1.40E-08	8.35

Treatment Sewsershed	Pre-GSI			Post-GI			Post-GI Summary Statistics			Post-AI ²			
	n	Control Median (lb/ac)	Treatment Median (lb/ac)	n	Control Median (lb/ac)	Treatment Median (lb/ac)	p-value	LSM % Phase Difference	n	Control Median (lb/ac)	Treatment Median (lb/ac)	p-value	LSM % Phase Difference
Blenheim	33	0.43	1.06	14	0.37	0.42	0.99	-39.12	20	0.43	0.49	0.90	-39.09
Cooke-Glenmont	16	0.59	0.77	44	0.40	0.51	0.10	-24.43	19	0.22	1.28	1.02E-07	367.79
Indian Springs	20	0.57	1.06	15	0.38	1.06	AOV not significant	-1.69	43	0.22	1.09	1.61E-06	39.13

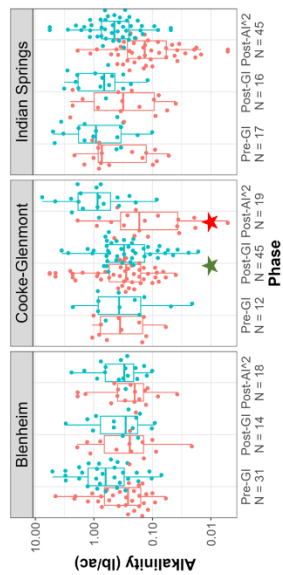
Figure 33: Summary statistics of Hardness in water quality samples collected from Clintonville sewersheds and results of analyses comparing project phases. Significant differences ($p < 0.05$), determined from Kruskal-Wallis/Dunn's test with Bonferroni corrections, are represented by different letters in box plots. Asterisk denotes differences were significant at $p < 0.1$.

Treatment Sewershed	Pre-GI		Post-GI		Post-GI Summary Statistics		Post-AI ²		Post-AI ² Summary Statistics			
	n	Control Median (mg/L)	Treatment Median (mg/L)	Control Median (mg/L)	Treatment Median (mg/L)	p-value	LSM % Phase Difference	n	Control Median (mg/L)	Treatment Median (mg/L)	p-value	LSM % Phase Difference
Blenheim	34	51.00	76.00	62.00	102.27	5.91E-07	-3.97	19	48.00	86.03	AOV not significant	18.61
Cooke-Glenmont	16	53.00	64.00	56.00	61.00	AOV not significant	53.09	25	43.00	84.00	8.16E-06	39.51
Indian Springs	18	57.00	92.50	66.00	74.00	AOV not significant	20.38	52	42.50	68.50	1.04E-06	-7.90



Swarm plot of control-paired alkalinity concentration data points

Treatment Sewershed	Pre-GI		Post-GI		Post-GI Summary Statistics		Post-AI ²		Post-AI ² Summary Statistics			
	n	Control Median (lb/ac)	Treatment Median (lb/ac)	Control Median (lb/ac)	Treatment Median (lb/ac)	p-value	LSM % Phase Difference	n	Control Median (lb/ac)	Treatment Median (lb/ac)	p-value	LSM % Phase Difference
Blenheim	31	0.26	0.63	0.24	0.29	0.78	-30.97	18	0.20	0.30	0.42	-22.70
Cooke-Glenmont	12	0.36	0.37	0.28	0.31	0.01	-10.08	19	0.17	0.87	3.95E-05	502.54
Indian Springs	17	0.73	0.92	0.32	0.67	AOV not significant	-1.89	45	0.14	0.45	0.29	-4.82



Swarm plot of control-paired alkalinity load data points

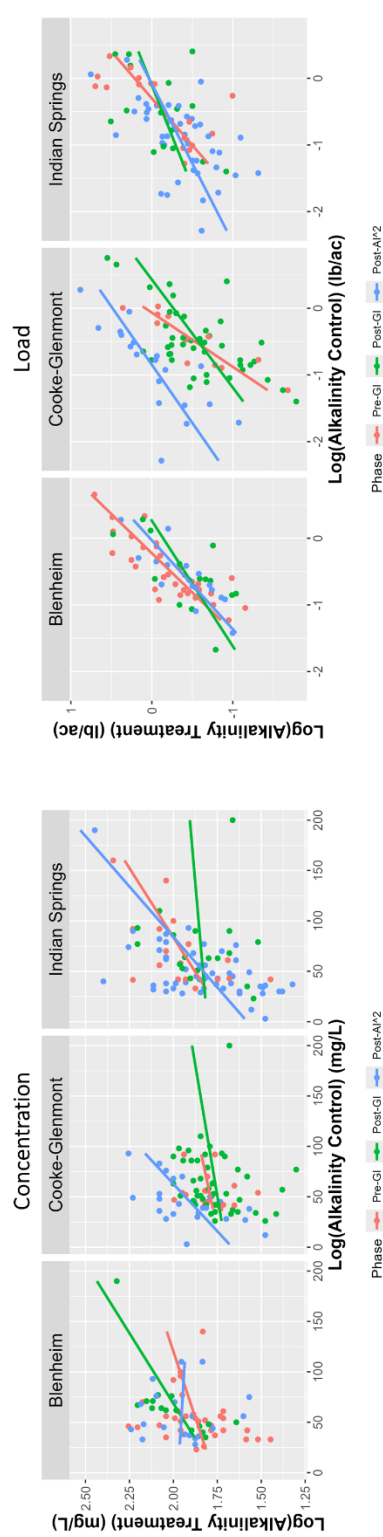
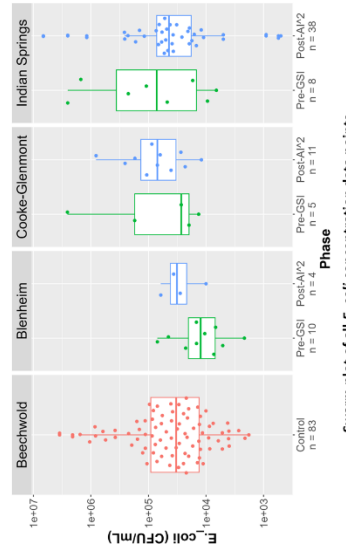


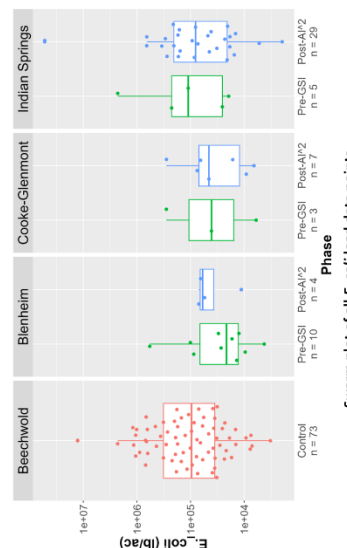
Figure 34: Summary statistics of Alkalinity in water quality samples collected from Clintonville sewersheds and results of analyses comparing project phases. Significant differences ($p < 0.05$), determined from Kruskal-Wallis/Dunn's test with Bonferroni corrections, are represented by different letters in box plots. Asterisk denotes differences were significant at $p < 0.1$.

Treatment Sewershed	Data Subset	Pre-GSI			Post-AI ²			Summary Statistics	
		n	Control Median	Treatment Median	n	Control Median	Treatment Median	p-value	LSM % Phase Difference
Blenheim	All	10	-	12550	4	-	32237	-	-
	Control-Paired	8	20000	12409	3	57300	36453	AOV not significant	74.09
Cooke-Glenmont	All	5	-	26900	11	-	70000	-	-
	Control-Paired	5	59000	26900	9	40000	70000	0.56	-15.30
Indian Springs	All	8	-	78100	38	-	44000	-	-
	Control-Paired	7	24110	47200	30	33000	43954	0.21	-63.61

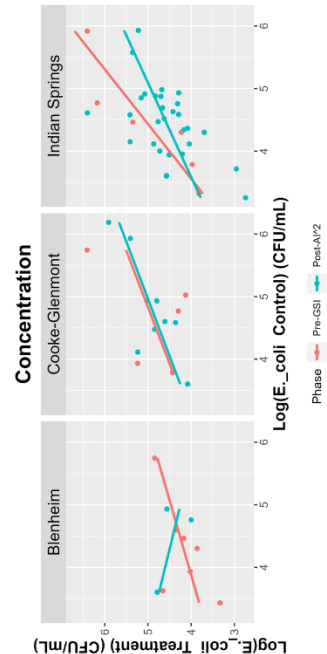
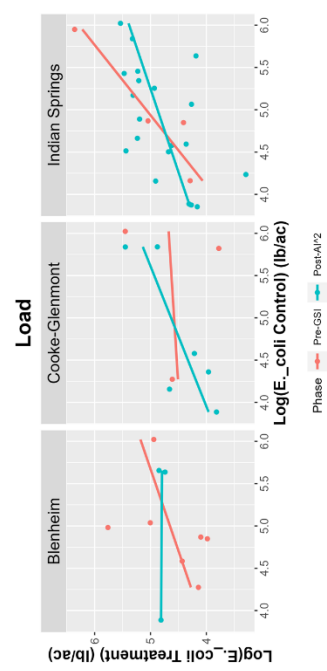


CONCENTRATION

Treatment Sewershed	Data Subset	Pre-GSI			Post-AI ²			Summary Statistics	
		n	Control Median	Treatment Median	n	Control Median	Treatment Median	p-value	LSM % Phase Difference
Blenheim	All	10	-	21939	4	-	59769	-	-
	Control-Paired	8	73888	21347	3	433202	64769	AOV not significant	41.21
Cooke-Glenmont	All	3	-	40633	7	-	45495	-	-
	Control-Paired	3	662420	40633	6	29499	27265	0.21	38.67
Indian Springs	All	5	-	110555	29	-	80754	-	-
	Control-Paired	4	72192	53208	21	59729	85119	0.70	-31.00



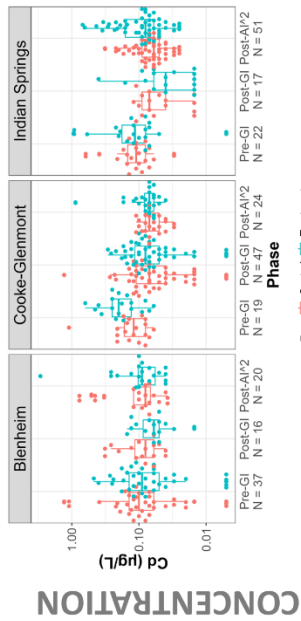
LOAD



ANCOVA

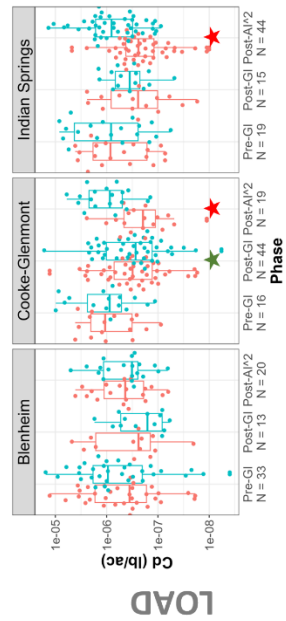
Figure 35: Summary statistics of *E. coli* in water quality samples collected from Clintonville sewersheds and results of analyses comparing project phases. Significant differences ($p < 0.05$), determined from Kruskal-Wallis/Dunn's test with Bonferroni corrections, are represented by different letters in box plots. Asterisk denotes differences were significant at $p < 0.1$.

Treatment Sewershed	Pre-GI			Post-GI			Post-GI Summary Statistics			Post-AI ²			Post-AI ² Summary Statistics					
	n	Control Median (µg/L)	Treatment Median (µg/L)	n	Control Median (µg/L)	Treatment Median (µg/L)	p-value	LSM % Phase Difference	n	Control Median (µg/L)	Treatment Median (µg/L)	p-value	LSM % Phase Difference	n	Control Median (µg/L)	Treatment Median (µg/L)	p-value	LSM % Phase Difference
Blenheim	37	0.10	0.09	16	0.08	0.06	AOV not significant	49.46	20	0.08	0.09	AOV not significant	26.17	20	0.08	0.09	AOV not significant	26.17
Cooke-Glenmont	19	0.12	0.20	47	0.07	0.08	0.47	18.93	24	0.07	0.07	AOV not significant	-48.14	24	0.07	0.07	AOV not significant	-48.14
Indian Springs	22	0.11	0.12	17	0.07	0.04	AOV not significant	117.43	51	0.06	0.08	AOV not significant	-1.75	51	0.06	0.08	AOV not significant	-1.75



Swarm plot of control-paired cadmium concentration data points

Treatment Sewershed	Pre-GI			Post-GI			Post-GI Summary Statistics			Post-AI ²			Post-AI ² Summary Statistics					
	n	Control Median (lb/ac)	Treatment Median (lb/ac)	n	Control Median (lb/ac)	Treatment Median (lb/ac)	p-value	LSM % Phase Difference	n	Control Median (lb/ac)	Treatment Median (lb/ac)	p-value	LSM % Phase Difference	n	Control Median (lb/ac)	Treatment Median (lb/ac)	p-value	LSM % Phase Difference
Blenheim	33	3.58E-07	9.45E-07	13	2.39E-07	1.60E-07	0.05	-51.32	20	4.34E-07	3.21E-07	0.11	-23.46	20	4.34E-07	3.21E-07	0.11	-23.46
Cooke-Glenmont	16	1.07E-06	8.75E-07	44	3.12E-07	2.72E-07	0.01	-40.40	19	1.95E-07	8.65E-07	0.04	109.25	19	1.95E-07	8.65E-07	0.04	109.25
Indian Springs	19	8.45E-07	8.20E-07	15	2.44E-07	3.54E-07	AOV not significant	-40.98	44	2.40E-07	8.07E-07	0.01	66.48	44	2.40E-07	8.07E-07	0.01	66.48



Swarm plot of control-paired cadmium load data points

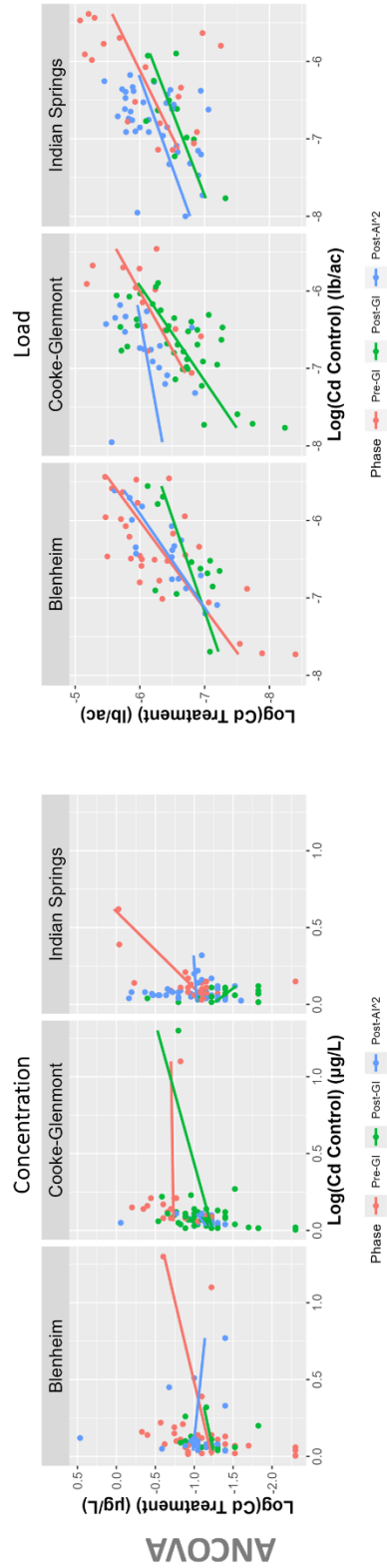
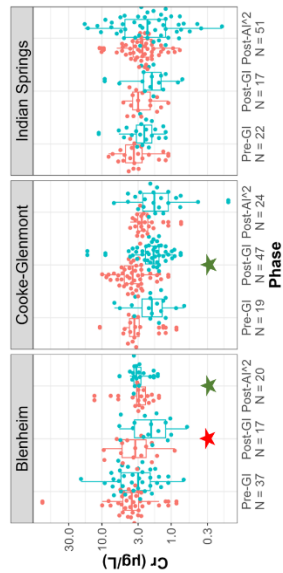


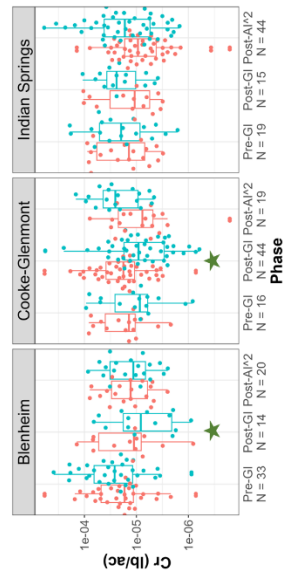
Figure 36: Summary statistics of Cadmium in water quality samples collected from Clintonville sewersheds and results of analyses comparing project phases. Significant differences ($p < 0.05$), determined from Kruskal-Wallis/Dunn's test with Bonferroni corrections, are represented by different letters in box plots. Asterisk denotes differences were significant at $p < 0.1$.

Treatment Sewershed	Pre-GI			Post-GI			Post-GI Summary Statistics			Post-AI ²			Post-AI ² Summary Statistics		
	n	Control Median (µg/L)	Treatment Median (µg/L)	n	Control Median (µg/L)	Treatment Median (µg/L)	p-value	LSM % Phase Difference	n	Control Median (µg/L)	Treatment Median (µg/L)	p-value	LSM % Phase Difference		
Blenheim	37	3.70	3.00	17	3.30	1.95	6.66E-04	50.98	20	2.94	3.18	3.38E-04	-1.92		
Cooke-Glenmont	19	3.40	1.90	47	3.60	1.80	1.23E-08	-14.74	24	2.65	1.75	AOV not significant	-21.89		
Indian Springs	22	3.45	2.45	17	3.00	1.90	AOV not significant	8.40	51	2.60	2.20	AOV not significant	-11.14		



Swarm plot of control-paired chromium concentration data points

Treatment Sewershed	Pre-GI			Post-GI			Post-GI Summary Statistics			Post-AI ²			Post-AI ² Summary Statistics		
	n	Control Median (lb/ac)	Treatment Median (lb/ac)	n	Control Median (lb/ac)	Treatment Median (lb/ac)	p-value	LSM % Phase Difference	n	Control Median (lb/ac)	Treatment Median (lb/ac)	p-value	LSM % Phase Difference		
Blenheim	33	1.69E-05	2.62E-05	14	1.17E-05	8.54E-06	0.03	-62.26	20	1.29E-05	1.15E-05	0.37	-30.30		
Cooke-Glenmont	16	1.39E-05	8.60E-06	44	1.78E-05	9.11E-06	0.02	-26.03	19	7.68E-06	2.54E-05	AOV not significant	203.71		
Indian Springs	19	1.39E-05	1.97E-05	15	1.08E-05	2.40E-05	AOV not significant	8.96	44	9.34E-06	1.67E-05	0.09	41.27		



Swarm plot of control-paired chromium load data points

CONCENTRATION

LOAD

ANCOVA

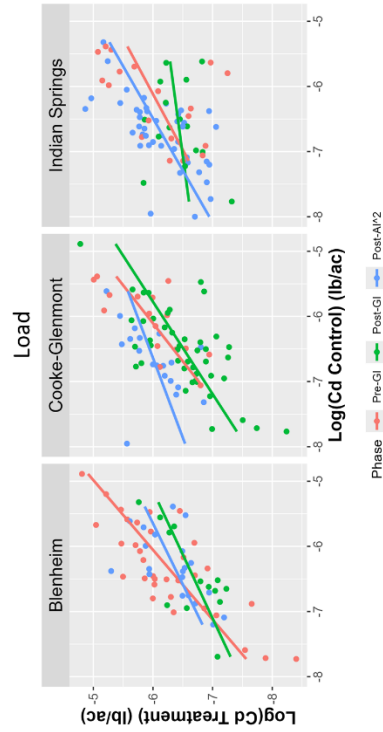
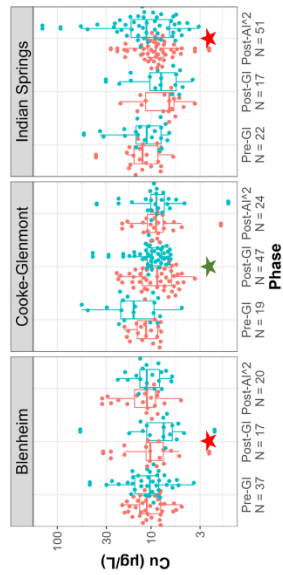
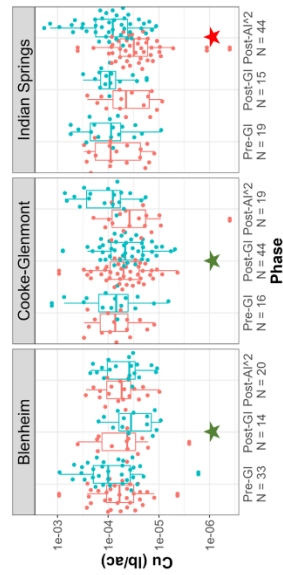


Figure 37: Summary statistics of Chromium in water quality samples collected from Clintonville sewersheds and results of analyses comparing project phases. Significant differences ($p < 0.05$), determined from Kruskal-Wallis/Dunn's test with Bonferroni corrections, are represented by different letters in box plots. Asterisk denotes differences were significant at $p < 0.1$.

Treatment Sewershed	Pre-GSI			Post-GI			Post-GI Summary Statistics			Post-AI ²			Post-AI ² Summary Statistics		
	n	Control Median (µg/L)	Treatment Median (µg/L)	n	Control Median (µg/L)	Treatment Median (µg/L)	p-value	LSM % Phase Difference	n	Control Median (µg/L)	Treatment Median (µg/L)	p-value	LSM % Phase Difference		
Blenheim	37	11.10	10.30	17	10.20	7.33	6.29E-04	19.21	20	11.05	11.13	AOV not significant	-5.84		
Cooke-Glenmont	19	11.30	15.35	47	8.60	9.80	7.34E-06	-11.34	24	8.85	8.75	AOV not significant	-39.87		
Indian Springs	22	12.30	11.15	17	6.40	7.80	0.48	28.83	51	8.90	11.20	0.02	8.44		

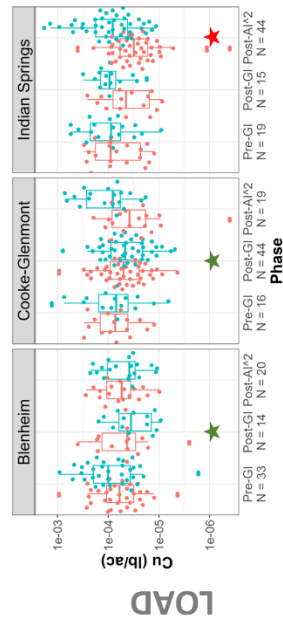


swarm plot of control-paired copper concentration data points



swarm plot of control-paired copper load data points

Treatment Sewershed	Pre-GSI			Post-GI			Post-GI Summary Statistics			Post-AI ²			Post-AI ² Summary Statistics		
	n	Control Median (lb/ac)	Treatment Median (lb/ac)	n	Control Median (lb/ac)	Treatment Median (lb/ac)	p-value	LSM % Phase Difference	n	Control Median (lb/ac)	Treatment Median (lb/ac)	p-value	LSM % Phase Difference		
Blenheim	33	5.98E-05	9.98E-05	14	4.22E-05	3.56E-05	0.02	-53.77	20	5.45E-05	3.84E-05	0.48	-39.30		
Cooke-Glenmont	16	7.26E-05	6.95E-05	44	4.98E-05	4.63E-05	0.02	-29.69	19	3.80E-05	8.11E-05	AOV not significant	124.35		
Indian Springs	19	8.91E-05	8.77E-05	15	4.45E-05	9.41E-05	AOV not significant	2.57	44	3.14E-05	8.13E-05	3.53E-09	51.09		



swarm plot of control-paired copper load data points

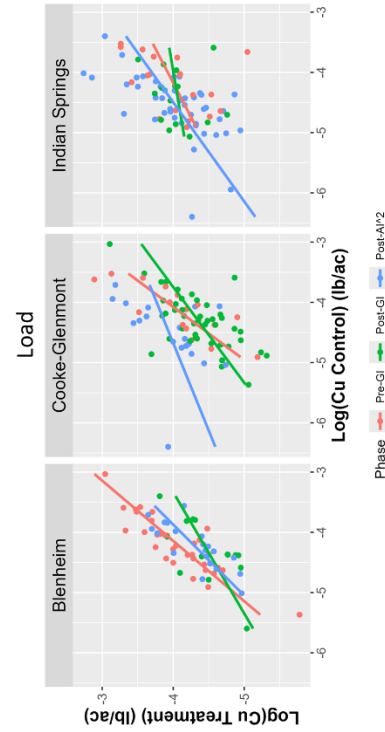
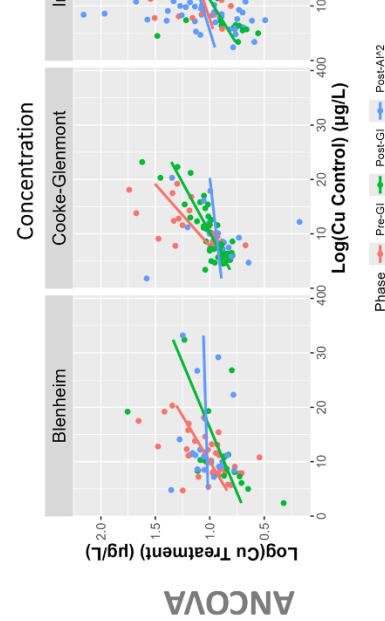
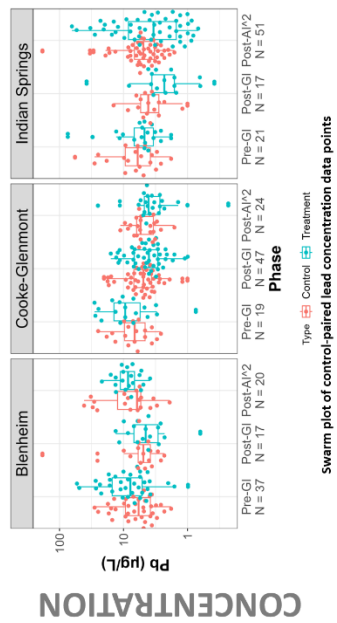


Figure 38: Summary statistics of Copper in water quality samples collected from Clintonville sewersheds and results of analyses comparing project phases. Significant differences ($p < 0.05$), determined from Kruskal-Wallis/Dunn's test with Bonferroni corrections, are represented by different letters in box plots. Asterisk denotes differences were significant at $p < 0.1$.

Treatment Sewershed	Pre-GI			Post-GI			Post-GI Summary Statistics			Post-AI ²			Post-AI ² Summary Statistics		
	n	Control Median (µg/L)	Treatment Median (µg/L)	n	Control Median (µg/L)	Treatment Median (µg/L)	p-value	LSM % Phase Difference	n	Control Median (µg/L)	Treatment Median (µg/L)	p-value	LSM % Phase Difference		
Blenheim	37	5.80	7.80	17	4.90	4.50	AOV not significant	71.26	20	6.15	8.50	AOV not significant	-6.15		
Cooke-Glenmont	19	6.70	9.40	47	4.90	4.00	0.22	-16.20	24	5.40	4.05	AOV not significant	-46.59		
Indian Springs	21	6.00	4.70	17	4.10	2.30	AOV not significant	54.62	51	4.90	3.40	AOV not significant	-24.06		



Treatment Sewershed	Pre-GI			Post-GI			Post-GI Summary Statistics			Post-AI ²			Post-AI ² Summary Statistics		
	n	Control Median (lb/ac)	Treatment Median (lb/ac)	n	Control Median (lb/ac)	Treatment Median (lb/ac)	p-value	LSM % Phase Difference	n	Control Median (lb/ac)	Treatment Median (lb/ac)	p-value	LSM % Phase Difference		
Blenheim	33	3.80E-05	6.90E-05	14	2.09E-05	1.48E-05	0.03	-63.24	20	3.60E-05	2.96E-05	0.42	-38.92		
Cooke-Glenmont	16	4.38E-05	4.04E-05	44	2.63E-05	1.88E-05	0.35	-39.07	19	1.44E-05	4.21E-05	0.26	112.84		
Indian Springs	18	3.38E-05	4.92E-05	15	2.04E-05	2.47E-05	AOV not significant	-28.73	44	1.72E-05	2.78E-05	0.03	35.58		

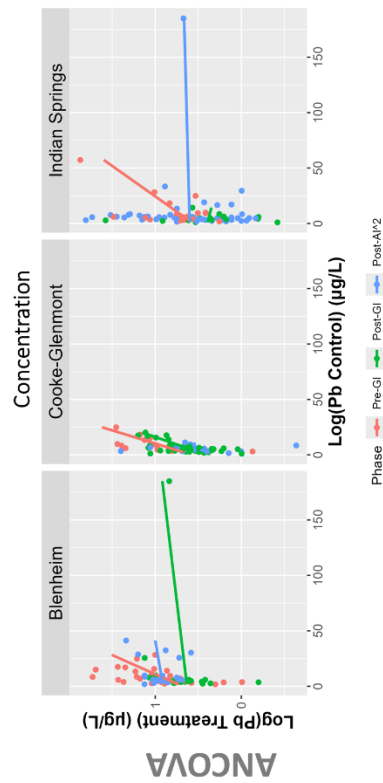
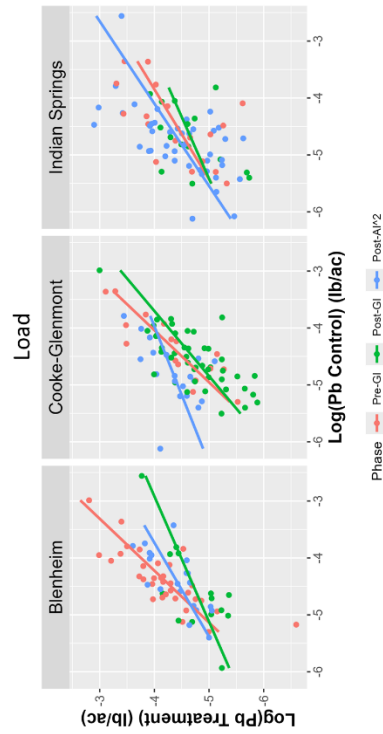
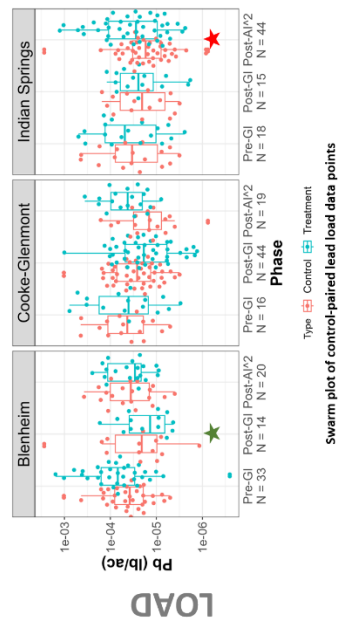
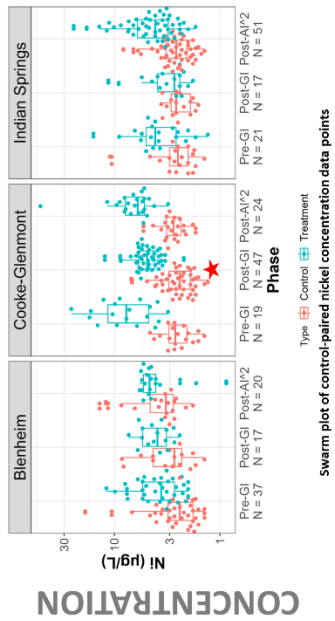


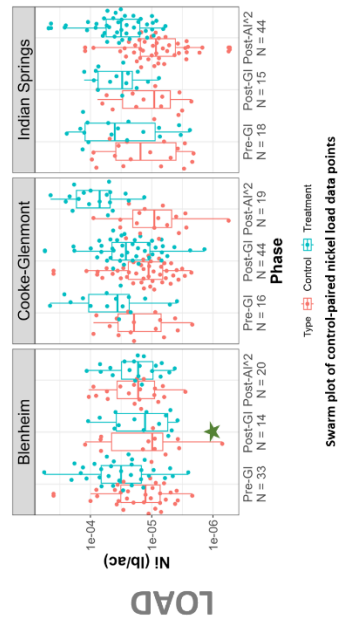
Figure 39: Summary statistics of Lead in water quality samples collected from Clintonville sewersheds and results of analyses comparing project phases. Significant differences ($p < 0.05$), determined from Kruskal-Wallis/Dunn's test with Bonferroni corrections, are represented by different letters in box plots. Asterisk denotes differences were significant at $p < 0.1$.

Treatment Sewershed	Pre-GI			Post-GI			Post-GI Summary Statistics			Post-AI ²			Post-AI ² Summary Statistics					
	n	Control Median (µg/L)	Treatment Median (µg/L)	n	Control Median (µg/L)	Treatment Median (µg/L)	p-value	LSM % Phase Difference	n	Control Median (µg/L)	Treatment Median (µg/L)	p-value	LSM % Phase Difference	n	Control Median (µg/L)	Treatment Median (µg/L)	p-value	LSM % Phase Difference
Blenheim	37	2.40	3.60	17	2.70	3.91	AOV not significant	-2.66	20	3.25	4.66	AOV not significant	1.46	20	3.25	4.66	AOV not significant	1.46
Cooke-Glenmont	19	2.65	7.70	47	2.40	4.90	4.34E-17	30.74	24	2.75	6.00	AOV not significant	-15.79	24	2.75	6.00	AOV not significant	-15.79
Indian Springs	21	2.50	4.10	17	2.60	2.70	AOV not significant	33.18	51	2.60	4.10	AOV not significant	17.77	51	2.60	4.10	AOV not significant	17.77



Swarm plot of control-paired nickel concentration data points

Treatment Sewershed	Pre-GI			Post-GI			Post-GI Summary Statistics			Post-AI ²			Post-AI ² Summary Statistics					
	n	Control Median (lb/ac)	Treatment Median (lb/ac)	n	Control Median (lb/ac)	Treatment Median (lb/ac)	p-value	LSM % Phase Difference	n	Control Median (lb/ac)	Treatment Median (lb/ac)	p-value	LSM % Phase Difference	n	Control Median (lb/ac)	Treatment Median (lb/ac)	p-value	LSM % Phase Difference
Blenheim	33	1.27E-05	3.16E-05	14	9.83E-06	1.29E-05	0.02	-45.20	20	1.67E-05	1.67E-05	0.09	-51.65	20	1.67E-05	1.67E-05	0.09	-51.65
Cooke-Glenmont	16	1.95E-05	3.62E-05	44	1.13E-05	2.65E-05	0.06	-41.10	19	9.07E-06	7.08E-05	0.18	150.57	19	9.07E-06	7.08E-05	0.18	150.57
Indian Springs	18	1.63E-05	4.05E-05	15	9.11E-06	3.03E-05	AOV not significant	16.34	44	8.54E-06	3.16E-05	0.06	53.01	44	8.54E-06	3.16E-05	0.06	53.01



Swarm plot of control-paired nickel load data points

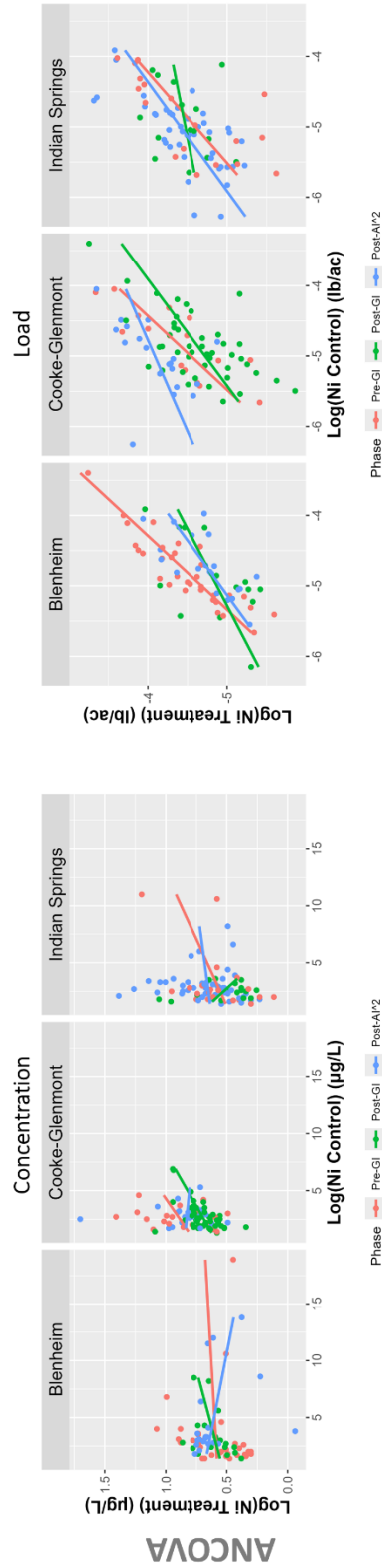
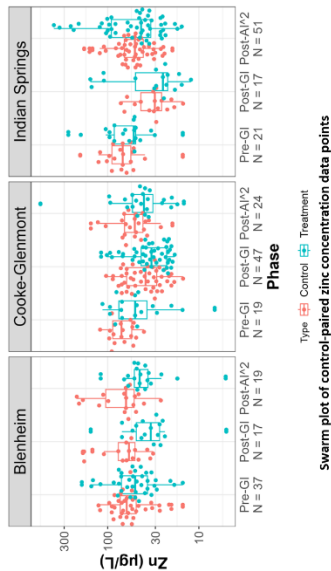


Figure 40: Summary statistics of Nickel in water quality samples collected from Clintonville sewersheds and results of analyses comparing project phases. Significant differences ($p < 0.05$), determined from Kruskal-Wallis/Dunn's test with Bonferroni corrections, are represented by different letters in box plots. Asterisk denotes differences were significant at $p < 0.1$.

Treatment Sewershed	Pre-GI			Post-GI			Post-GI Summary Statistics			Post-AI2			Post-AI2 Summary Statistics	
	n	Control Median (µg/L)	Treatment Median (µg/L)	n	Control Median (µg/L)	Treatment Median (µg/L)	p-value	LSM % Phase Difference	n	Control Median (µg/L)	Treatment Median (µg/L)	p-value	LSM % Phase Difference	
Blenheim	37	61.80	50.00	17	58.40	33.65	AOV not significant	6.58	19	62.90	44.55	AOV not significant	-31.59	
Cooke-Glenmont	19	70.60	50.00	47	38.40	33.10	0.44	-2.64	24	50.40	40.05	0.47	24.36	
Indian Springs	21	68.40	51.80	17	30.40	24.80	AOV not significant	19.65	51	50.30	43.00	AOV not significant	-2.49	



Treatment Sewershed	Pre-GI			Post-GI			Post-GI Summary Statistics			Post-AI2			Post-AI2 Summary Statistics	
	n	Control Median (lb/ac)	Treatment Median (lb/ac)	n	Control Median (lb/ac)	Treatment Median (lb/ac)	p-value	LSM % Phase Difference	n	Control Median (lb/ac)	Treatment Median (lb/ac)	p-value	LSM % Phase Difference	
Blenheim	33	2.78E-04	4.23E-04	14	2.46E-04	1.36E-04	0.03	-63.63	19	3.17E-04	2.04E-04	0.15	-57.66	
Cooke-Glenmont	16	4.13E-04	1.95E-04	44	2.02E-04	1.58E-04	0.01	5.96	19	2.13E-04	6.47E-04	0.54	306.57	
Indian Springs	18	2.85E-04	4.81E-04	15	1.81E-04	3.31E-04	AOV not significant	8.63	44	1.67E-04	3.60E-04	0.27	57.29	

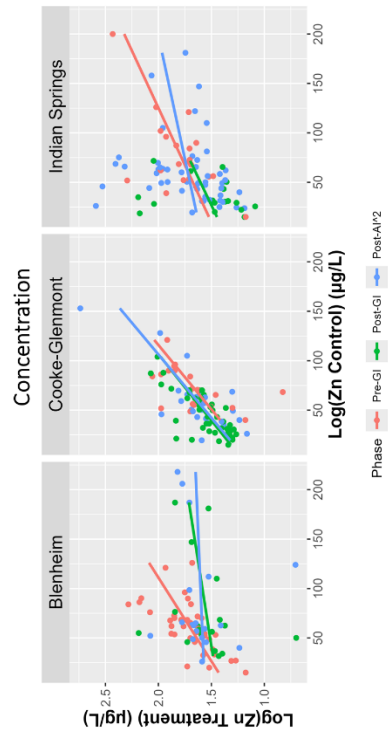
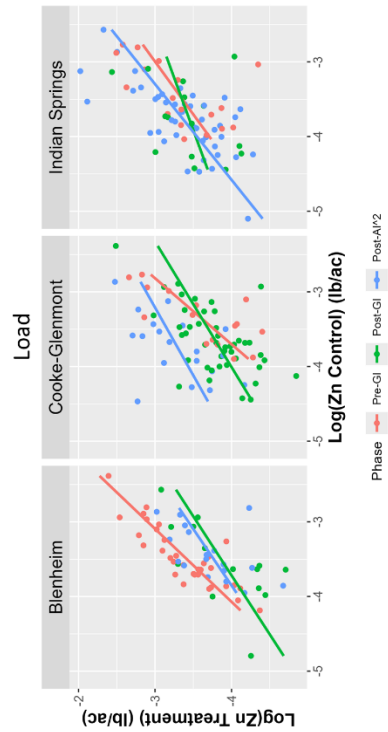
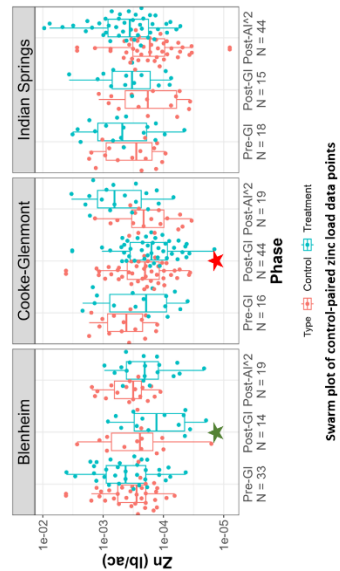


Figure 41: Summary statistics of Zinc in water quality samples collected from Clintonville sewersheds and results of analyses comparing project phases. Significant differences ($p < 0.05$), determined from Kruskal-Wallis/Dunn's test with Bonferroni corrections, are represented by different letters in box plots. Asterisk denotes differences were significant at $p < 0.1$

Appendix D: Rainfall-Water Quality Correlation Analysis

Rainfall characteristics were paired with pollutant concentration and load data for all available data points, and the relationship between rainfall and water quality variables was assessed. Data were subset by site and assessed for normality. Non-parametric Spearman correlations were generated between water quality and rainfall characteristics for each project site for each phase.

Correlation analyses between rainfall characteristics and water quality parameters generally demonstrate that substantial changes occurred between project phases in each watershed. Rainfall depth tended to be positively correlated with pollutant loads in the pre-GI phase; however, those correlations were almost universally weakened or lost in the post-GI phase. Correlations between rainfall intensity (both peak 5-minute and average) and metals (both concentration and load) at CG and IS underwent sizeable shifts in magnitude and direction across project phases. Metal loads at both CG and IS were almost completely decoupled from rainfall factors following the installation of GI. In the post-AI² phase at IS, these relationships reemerged and loosely resembled pre-GI conditions. The relationships between nutrient concentrations and rainfall characteristics at BG were strongest during the post-AI² phase. Nutrient loads at BG were mostly driven by peak 5-minute rainfall intensity in the post-GI phase and by rainfall depth in the post-AI² phase. This change was likely driven by the establishment of the Park of Roses constructed wetland which received low flows from the BG watershed. Correlations between rainfall depth and duration and nutrient loads at CG was mostly reduced post-GI and generally absent in the post-AI² phase.

Blenheim

Correlation analyses showed that concentrations of most nutrient species (i.e., TAN, TKN, OrgN, PBP, OP, TP) were positively correlated with peak 5-minute rainfall intensity and negatively correlated with rainfall depth at BG during the pre-GI phase (Figure 42). Metals concentrations and rainfall characteristics were often not significantly correlated in this phase with the exception of a single negative correlation between Pb and rainfall duration. In the post-GI phase, all positive correlations between nutrient concentrations and peak 5-minute rainfall intensity observed in the pre-GI phase disappeared, while negative correlations emerged for NO₂₋₃, InOrgN, and TN concentrations. Significant correlations between concentrations of Cd, Cr, and Pb and rainfall duration (positive), peak 5-minute rainfall intensity (negative), and average rainfall intensity were observed in the post-GI phase. Cu concentrations were also negatively correlated with average rainfall intensity in the post-GI phase. Unlike other phases, correlations between rainfall characteristics and nutrient concentrations were found to be highly species-specific in the post-AI² phase. Concentrations of NO₂₋₃, InOrgN, and TN were all positively correlated with rainfall depth, peak 5-minute rainfall intensity, and average rainfall intensity; PBP and TP concentrations were negatively correlated with these rainfall characteristics. Negative correlations between TAN and rainfall depth and peak 5-minute rainfall intensity and also TKN and peak 5-minute rainfall intensity and average rainfall intensity were also observed in the post-AI² phase. Concentrations of Cr, Cu, and Pb were negatively correlated with rainfall depth while Ni was positively correlated with these parameters. Ni was also negatively correlated with average rainfall intensity.

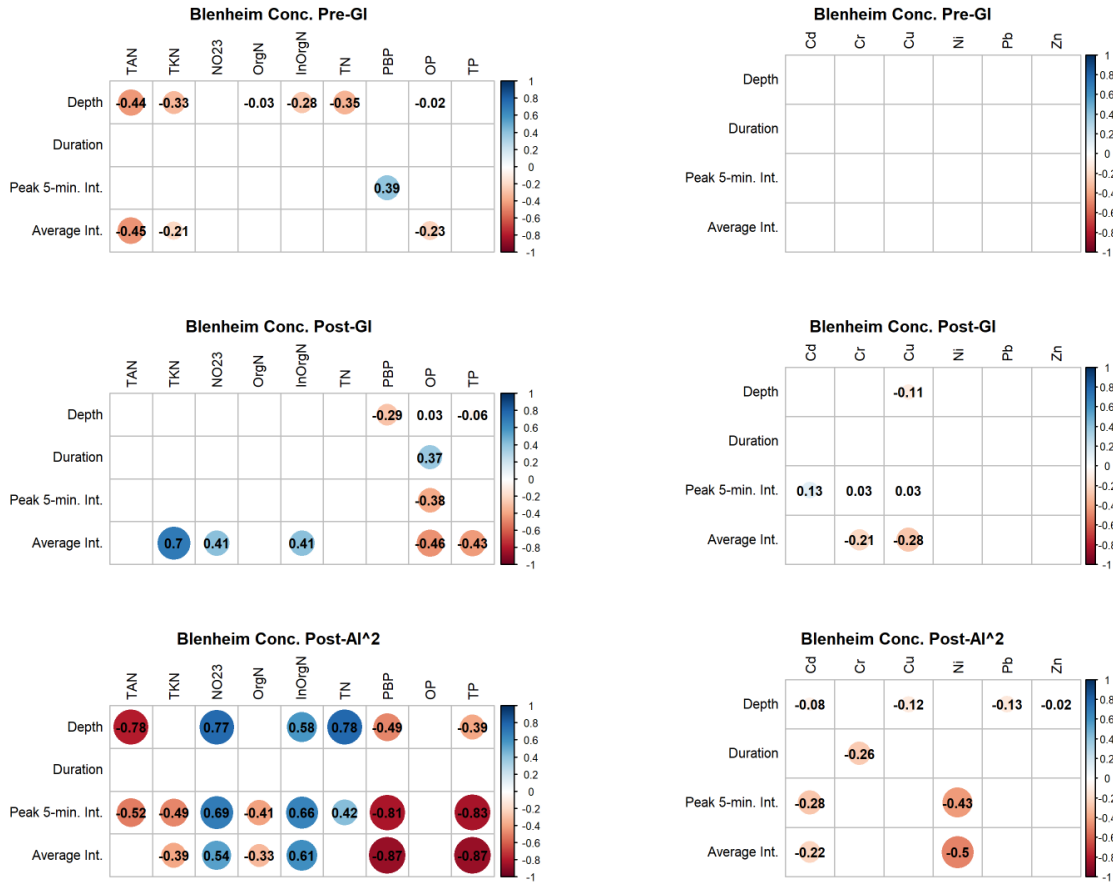


Figure 42: Spearman correlation matrices at Blenheim between rainfall characteristics and nutrient and metal concentrations across project phases. Statistically significant ($p < 0.05$) concentrations shown in correlograms.

During the pre-GI phase, correlation analyses revealed that loads for several nutrient species (i.e., TKN, OrgN, TN, PBP, TP) were positively correlated with rainfall depth at BG; some positive correlations between average rainfall intensity were also observed (i.e., OrgN, TN, TP) (Figure 43). Aside from Cd, loads of all metals species were positively correlated with depth in the pre-GI phase. Nutrient loads for all studied species were negatively correlated with peak 5-minute rainfall intensity during the post-GI phase, while metal loads were positively correlated with rainfall duration for all species except Zn. In the post-AI² phase, nutrient loads for all studied species were positively correlated with rainfall depth with the exception of TAN (negative correlation). Positive correlations were observed between loads of TN, TP, and PBP

and rainfall duration during this phase. Cu and Ni loads were positively correlated with rainfall depth.

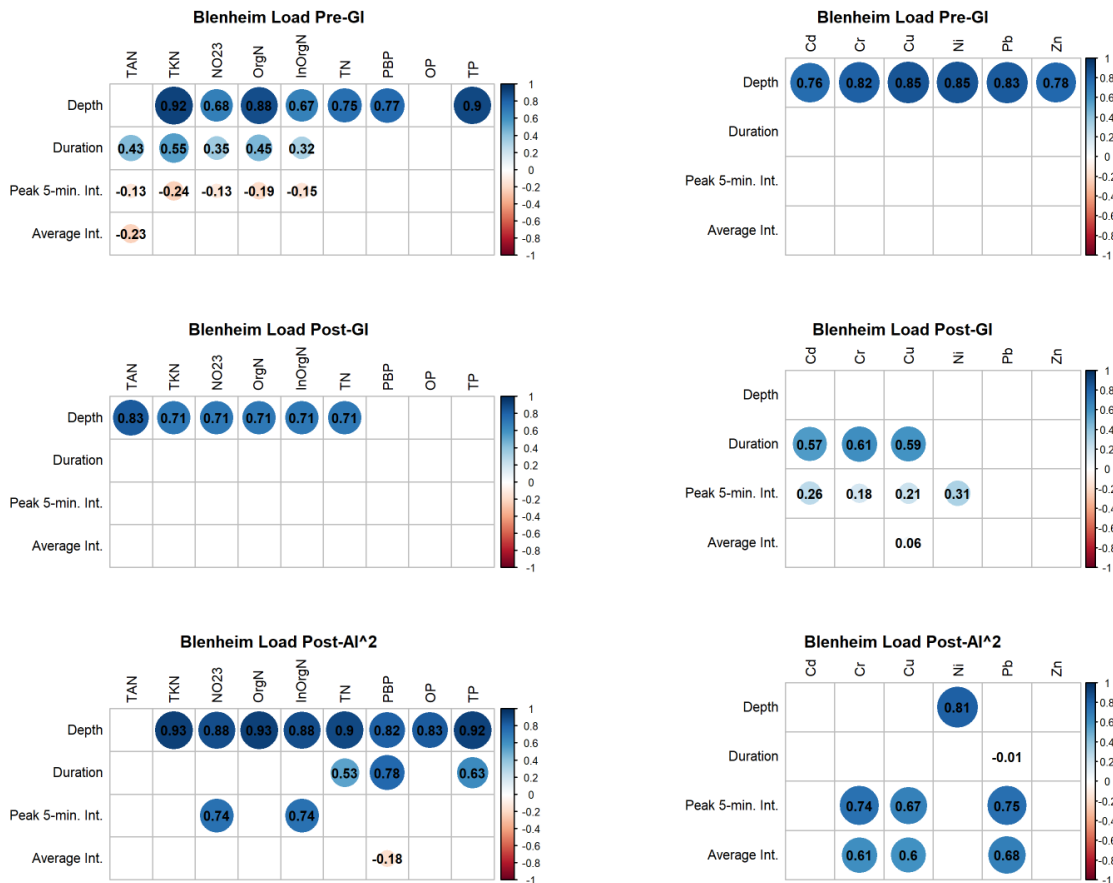


Figure 43: Spearman correlation matrices at Blenheim between rainfall characteristics and nutrient and metal loads across project phases. Statistically significant ($p < 0.05$) concentrations shown in correlograms.

Cooke-Glenmont

In the pre-GI phase at CG, InOrgN, concentrations of TN, and OP were positively correlated with rainfall depth, peak 5-minute intensity, and average intensity (Figure 44). Meanwhile, TKN, OrgN, PBP, and TP concentrations were negatively correlated with rainfall duration. Weak correlations were observed between the concentration of many metals species and rainfall characteristics in the pre-GI phase at CG. In the post-GI phase, concentrations of

TKN, OrgN, TN, PBP, and TP were all negatively correlated with rainfall depth and duration. Statistically significant correlations between rainfall characteristics and metals concentrations were generally absent in the post-GI at CG. In the post-AI² phase, concentrations of almost all nutrients were negatively correlated with average rainfall intensity. Concentrations of NO₂₋₃, InOrgN, and TN were positively correlated with rainfall duration, while TAN was negatively correlated with this parameter. Concentrations of Cd, Cr, Ni, and Pb were negatively correlated with peak 5-minute rainfall intensity during the post-AI² phase. Some negative correlations between metals concentrations and rainfall depth (Cd and Ni) and average rainfall intensity (Cr and Pb) were also observed during this phase.

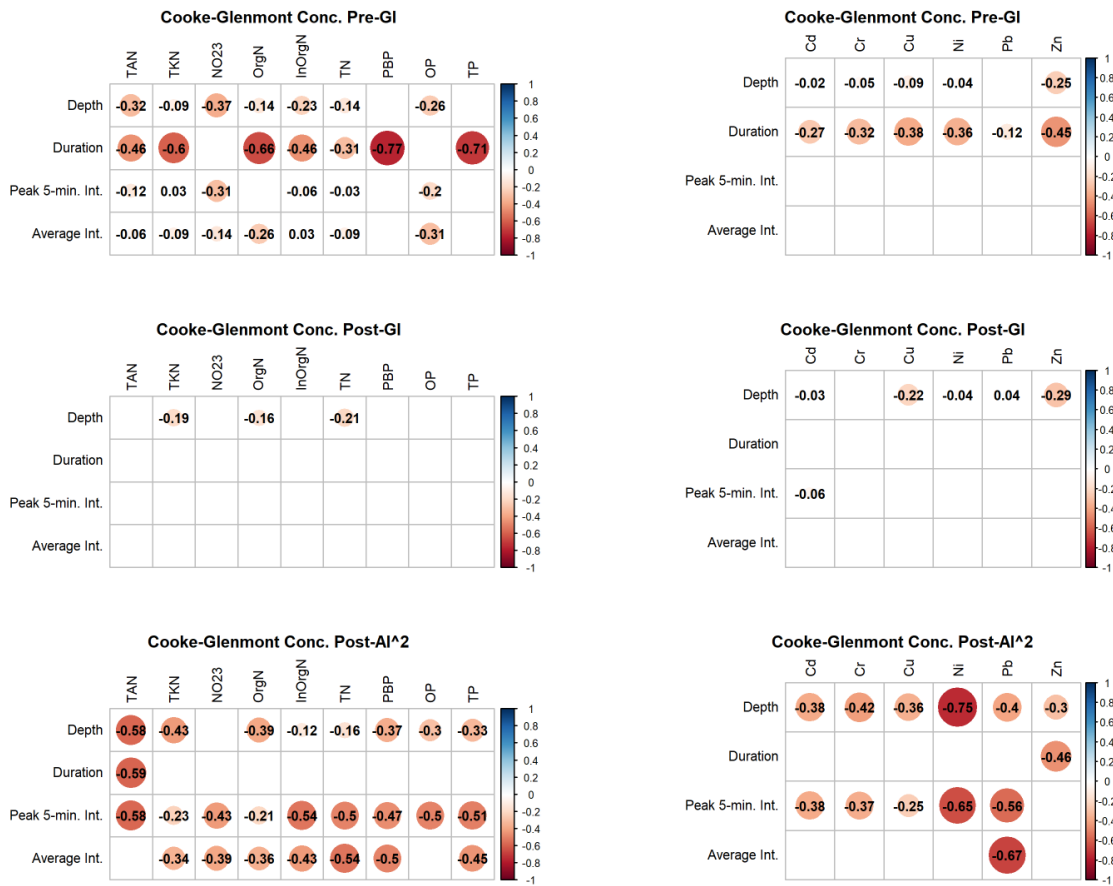


Figure 44: Spearman correlation matrices at Cooke-Glenmont between rainfall characteristics and nutrient and metal concentrations across project phases. Statistically significant ($p < 0.05$) concentrations shown in correlograms.

Pre-GI load correlations at CG showed that TAN was negatively associated with TAN for all rainfall characteristics, and all other nutrient loads were positively correlated with all rainfall characteristics (Figure 45). All metals were positively correlated with peak 5-minute rainfall intensity during the pre-GI phase at CG. In the post-GI phase, mostly nutrient species were positively correlated with rainfall depth, duration, and peak 5-minute intensity. No significant correlations were detected between rainfall characteristics and metals loads during this phase. In the post-AI² phase, most nutrient loads were negatively associated with both peak 5-minute and

average rainfall intensity. Correlations between metal loads and peak 5-minute and average rainfall intensity were detected in the post-AI² phase at CG, but these correlations were small.

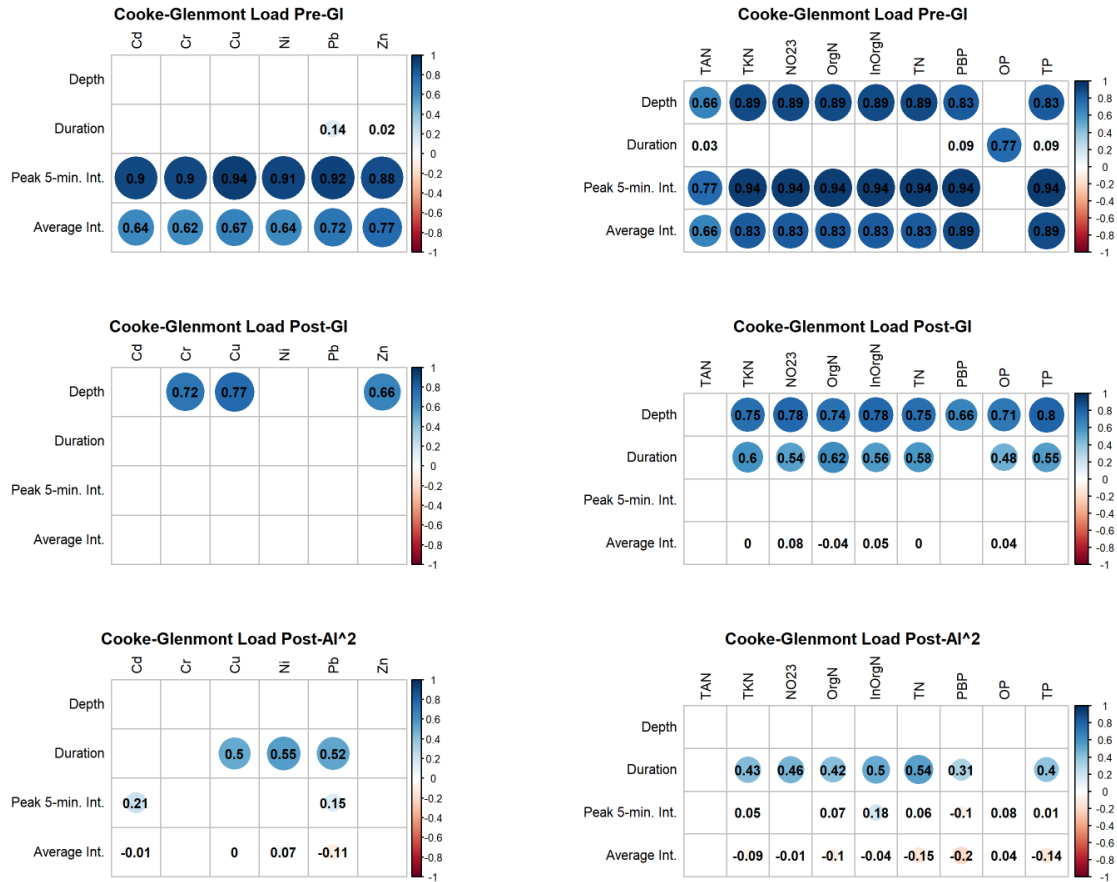


Figure 45: Spearman correlation matrices at Cooke-Glenmont between rainfall characteristics and nutrient and metal loads across project phases. Statistically significant ($p < 0.05$) concentrations shown in correlograms.

Indian Springs

In the pre-GI phase at IS, most nutrient concentrations were positively correlated with rainfall depth (TAN, TKN, OrgN, TN, TP) and duration (TAN, TKN, OrgN, TN, PBP, TP) (Figure 46). Notably, NO₂₋₃ was negatively correlated with depth and duration while InOrgN was negatively correlated with duration. Some metal concentrations were negatively correlated with rainfall depth (Cr, Cu, Zn) and peak 5-minute rainfall intensity (Cd, Ni). Of the studied sites,

changes in correlations between pre-GI and post-GI for nutrient concentrations were most similar at IS. Rainfall duration, average intensity, and depth had mixed positive and negative correlations across nutrient concentrations. In the post-GI phase, select metal concentrations were positively correlated with rainfall duration (Cr, Pb, Zn) and negatively correlated with peak 5-minute (Cr, Pb, Zn) and average rainfall intensity (Cr, Zn). In the post-AI² phase, most nutrient concentrations were negatively correlated with rainfall depth (NO₂₋₃, OrgN, TN, PBP, OP, TP) and some with duration (NO₂₋₃, InOrgN, TN). Positive correlations were also detected between peak 5-minute (TAN, NO₂₋₃, InOrgN) and average (NO₂₋₃, InOrgN) rainfall intensities. Most metal concentrations were negatively correlated with average rainfall intensity (Cr, Cu, Pb, Zn).

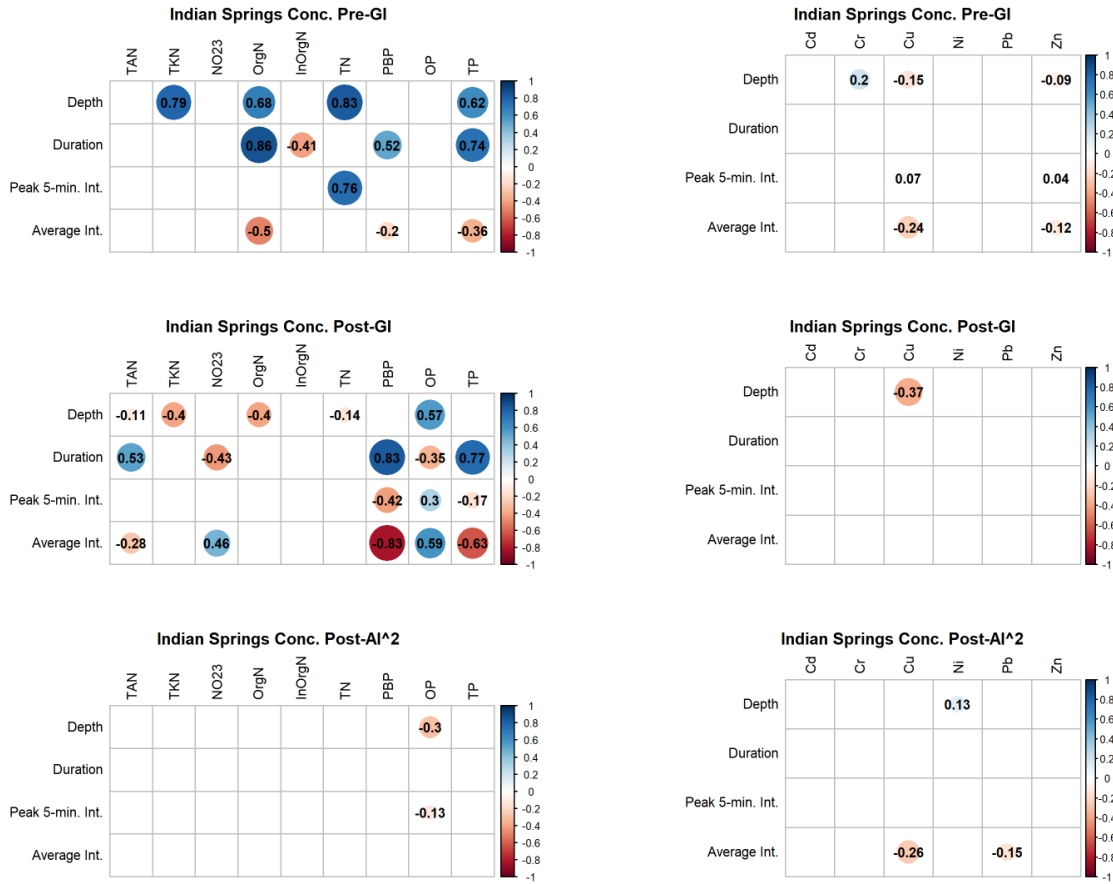


Figure 46: Spearman correlation matrices at Indian Springs between rainfall characteristics and nutrient and metal concentrations across project phases. Statistically significant ($p < 0.05$) concentrations shown in correlograms.

In the pre-GI phase at IS, loads of several nutrients were negatively correlated with peak 5-minute (NO₂₋₃, OrgN, PBP, OP, TP) and average rainfall intensity (PBP, TP) (Figure 47). Positive correlations were also identified between rainfall depth (TAN, InOrgN) and duration (PBP, TP). Metal loads were all positively correlated with rainfall depth and duration. In the post-GI phase, correlations between nutrient loads and rainfall characteristics were highly varied. Loads of several nutrients were significantly correlated with rainfall depth (negative: TKN; positive: OP), duration (negative: NO₂₋₃, OrgN, InOrgN, TN; positive: TAN, PBP, TP), and average intensity (negative: TAN, PBP, TP; positive: NO₂₋₃, InOrgN, TN). The only significant relationship between metals loads at IS in the post-GI phase was a positive correlation between

Zn and duration. In the post-AI² phase, nutrient loads were mostly positively correlated with rainfall duration (TKN, OrgN, TN, PBP, OP, TP) and depth (NO₂₋₃, OrgN, TN). TAN loads were negatively correlated with both rainfall characteristics. Negative correlations were also detected between average rainfall intensity (TKN, OrgN, PBP, OP, TP). All metals except Cd were positively correlated with rainfall duration and negatively correlated with average intensity in the post-AI² phase.

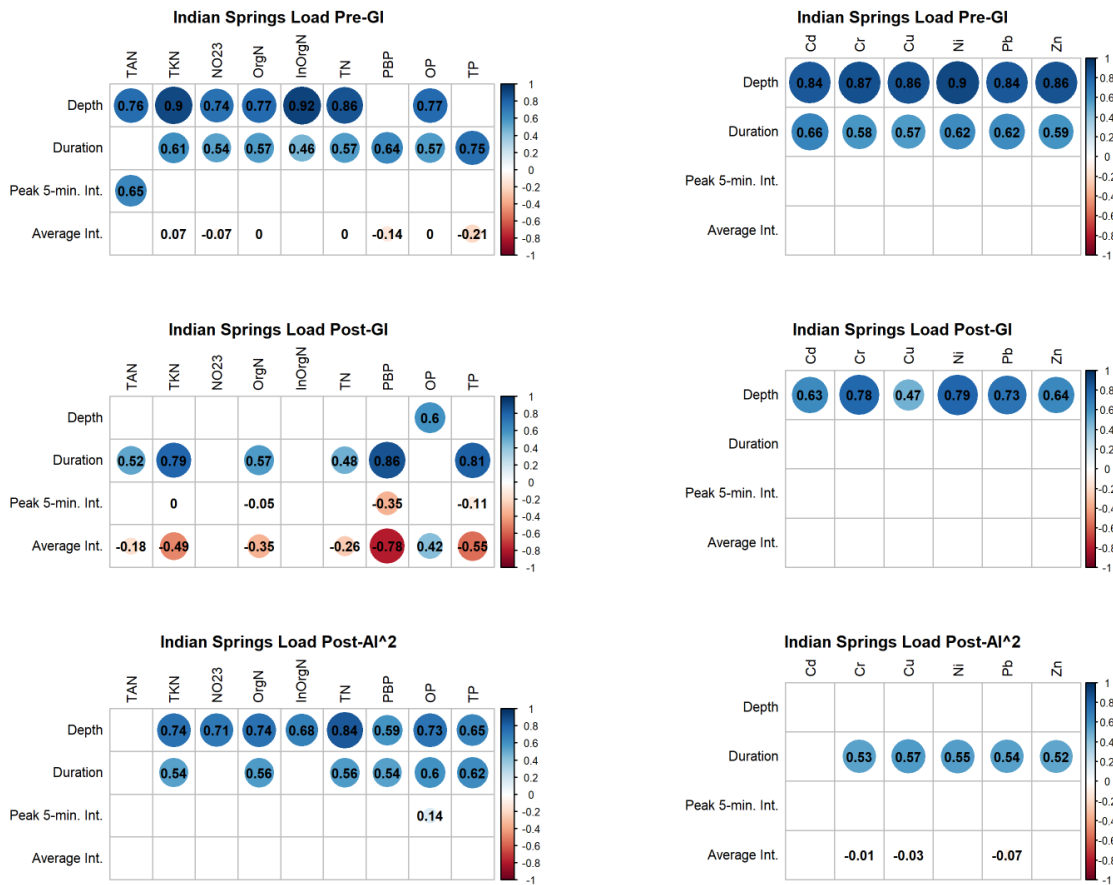


Figure 47: Spearman correlation matrices at Indian Springs between rainfall characteristics and nutrient and metal loads across project phases. Statistically significant ($p < 0.05$) concentrations shown in correlograms.

Appendix E: Wetland Inlet and Outlet Pollutant Concentration Summary Table and Figures

Table 12: Summary statistics for wetland inlet and outlet data points for all monitored pollutants. Reported p-values based on Unpaired T-Test with Welch Corrections or Uncorrected Mann-Whitney test (based on normality). Significant p-values in bold; corresponding median percent reductions bolded and colored according to direction of change (green = decrease, red = increase).

Pollutant	n		Median		Summary Statistics	
	Wetland Inlet	Wetland Outlet	Wetland Inlet	Wetland Outlet	p-value	Median % Reduction
Alkalinity (mg/L)	49	49	74.00	140.00	1.25E-11	-95.65
Cd (µg/L)	48	48	0.09	0.04	1.02E-09	53.83
Cr (µg/L)	48	48	2.98	1.45	3.22E-07	50.00
Cu (µg/L)	48	48	10.75	3.35	1.04E-13	69.01
<i>E. coli</i> (CFU/L)	18	18	2.80E+04	6.76E+03	7.04E-04	73.69
Hardness (mg/L)	48	48	120.00	185.00	6.61E-05	-47.06
InOrgN (mg/L)	48	48	0.60	0.14	8.39E-09	71.30
Ni (µg/L)	48	48	4.40	4.30	0.90	0.00
Nitrate (mg/L)	40	40	0.61	0.12	1.53E-13	79.30
Nitrite (mg/L)	39	39	0.02	0.02	0.0132900 52	0.00
NO ₂₋₃ (mg/L)	39	39	0.69	0.14	2.81E-13	79.22
OP (mg/L)	19	19	0.08	0.03	2.38E-04	40.00
OrgN (mg/L)	47	47	1.19	0.79	1.99E-05	32.14
Pb (µg/L)	48	48	8.75	1.50	1.32E-15	82.02
PBP (mg/L)	42	42	0.24	0.09	9.06E-05	57.52
TAN (mg/L)	48	48	0.06	0.01	2.82E-03	27.78
TKN (mg/L)	48	48	1.25	0.87	5.81E-06	30.06
TN (mg/L)	48	48	1.86	0.98	1.00E-10	45.65
TP (mg/L)	48	48	0.23	0.12	1.25E-05	42.04
TSS (mg/L)	49	49	47.00	19.00	2.36E-09	69.64
Zn (µg/L)	48	48	47.05	18.65	1.59E-08	64.37

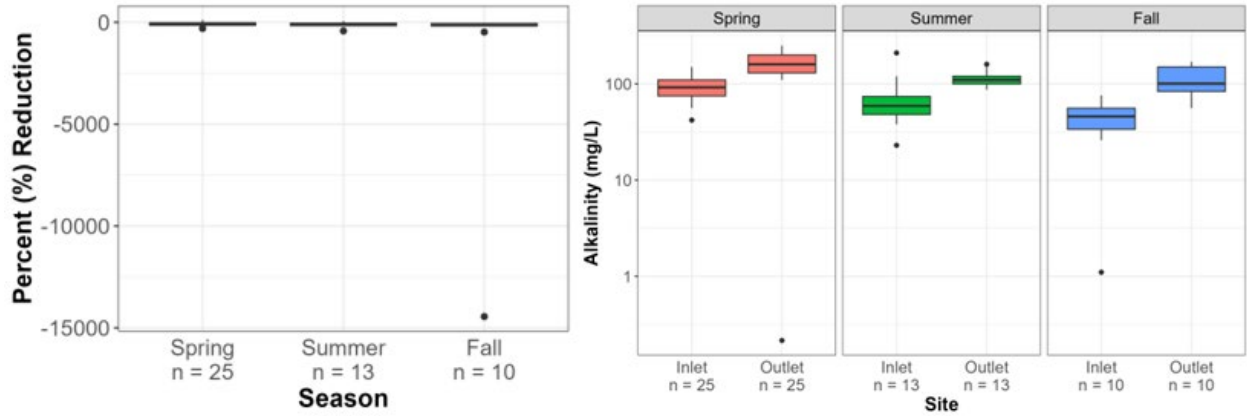


Figure 48: Summary statistics of alkalinity in water quality samples collected from the constructed wetland at the Clintonville Park of Roses receiving low flows from the Blenheim sewershed and results of analyses comparing season of collection.

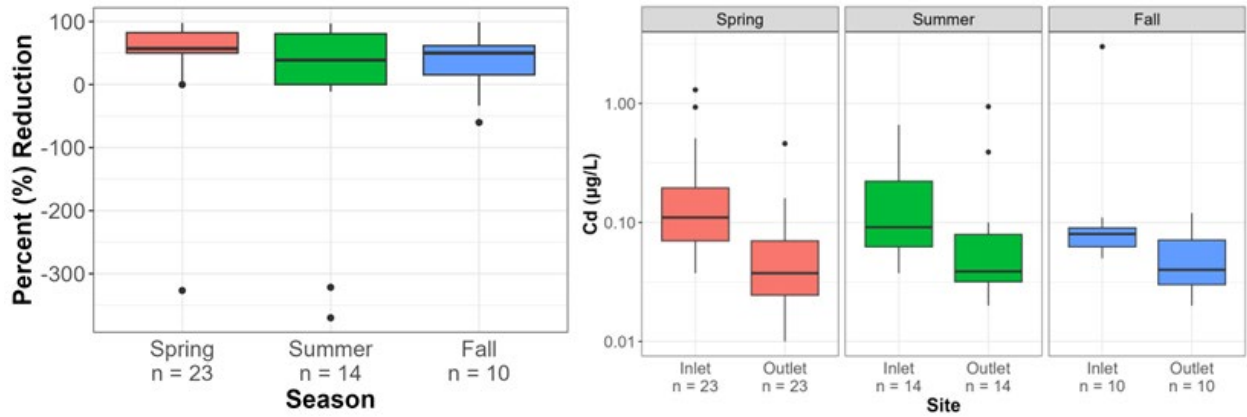


Figure 49: Summary statistics of cadmium in water quality samples collected from the constructed wetland at the Clintonville Park of Roses receiving low flows from the Blenheim sewershed and results of analyses comparing season of collection.

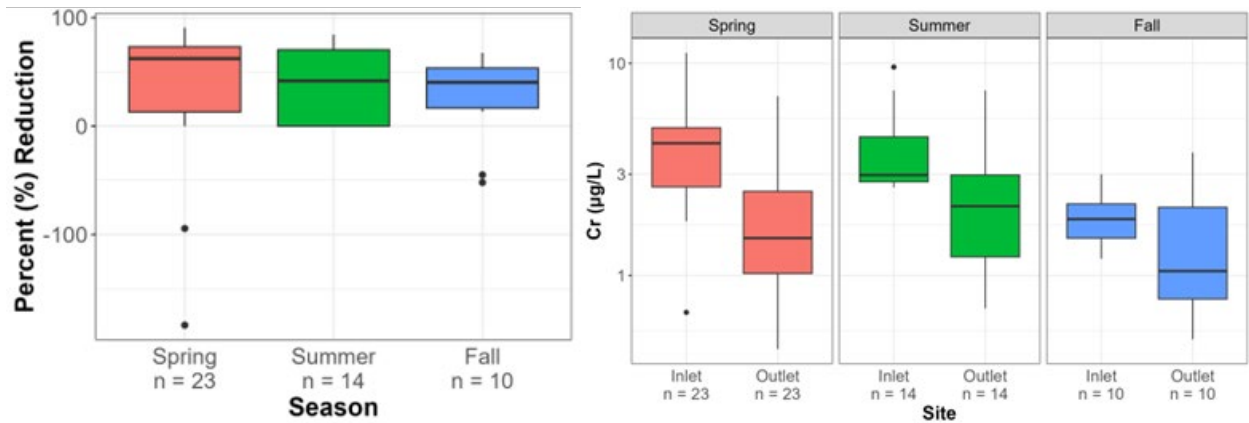


Figure 50: Summary statistics of chromium in water quality samples collected from the constructed wetland at the Clintonville Park of Roses receiving low flows from the Blenheim sewershed and results of analyses comparing season of collection.

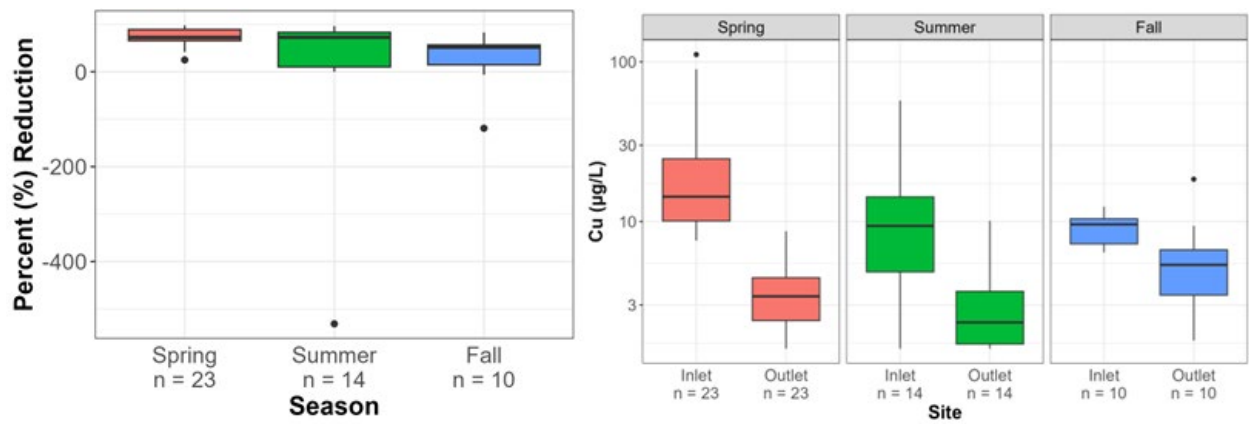


Figure 51: Summary statistics of copper in water quality samples collected from the constructed wetland at the Clintonville Park of Roses receiving low flows from the Blenheim sewershed and results of analyses comparing season of collection.

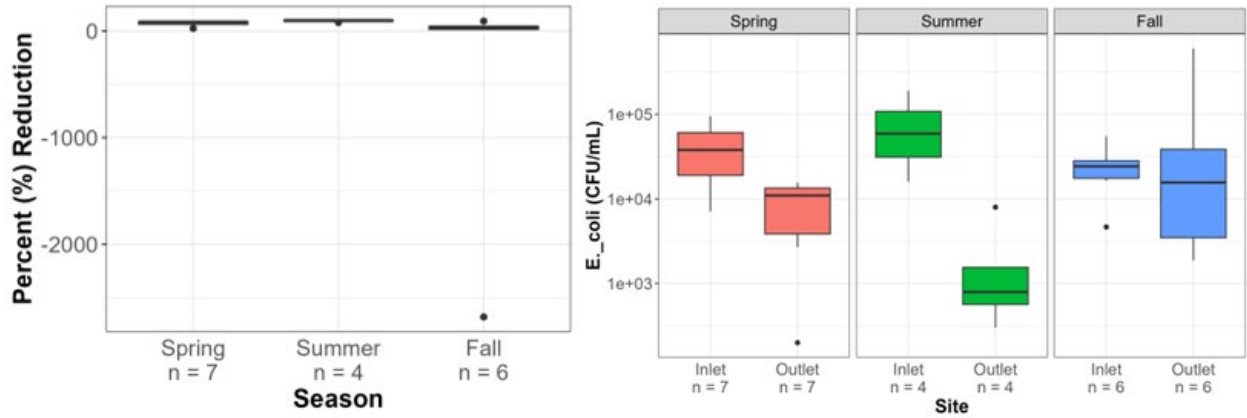


Figure 52: Summary statistics of *E. coli* in water quality samples collected from the constructed wetland at the Clintonville Park of Roses receiving low flows from the Blenheim sewershed and results of analyses comparing season of collection.

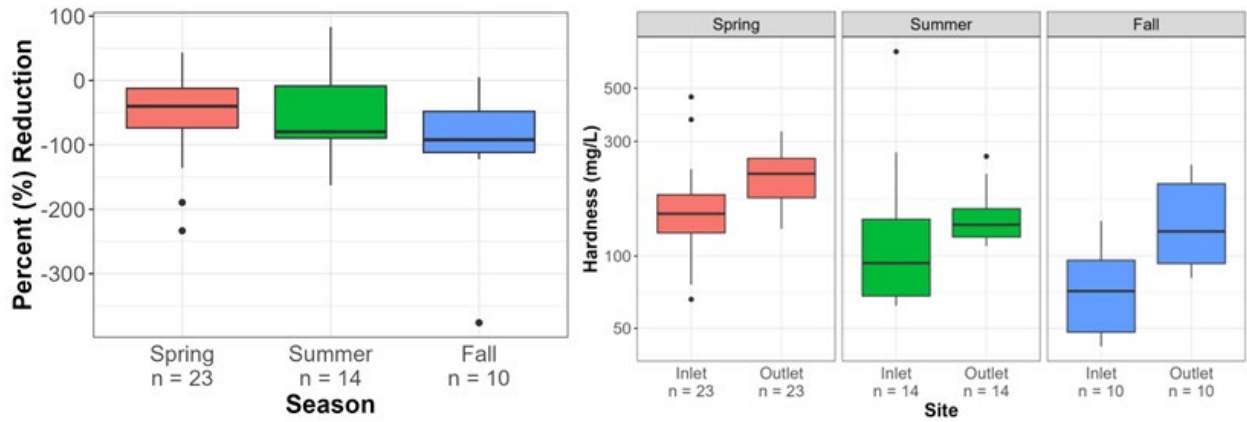


Figure 53: Summary statistics of hardness in water quality samples collected from the constructed wetland at the Clintonville Park of Roses receiving low flows from the Blenheim sewershed and results of analyses comparing season of collection.

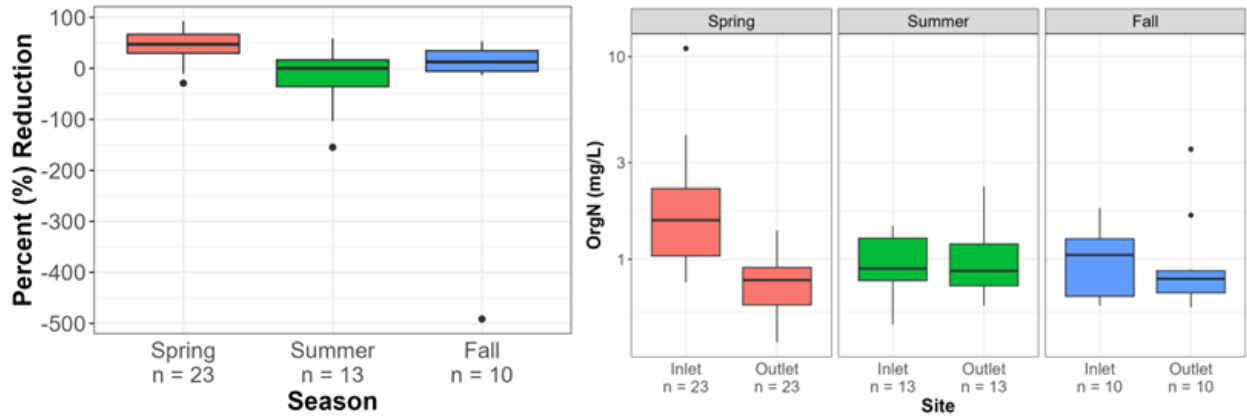


Figure 54: Summary statistics of organic nitrogen in water quality samples collected from the constructed wetland at the Clintonville Park of Roses receiving low flows from the Blenheim sewershed and results of analyses comparing season of collection.

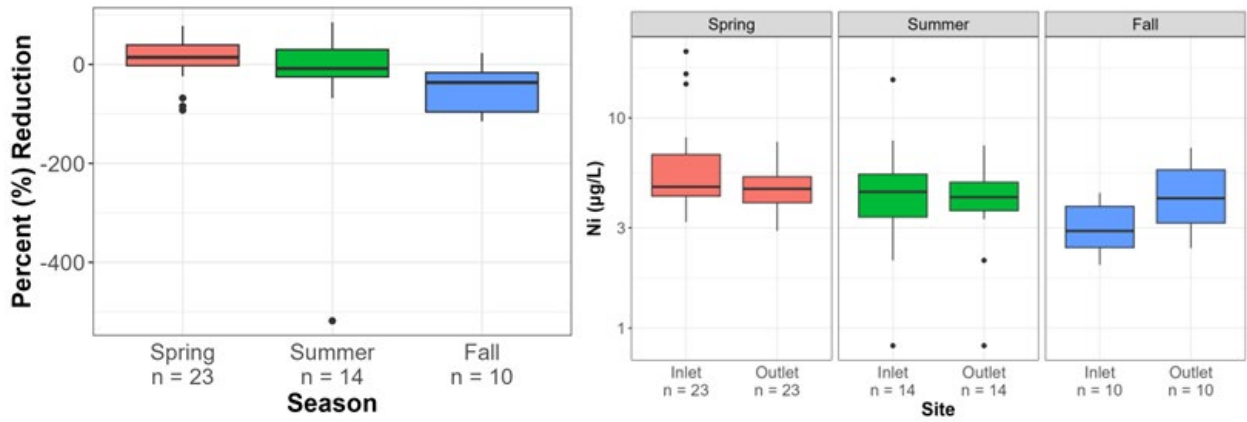


Figure 55: Summary statistics of nickel in water quality samples collected from the constructed wetland at the Clintonville Park of Roses receiving low flows from the Blenheim sewershed and results of analyses comparing season of collection.

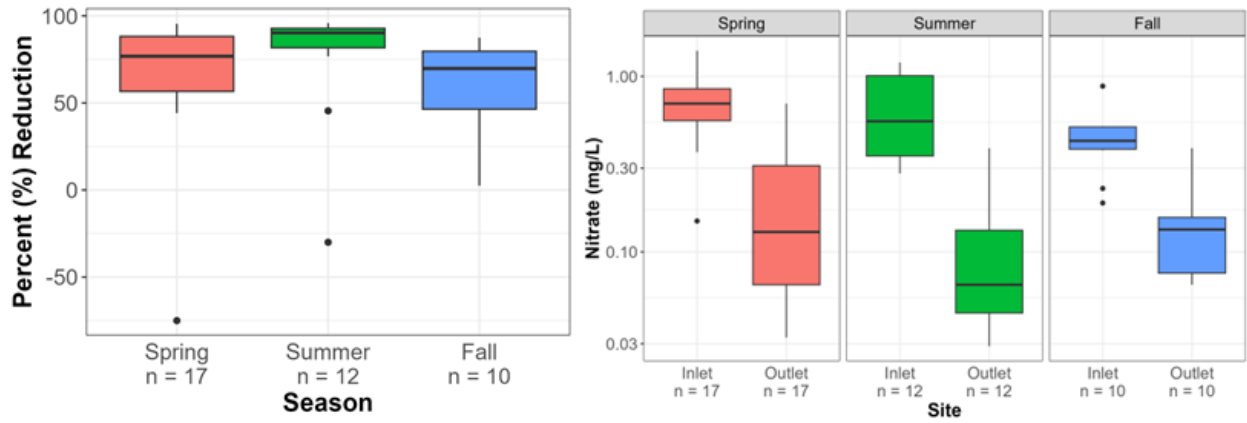


Figure 56: Summary statistics of nitrate in water quality samples collected from the constructed wetland at the Clintonville Park of Roses receiving low flows from the Blenheim sewershed and results of analyses comparing season of collection.

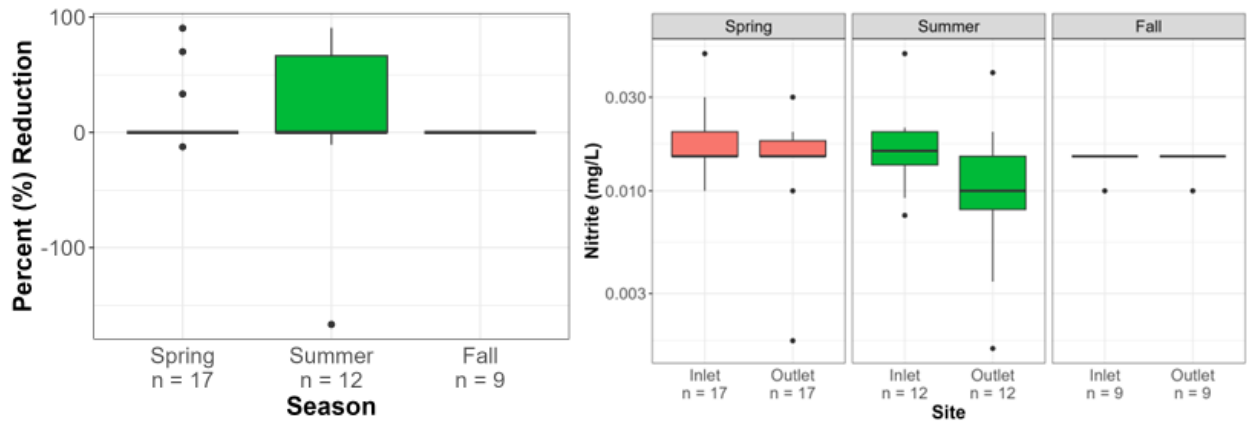


Figure 57: Summary statistics of nitrite in water quality samples collected from the constructed wetland at the Clintonville Park of Roses receiving low flows from the Blenheim sewershed and results of analyses comparing season of collection.

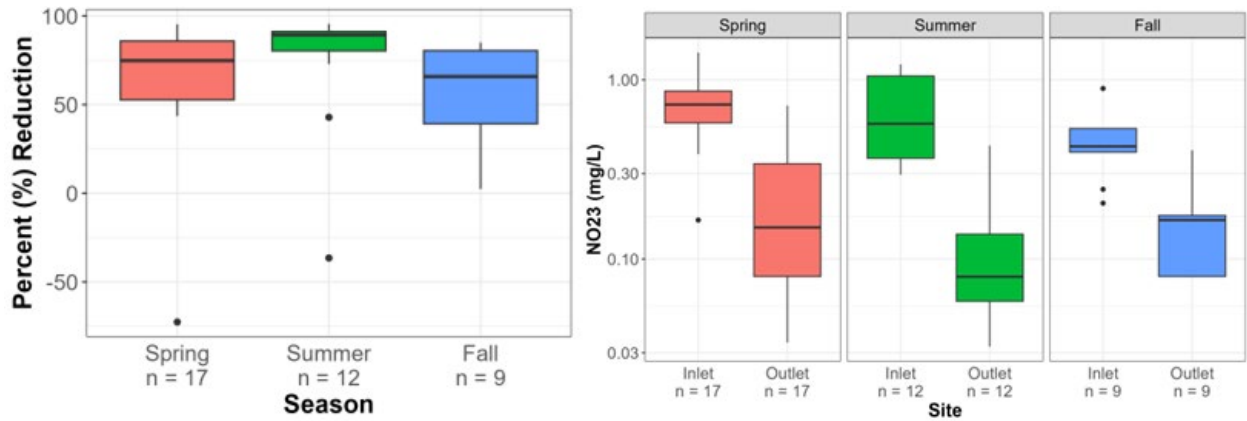


Figure 58: Summary statistics of NO₂₃ in water quality samples collected from the constructed wetland at the Clintonville Park of Roses receiving low flows from the Blenheim sewershed and results of analyses comparing season of collection.

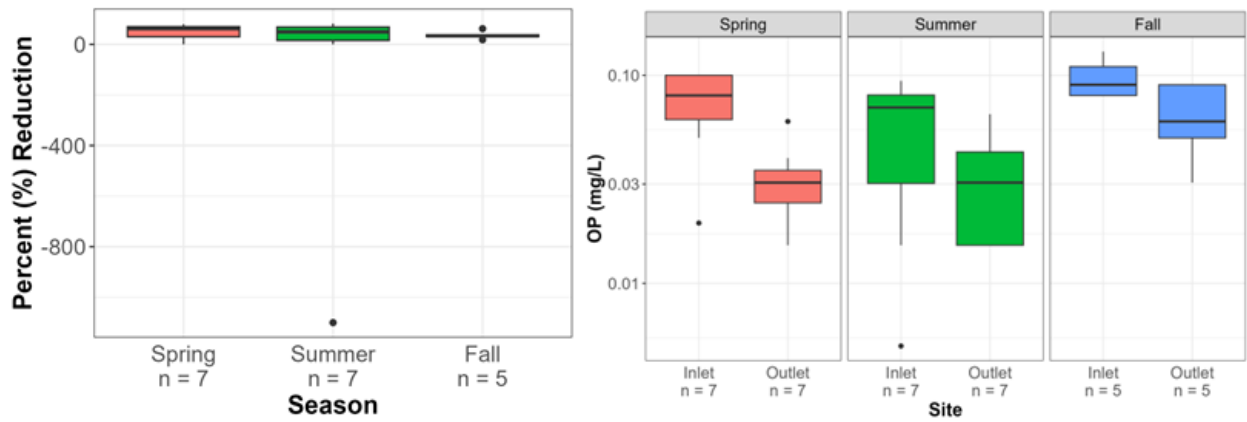


Figure 59: Summary statistics of orthophosphate in water quality samples collected from the constructed wetland at the Clintonville Park of Roses receiving low flows from the Blenheim sewershed and results of analyses comparing season of collection.

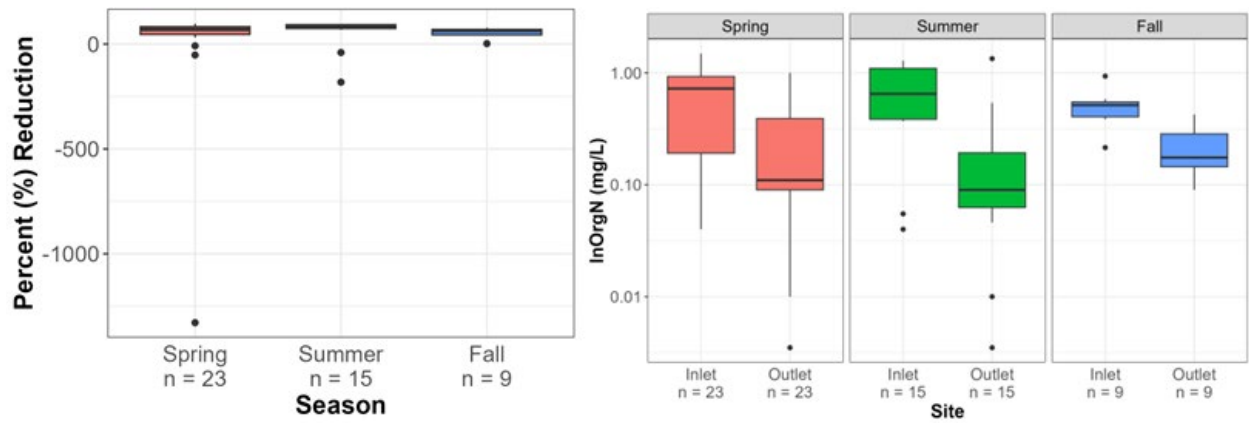


Figure 60: Summary statistics of inorganic nitrogen in water quality samples collected from the constructed wetland at the Clintonville Park of Roses receiving low flows from the Blenheim sewershed and results of analyses comparing season of collection.

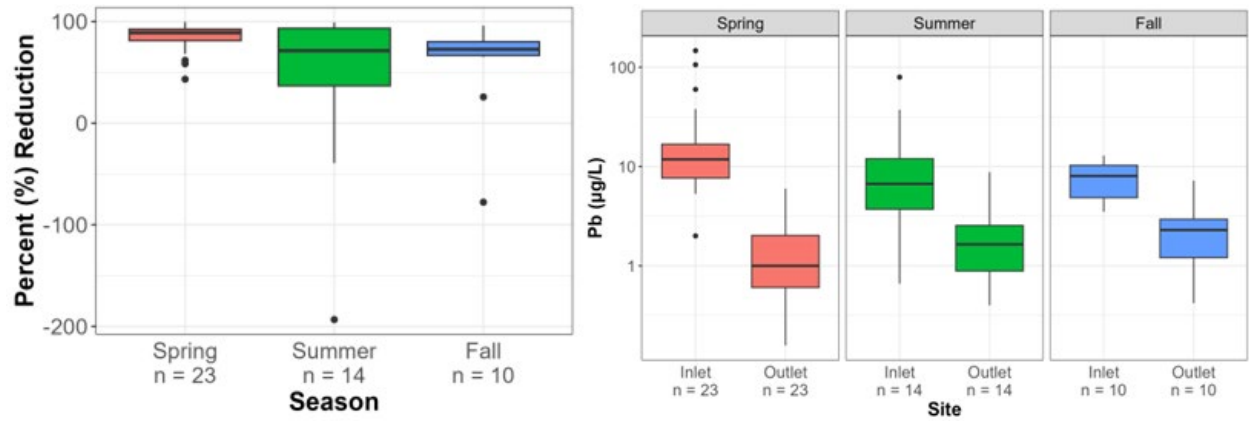


Figure 61: Summary statistics of lead in water quality samples collected from the constructed wetland at the Clintonville Park of Roses receiving low flows from the Blenheim sewershed and results of analyses comparing season of collection.

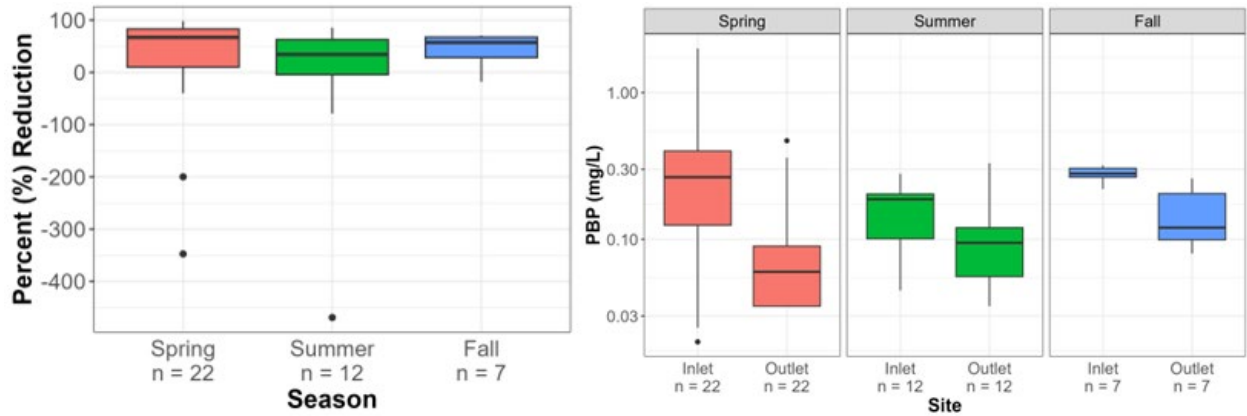


Figure 62: Summary statistics of particle-bound phosphorus in water quality samples collected from the constructed wetland at the Clintonville Park of Roses receiving low flows from the Blenheim sewershed and results of analyses comparing season of collection.

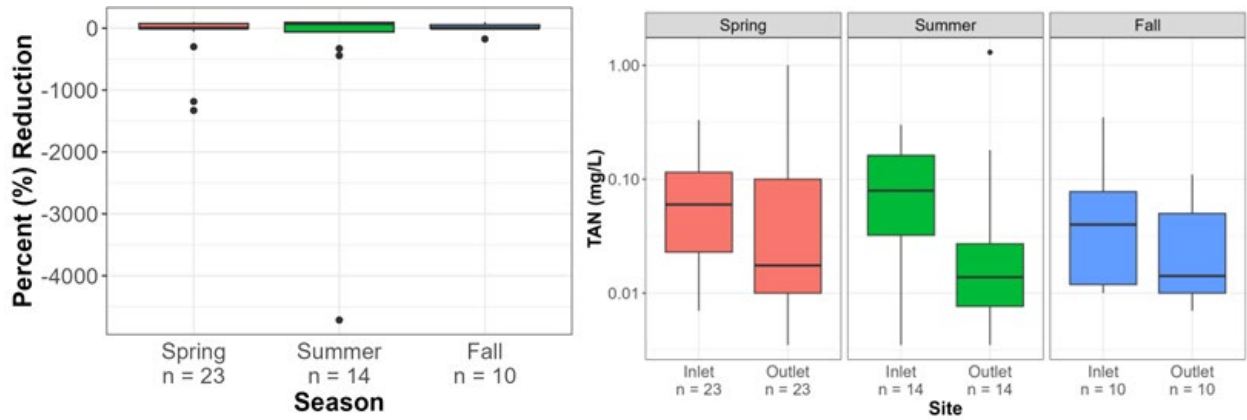


Figure 63: Summary statistics of total ammoniacal nitrogen in water quality samples collected from the constructed wetland at the Clintonville Park of Roses receiving low flows from the Blenheim sewershed and results of analyses comparing season of collection.

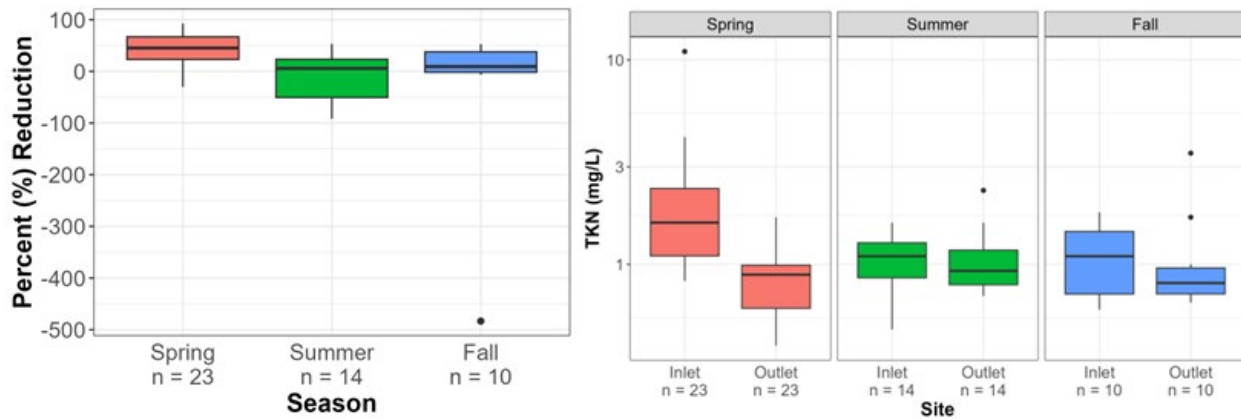


Figure 64: Summary statistics of total Kjeldahl nitrogen in water quality samples collected from the constructed wetland at the Clintonville Park of Roses receiving low flows from the Blenheim sewershed and results of analyses comparing season of collection.

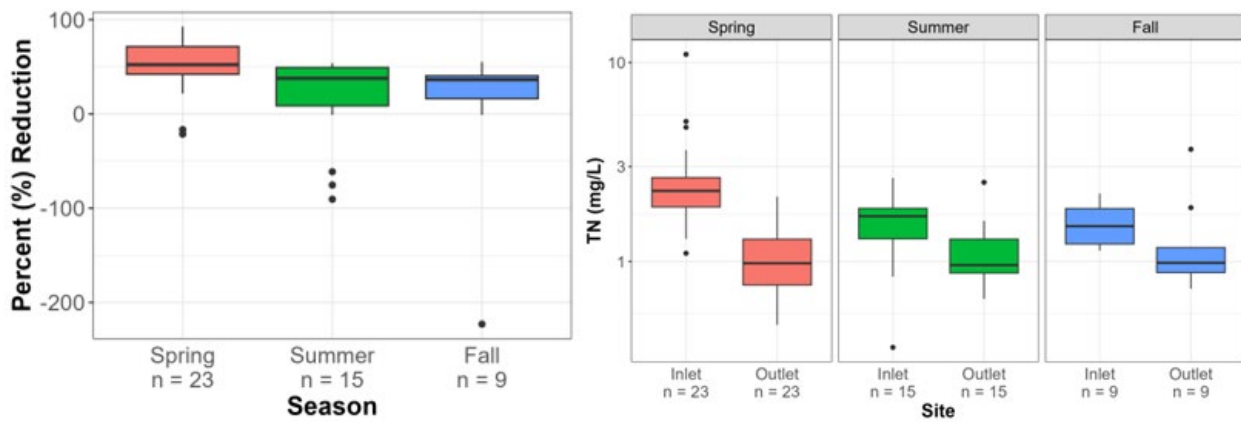


Figure 65: Summary statistics of total nitrogen in water quality samples collected from the constructed wetland at the Clintonville Park of Roses receiving low flows from the Blenheim sewershed and results of analyses comparing season of collection.

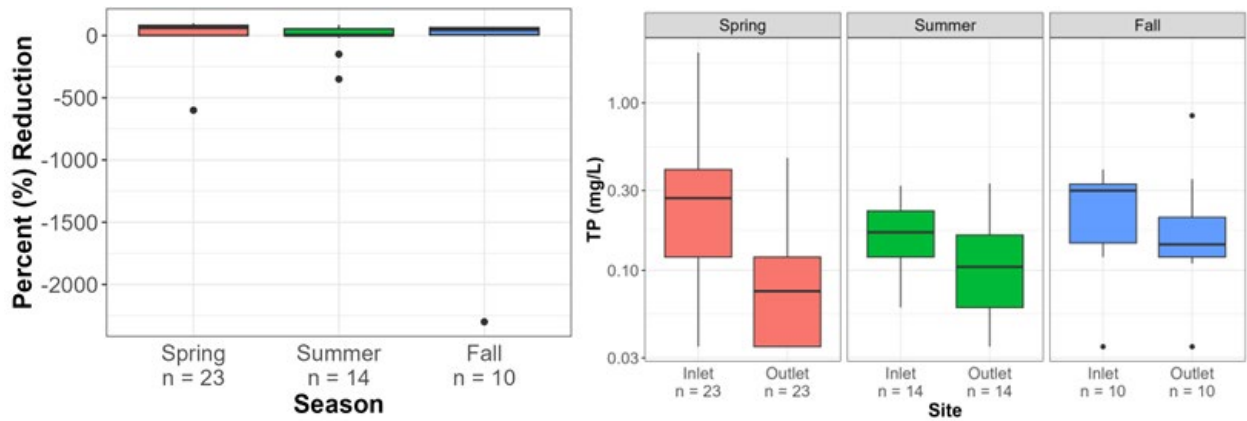


Figure 66: Summary statistics of total phosphorus in water quality samples collected from the constructed wetland at the Clintonville Park of Roses receiving low flows from the Blenheim sewershed and results of analyses comparing season of collection.

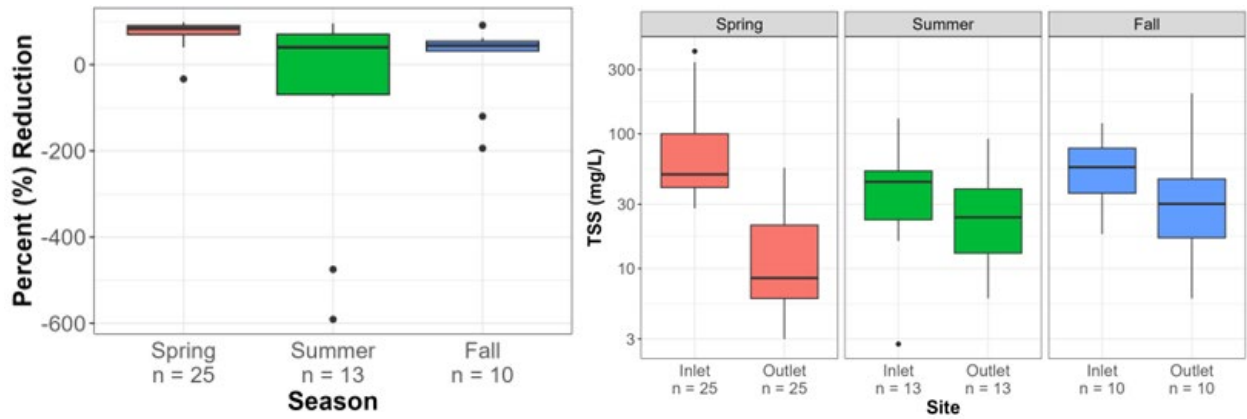


Figure 67: Summary statistics of total suspended solids in water quality samples collected from the constructed wetland at the Clintonville Park of Roses receiving low flows from the Blenheim sewershed and results of analyses comparing season of collection.

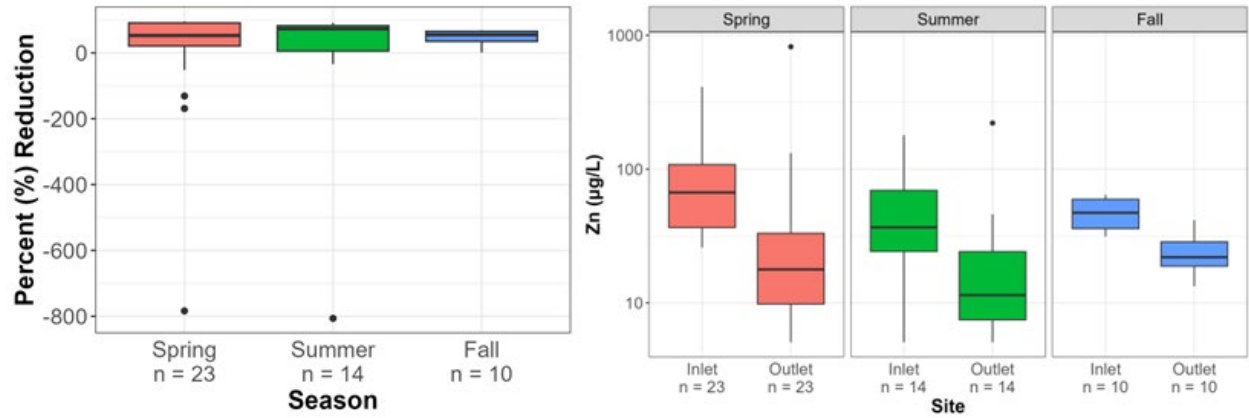


Figure 68: Summary statistics of zinc in water quality samples collected from the constructed wetland at the Clintonville Park of Roses receiving low flows from the Blenheim sewershed and results of analyses comparing season of collection.

Appendix F: Laboratory Methods

Table 13: Sample collection, preservation, and laboratory testing methods as well as method detection limits (MDLs) for pollutants analyzed herein.

Parameter	Laboratory Method	Sampling Method	Container	Preservation	MDL (mg/L)
TKN	EPA Method 351.21	Composite	Plastic	H ₂ SO ₄ (<2 pH), <4°C	0.078
NO ₂	EPA Method 353.2	Composite	Plastic	H ₂ SO ₄ (<2 pH), <4°C	0.018
NO ₃	EPA Method 353.2	Composite	Plastic	<4°C	0.043
TN	Calculated as TKN + NO ₂ + NO ₃	Composite	Plastic	NA	NA
TAN ¹	EPA Method 350.1	Composite	Plastic	H ₂ SO ₄ (<2 pH), <4°C	0.0031
ON	Calculated as TKN-TAN	Composite	Plastic	NA	NA
OP	EPA Method 365.2	Composite	Plastic	<4°C	0.01
PBP	Calculated as TP-OP	Composite	Plastic	NA	NA
TP	EPA Method 365.2	Composite	Plastic	<4°C	0.1
TSS	Standard Methods 2540D2	Composite	Plastic	<4°C	2
Total Alkalinity	Standard Methods 2320	Composite	Plastic	<4°C	6.61
Hardness	Standard Methods 4500-SiO ₂ D	Composite	Plastic	HNO ₃ (<2 pH), <4°C	0.027
Cyanide ²	EPA Method 335.4	Grab	Glass	4-6 pellets NaOH	0.0019
Oil and Grease ²	Standard Methods 2130 B	Grab	Glass	H ₂ SO ₄ (<2 pH), <4°C	0.15
COD ²	EPA Method 410.3	Composite	Plastic	H ₂ SO ₄ (<2 pH), <4°C	5.9
cBOD, 5 day ²	Standard Methods 5210B	Composite	Plastic	<4°C	0.59
BOD, 5 day ²	Standard Methods 5210A	Composite	Plastic	<4°C	0.31
Parameter	Laboratory Method	Sampling Method	Container	Preservation	MDL
E. coli	EPA Method 1603	Composite	Plastic	<4°C	1 CFU/100mL
Microbial source tracking	Quantitative PCR	Composite	Plastic	-80°C	5 gene copies/reaction
Microbiome	Metagenomics	Composite	Plastic	-80°C	10 read count
Resistome	Metagenomics	Composite	Plastic	-80°C	read count
Virulence gene	Metagenomics	Composite	Plastic	-80°C	10 read count
Parameter	Laboratory Method	Sampling Method	Container	Preservation	MDL (µg/L)
Cd		Composite	Plastic		0.013
Cr		Composite	Plastic		0.036
Cu	EPA 200.8	Composite	Plastic	HNO ₃ (<2 pH), <4°C	0.26
Pb		Composite	Plastic		0.0086
Ni		Composite	Plastic		0.025
Zn		Composite	Plastic		0.7

¹TAN is equal to the laboratory reported NH₃ (ammonia) concentration.

²Samples obtained once per quarter for NPDES compliance.